ENHANCING THE STRUCTURAL PERFORMANCE WITH ACTIVE AND SEMI-ACTIVE DEVICES USING ADAPTIVE CONTROL STRATEGY

A Dissertation

by

MARYAM BITARAF

Submitted to the Office of Graduate Studies of
Texas A&M University
in partial fulfillment of the requirements for the degree of

DOCTOR OF PHILOSOPHY

May 2011

Major Subject: Civil Engineering

Enhancing the Structural Performance with Active and Semi-active Devices Using Adaptive Control Strategy

ENHANCING THE STRUCTURAL PERFORMANCE WITH ACTIVE AND SEMI-ACTIVE DEVICES USING ADAPTIVE CONTROL STRATEGY

A Dissertation

by

MARYAM BITARAF

Submitted to the Office of Graduate Studies of
Texas A&M University
in partial fulfillment of the requirements for the degree of

DOCTOR OF PHILOSOPHY

Approved by:

Chair of Committee,	Stefan Hurlebaus
Committee Members,	Luciana Barroso
	Jose Roesset
	Paolo Gardoni
	Reza Langari
Head of Department,	John Niedzwecki

May 2011

Major Subject: Civil Engineering

ABSTRACT

Enhancing the Structural Performance with Active and Semi-Active Devices Using Adaptive Control Strategy. (May 2011)

Maryam Bitaraf, B.Sc., University of Tehran, Iran;

M.Sc., University of Tehran, Iran

Chair of Advisory Committee: Dr. Stefan Hurlebaus

Changes in the characteristics of the structure, such as damage, have not been considered in most of the active and semi-active control methods that have been used to control and optimize the response of civil engineering structures. In this dissertation, a direct adaptive control which can deal with the existence of measurement errors and changes in structural characteristics or load conditioning is used to control the performance of structures. A Simple Adaptive Control Method (SACM) is modified to control civil structures and improve their performance. The effectiveness of the SACM is verified by several numerical examples. The SACM is used to reduce the structural response such as drift and acceleration using active and semi-active devices, and its performance is compared with that of other control methods. Also, a probabilistic indirect adaptive control method is developed and its behavior is compared to the SACM using a simple numerical example. In addition to the simplicity of the SACM implementation, the results show that SACM is very effective to reduce the response of structures with linear and non-linear behavior in comparison with other control methods.

DEDICATION

To My Grandmother, My Father, My Mother, My sisters and Ali

ACKNOWLEDGEMENTS

The research presented in this dissertation would not have been possible without the support that I received from my advisor, Dr. Hurlebaus. I would like to thank him for his advice and encouragement to work on my own research interests. Without his help, I would have not managed to write many journal and conference papers. I would also like to thank Dr. Barroso for her support, understanding and especially for her kindness. I want to thank Dr. Langari for his professional advice on adaptive control methods.

Special thanks go to Dr. Roesset for his friendship and invaluable help during my doctoral study. I am so proud and honored that I am one of his students. I want to thank my dear Iranian friends in College Station who made me enjoy my life more than what I could have imagined during these past four years.

Finally, I would like to acknowledge the support of my family. I want to thank my dear parents and sisters whose love and support were critical in the completion of this dissertation. I would like to thank my dearest husband, Dr. Ali Sadighi, who always supports and helps me, especially in very difficult situations. I can always feel confident in every situation because I know he is backing me up.

TABLE OF CONTENTS

Page

Page

LIST OF FIGURES

Page

Page

Page

Page

Page

LIST OF TABLES

Page

1. INTRODUCTION

Many severe events such as earthquakes and winds might happen to a structural system, impacting its structural performance and causing extensive damage. Structural damage resulting from natural hazards may cause human tragedies and enormous economic repercussions (Huang et al. 2004). For example, the Kobe earthquake (in January 1995 in Japan), with a 6.9 Richter magnitude, was very devastating. It took an estimated 5,500 lives, more than 36,000 people were injured, and over 200,000 buildings were either damaged or destroyed (Figure 1.1). The economic damage amounted to roughly $200 billion.

[http://library.thinkquest.org/03oct/00904/eng/elmeny.htm]

[http://www.smate.wwu.edu/teched/geology/GeoHaz/eq-Kobe/]

Figure 1.1: Earthquake damage in Kobe, Japan.

This dissertation follows the style of *Journal of Engineering Mechanics*.

About 31,000 people perished and a further 30,000 were injured because of an earthquake which occurred in Bam, Iran in 2003. The economic loss was estimated at around $32.7 million. Eastern Sichuan in China was destroyed with the loss of 69,000 people because of an earthquake with magnitude of 7.9 which happened in 2008. About 374,000 people were injured and more than 5 million buildings collapsed while about 21 million buildings were damaged. Experts estimated over $86 billion economic loss for that hazard. In addition to earthquakes, strong winds can also cause human and economic loss. For example, Hurricane Katrina (2005) which is the fifth deadliest hurricane in the US killed at least 1,800 people and caused $81 billion in property damage.

One of the challenging tasks for civil engineers is to mitigate the response of a structure subjected to dynamic loads in order to reduce the risks of damage and injuries caused by extreme hazards such as earthquakes and strong winds. One of the solutions to reduce tragic consequences of natural hazards is using supplemental control devices which can reduce the deformation or acceleration response of civil engineering structures and protect them from damage under external loadings (Adeli and Saleh 1999; Chase et al. 2006; McCormick et al. 2006; Padgett and DesRoches 2008). There are mainly three classes of control devices, which are passive, active and semi-active devices (Housner et al. 1997; Hurlebaus and Gaul 2006). Passive devices are reliable and never destabilize the structure. They need no external power for operation and use the motion of the structure to develop the control forces (Wilde et al. 2000; Kim and Adeli 2005). However, they have low adaptability to change of external loading conditions or

usage patterns used in their design. Many passive control devices, such as viscoelastic dampers and tuned mass dampers have been used to reduce the structural response of civil engineering systems (Hoang et al. 2008).

On the other hand, active control devices which typically require a large power source for operation are adaptive to varying usage patterns and loading conditions and capable of generating relatively large forces with a relatively small response time (Kerber et al. 2007; Jiang and Adeli 2008). However, their stability problems, reliability and large power consumption are major concerns to engineers. Servo-hydraulic actuators are one class of active devices. They usually consist of a hydraulic power supply, a control element such as a valve, and an actuating element such as a motor (Chen 2007). Very high forces at very high power levels can be provided by hydraulic actuators (DeSilva 1989).

Semi-active devices which are the third class of structural control systems have attracted considerable attention for the seismic protection of structures in recent years (Gaul et al. 2008). These devices only absorb or store the vibratory energy and they do not inject energy to the system. Therefore, they do not induce adverse effects on the stability of the system. The versatility and adaptability of the active devices and the reliability of the passive devices are offered by semi-active devices. A variety of semi-active devices such as variable orifice dampers, variable friction devices, adjustable tuned liquid dampers, variable stiffness dampers and controllable fluid dampers have been proposed for vibration control of structures (Yi et al. 2001; Casciati et al. 2006). One of the most promising semi-active devices is the magnetorheological (MR) damper.

1.1. Survey of Relevant Work

One of the challenges in the application of active and semi-active control devices is using an appropriate control algorithm to determine the control command to the control device. Many control algorithms have been proposed to control the performance of structure equipped with active or semi-active devices.

1.1.1. Active Control Systems

Different control methods such as feedback control algorithms, fuzzy logic control, and Linear Quadratic Gaussian (LQG) control have been used to actively control the structural response of civil engineering systems (Wilde et al. 2001). Linear quadratic regulator theory was applied to a structure equipped with active devices by Chung et al. (1989) and Reinhorn et al. (1989). LQG/H_2 has been applied to actively control the performance of civil engineering structures by Suhardjo et al. (1992), Kozodoy and Spanos (1995), Quast et al. (1995), Dyke et al. (1996a) and Zhu et al. (1997). The performance of active tendon control of cable-stayed bridges was studied analytically and experimentally by Warnitchai et al. (1993). Active Tuned Liquid Damper (TLD) with Magnetic Fluid was proposed as an active device by Abe et al. (1998). A rule-based control law was used to control the proposed active device and its performance was verified experimentally. A H_∞ control of an active mass damper (AMD) was used to reduce the response of a building with mass and stiffness uncertainties by Huo et al. (2008). To model uncertainty, linear fractional transformation (LFT) was utilized and the acceleration signal was used for feedback. The effectiveness

of compensation algorithm for AMD was studied by Sasajima et al. (2010). Ishiola et al. (2010) used the variable gain control algorithm to control the response of high-rise buildings equipped with AMD analytically and experimentally.

More than 30 buildings in Japan were built using different types of structural control systems. The Kyobashi Seiwa building was the first full-scale actively controlled building equipped with AMD (Sakamoto et al. 1994). Kyobashi Seiwa is an eleven-story steel building constructed in Tokyo, Japan in 1989. The Sendagaya INTES Building (1992), Applause Tower Building (1994), Riverside Sumida Building (1994), and the HERBIS Osaka Building (1997) are some other buildings which employed active control systems to improve their performance (Nishitani and Inoue 2001).

1.1.2. Semi-active Control Systems

In the past two decades, many control methods have also been used to control the behavior of structural systems with semi-active devices. Decentralized bang-bang control (Feng and Shinozuka 1990), the methods based on the Lyapunov theory to minimize the rate of change of a Lyapunov function (Brogan 1991), the method which decreases the total energy of the structure (McClamroch and Gavin 1995), the modified linear quadratic regulator (LQR) (Johnson and Erkus 2007), clipped-optimal control (Dyke and Spencer 1996) and modulated homogeneous friction control (Inaudi 1997) are some of the control algorithms used for semi-active control devices.

Spencer et al. (1997) used acceleration feedback control and MR dampers to control the performance of a structure. A semi-active control method which considers

the dynamics of the disturbance was applied by Yoshida et al. (1999) to suppress the effect of external loads on structural response. They suggested including feedforward information of disturbance in the process of the control algorithm. The response of elevated highway bridges controlled with active, semi-active and passive systems under seismic loads were studied by Erkus et al. (2002). They used LQR and LQR-based clipped optimal control to control the active and semi-active systems. It was shown that MR dampers can reach the active control performance depending on the goal design. The effectiveness of using MR dampers combined with a semi-active independently variable stiffness (SAIVS) to reduce the response of a base isolated structure subjected to earthquakes was experimentally and analytically studied by Nagarajaiah et al. (2006a). A nonlinear tangential stiffness moving average control and Lyapunov based control algorithms were used to control SAIVS and MR dampers, respectively (Sahasrabudhe and Nagarajaiah 2005b; Nagarajaiah et al. 2006a).

Semi-active control of cable-stayed bridges was studied by Johnson et al. (2007) and compared with active and passive devices. The semi-active damper was as successful as the active damper in reducing the structural response. In comparison with passive dampers, the semi-active damper was very effective in decreasing response and absorbing energy (Johnson et al. 2007). Yuen et al. (2007) proposed a clipped robust reliability-based control and MR dampers to protect structures against external loads. They used a robust reliability-based active linear control methodology to calculate the forces generated by the MR dampers (Yuen et al. 2007). Lyapunov-based control approach is proposed by Ha et al. (2008) to mitigate seismic responses of building with

MR dampers. The supply current applied to MR dampers was controlled directly using their method. Fuzzy logic control methods have been investigated for active and semi-active control of civil engineering structures by many researchers (Faravelli and Yao 1996; Subramaniam et al. 1996; Ahlawat and Ramaswamy 2001; Zhou et al. 2003; Al-Dawod et al. 2004; Choi et al. 2004; Kim et al. 2010).

The first full-scale application of MR dampers in civil engineering structures was the Nihon-Kagaku-Miraikan, the Tokyo National Museum of Emerging Science and Innovation in 2001 (Figure 1.2). Two 30-ton MR dampers are located between the third and fifth story of the building (Spencer and Nagarajaiah 2003). In 2003, 40-ton MR dampers were installed in a residential building in Japan (Spencer and Nagarajaiah 2003). The first world implementation of MR dampers for bridges is on the Dongting Lake Bridge, China. A MR damping system was installed on the cables of the bridge in 2002 (Chen et al. 2004). The Shandong Binzhou Yellow River Highway Bridge in Shandong Province, China is also equipped with MR dampers to have more desirable performance under dynamic loads (Li et al. 2007).

The variable friction damper (VFD) is a semi-active device that appears to be promising for structural control applications. Symans and Kelly investigated the performance of a variable viscous damper modulated by a fuzzy controller for seismic protection of an isolated bridge (Symans and Kelly 1999). In another study, Nagarajaiah and Sahasrabudhe (2006b) proposed a variable stiffness device that is used in a sliding isolation system to reduce seismic response of a base-isolated building and the effectiveness of the proposed semi-active device was shown by performing analytical

and experimental studies. Madhekar and Jangid (2009) evaluated the dynamic response of a seismically isolated benchmark bridge equipped with viscous and variable dampers and assessed the performance of such dampers.

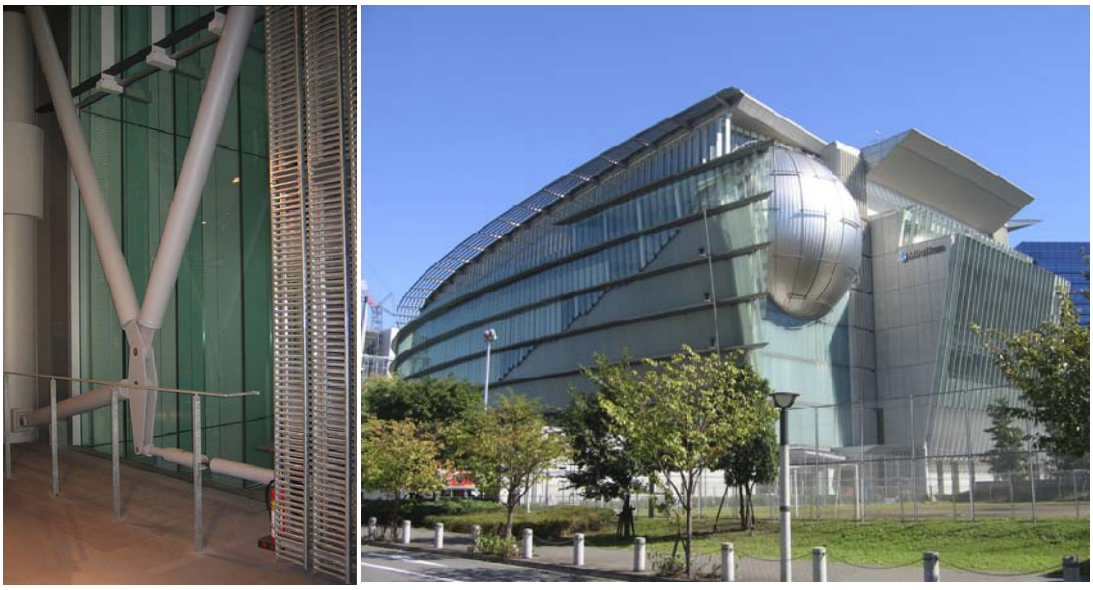

Figure 1.2: Nihon-Kagaku-Miraikan, the Tokyo National Museum of Emerging Science and Innovation, Japan.

Inaudi et al. (1997) developed a modulated homogenous friction (MHF) strategy that assumes the slip force of the damper is proportional to the absolute value of the prior local peak of the damper deformation. He et al. (2003) improved the MHF controller to enable the slippage in the damper at different levels of seismic loadings. Chen and Chen (2004) suggested a Viscous and Reid friction (VRF) control strategy where the control force is computed as a function of the displacement and velocity of the damper. Xu and Chen (2008) presented a modified VRF controller with a Kalman filter that uses acceleration response as a feedback signal. Lu and Lin (2009) proposed a control algorithm named predictive control that takes into account the features of friction dampers and predicts a slip force such that the damper remains in its slip state

throughout the excitation. Ng and Xu (2007) developed a non-sticking friction controller that uses the actuated velocity in the current state of damper to ensure a continuous slipping and energy dissipation.

1.2. Research Significance

Each of the above mentioned control strategies has its own merits and limitations depending on the application and desired response, and comparative studies are needed to evaluate the performance of each control method. The majority of the above-mentioned methods used to control the response of a structure with semi-active devices does not consider the possibility of any change in the characteristics of the controlled structure or the presence of noise in the output measurements. In this study, a direct adaptive control method is chosen to control the performance of the structural systems subjected to external dynamic loads which can perform well in the presence of noise or any change in structural characteristics (Bitaraf et al. 2010a; Bitaraf et al. 2010d).

However, even in the presence of supplemental control devices, extreme earthquakes, wind loads and deterioration caused by corrosion or fatigue may result in structural damage. Also, the characteristics of the structure such as mode shapes, natural frequencies and stiffness are different from the model of the structure due to structural modeling uncertainties. As a result, the environmental and operational conditions of the structure may vary within a rather large range and deviate substantially from those considered in the nominal ideal design. The use of an adaptive control strategy is particularly appropriate as it can address these changes (Sobel et al. 1982). An adaptive

controller has adjustable parameters and a mechanism for adjusting them. An adaptive control method can continuously monitor its own performance in relation to a given condition and has a means of modifying its own parameters by a closed loop action to approach optimum performance (Wen and Balas 1989; Barkana and Kaufman 1993). In this research, the Simple Adaptive Control Method (SACM), which is a type of direct adaptive control approach, is used to control the structural performance using semi-active devices. SACM is used to optimize the response of an undamaged structure and mitigate the undesirable behavior of a damaged structure subjected to an earthquake. Also, the effectiveness of SACM to control the behavior of the structure with active devices is studied and compared with the performance of the structure controlled with semi-active devices.

Two types of control devices are used to generate the required force to control the performance of the structure using SACM. An ideal active actuator and a hydraulic actuator are chosen as the active devices and the MR damper is selected as a semi-active device (Bitaraf and Barroso 2009; Bitaraf et al. 2010b). Also, a variable friction damper which is a semi-active device is used to improve the performance of the structural systems (Ozbulut et al. 2010; Bitaraf et al. 2010c). Three-story and twenty-story buildings designed for the SAC[1] Phase II project are used in this research to study the effectiveness of SACM in controlling the behavior of the structure subjected to the earthquake. SAC buildings were designed for the Los Angeles region and also utilized

[1] SAC is a joint venture of three nonprofit organizations: The Structural Engineers Association of California (SEAOC), the Applied Technology Council (ATC), and California Universities for Research in Earthquake Engineering (CUREE) (Ohtori et al., 2004).

for the third generation of the control benchmark problem. Both the linear and nonlinear behavior of the structure will be considered in controlling the structural performance using SACM.

1.3. Objectives of the Dissertation

The goal of the proposed work is to develop the Simple Adaptive Control Method (SACM) to enhance the performance of damaged and undamaged structures. The proposed work has the following four objectives:

Objective 1: Develop the Simple Adaptive Control Method to mitigate the undesirable behavior of a damaged structure.

When damage happens to a structure due to earthquakes, strong winds or deterioration, the structure doesn't respond like the undamaged structure with the acceptable performance. Increasing the maximum acceleration of the structure results in reducing its serviceability and increasing the maximum interstory drift causes a safety reduction. The objective is to mitigate the impact of damage on the performance of the damaged structure and to make the damaged structure behave like an undamaged one using the adaptive control method. It is assumed that the undamaged structure responds optimally under external loads.

Objective 2: Develop the Simple Adaptive Control Method to optimize the behavior of the controlled undamaged structure.

Three issues are considered to define a model for Simple Adaptive Control Method to optimize the response of the undamaged structure. The first issue is that the performance of the undamaged structure is not always better than that of the damaged structure and is dependent on the external loadings applied to the structure. Next, it is not always possible to measure the input force to the structure caused by winds or earthquakes. The final issue relates to the limitation of the control devices, such as MR dampers, in generating the required force. Therefore, a model in SACM which always makes the structure exhibit better performance is preferred. By considering all the noted terms, the model for the SACM in this research is defined as a structure having the output in a specific range. The objective is to optimize the response of the structure using the SACM, independent of the characteristics of the external loads.

Objective 3: Develop the Simple Adaptive Control Method to control the response of the structure with nonlinear behavior.

The third objective of this research is to consider the nonlinear behavior of the structure controlled with Simple Adaptive Control Method and study the effectiveness of this control method in controlling the system with nonlinear behavior.

Objective 4: Develop an indirect adaptive control method and compare its result with that of the Simple Adaptive Control Method

Simple Adaptive Control Method is a direct method that doesn't need system identification to update its parameters. For some control methods such as LQR and LQG, control parameters are not updated during the simulation. The objective is to

combine a system identification method with one of these control methods to update the control parameters when a change occurs in the structure, and then compare the response of that controlled structure with the response of the structure controlled with SACM.

1.4. Overview of the Dissertation

The focus of this dissertation is to study the effectiveness of using the Simple Adaptive Control Method to improve the performance of structural systems equipped with active and semi-active control devices.

Section 2 deals with different control algorithms. First, an optimal control and fuzzy logic control method are briefly explained. Then, the Simple Adaptive Control Method (SACM) which is developed to improve the structural response is described. Different reference models which are used in SACM to mitigate the damage impact and optimize the structural response are presented. Simple Adaptive Control for nonlinear problems is studied in this section. Also, Section 2 discusses how SACM can deal with uncertainties.

Section 3 provides background information concerning semi-active and active devices. Characteristics of semi-active devices are briefly explained followed by different dynamic models of MR damper and variable friction device behavior. Active control devices, especially hydraulic actuators, and the dynamic model of their behavior are discussed in Section 3.

Section 4 focuses on Simple Adaptive Control Method to mitigate the undesirable performance of damaged structures. The structure analyzed in this study is a

steel moment resisting frame building (SMRF), three-stories tall, and designed as part of a SAC steel project for the Los Angeles area. The behavior of both damaged and undamaged structures controlled by SACM is studied under three suites of earthquake records, also from the SAC Phase II project, representing three different return periods for the area. It is assumed that the building is equipped with MR dampers and ideal active actuators. The effectiveness of SACM to optimize the structural response of a three-story building is studied in Section 5. The performance of the structure with MR dampers and hydraulic actuators are compared. Also, the performance of SACM is compared with that of LQR and passive systems.

Section 6 compares SACM with other control strategies such as fuzzy logic control, Lyapunov controller, decentralized bang-bang, maximum energy dissipation, clipped-optimal, and modulated homogeneous friction. A numerical example which has been studied by Jansen and Dyke (2000) and Williams (2004) is used for this comparison. The numerical example consists of a six-story building with two MR dampers connected between the ground and first floors and two MR dampers connected between the first and second floors.

The performance of base-isolated structures against near-field earthquakes using a variable friction damper and controlled by SACM is studied in Section 7. Fuzzy logic control is also used to control the structural response of the building and its result is compared with SACM. A total of six historical earthquake records that are commonly used in structural control research are employed as external excitation in the numerical simulations.

Section 8 deals with the effectiveness of SACM in controlling the response of a structure with nonlinear behavior. A twenty-story building from SAC project is used to assess the performance of the Simple Adaptive Control Method in nonlinear problems. It is assumed that 1000 kN MR dampers are located on each level of the building as control devices.

In Section 9, an indirect adaptive control method is developed and its result is compared with that of the Simple Adaptive Control Method, which is a direct adaptive control approach. A probabilistic system identification method using Bayesian theory is used to update the structural parameters during the control process and LQG is utilized to control the performance of the structure equipped with semi-active devices. Finally, Section 10 presents the concluding remarks and potential directions for future work.

2. CONTROL METHODS

Supplemental control devices such as passive, active and semi-active control devices can protect structural systems against natural hazards. In order to utilize the full capabilities of active and semi-active devices employed in a structural system, an effective control algorithm that is practically viable is needed. In this section, the fuzzy logic control and the optimal control method are briefly explained. The Simple Adaptive Control Method (SACM) is studied in Section 2.3.

2.1. Fuzzy Logic Control Method

One of the effective methods to deal with complex nonlinear systems is the fuzzy logic approach. Fuzzy logic describes the relationship between inputs and outputs of a controller using simple verbal statements instead of complicated mathematical terms. Due to its inherent robustness and simplicity, several researchers have used fuzzy logic theory to develop controllers for semi-active devices (Subramaniam et al. 1996; Symans and Kelly 1999; Ahlawat and Ramaswamy 2001; Choi et al. 2004). The design of a fuzzy logic controller (FLC) involves four main steps: (i) fuzzification of variables, which includes the transformation of the crisp inputs to fuzzy variables by defining membership functions to each input, (ii) definition of a rule base that relates the inputs to output by means of if-then rules, (iii) definition of an inference engine that evaluates the rules to produce the system output and (iv) defuzzification, where the output variable that is a fuzzy quantity is transformed to a non-fuzzy discrete value.

The performance of a conventional FLC depends on various controller parameters such as the scaling factors, the membership functions and the rule base. It is especially important for a FLC to have an effective and reliable rule base to perform at the desired level. In order to improve the effectiveness of the controller, an adaptive FLC can be designed by altering each of the parameters. A general architecture of a fuzzy logic controller is given in Figure 2.1.

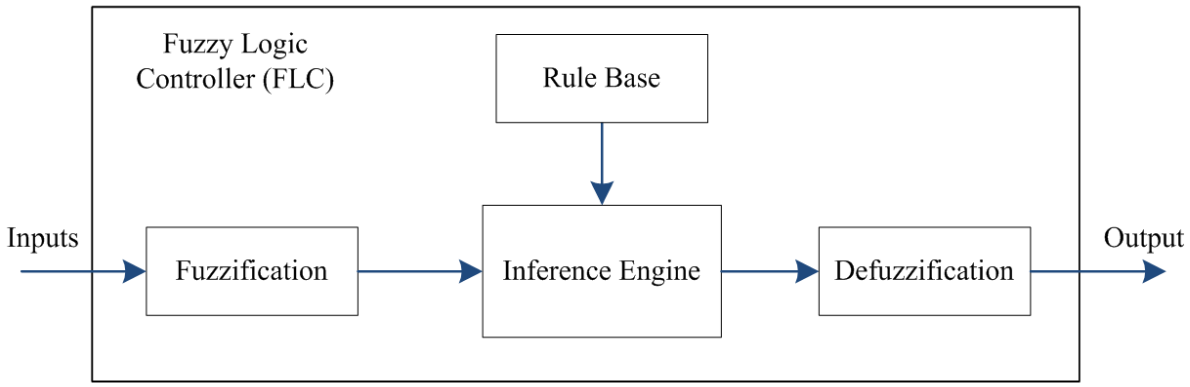

Figure 2.1: General architecture of a fuzzy logic controller.

2.2. Optimal Controller

Linear Quadratic Gaussian (LQG) control is an optimal control which combines a Kalman estimator and a Linear Quadratic Regulator (LQR) (Skogestad and Postlethwaite 2005). Assuming that the dynamic behavior of the controlled system (plant) is modeled in the form of

$$\dot{x}(t) = Ax(t) + Bu(t) + w(t) \tag{2.1}$$

$$y(t) = Cx(t) + v(t)\,, \tag{2.2}$$

where $w(t)$ and $v(t)$ are disturbance and measurement noise, respectively. It is assumed that $w(t)$ and $v(t)$ are zero-mean Gaussian noise. In LQG control design, the control command $u(t)$ is computed by minimizing

$$J_r = \int_0^\infty \left[x^T Q x + u^T R u \right] dt \tag{2.3}$$

where matrices R and Q are referred to as weighting parameters, whose magnitudes are assigned according to the relative importance attached to the state variables and to the control force in minimization procedure. The optimal solution is

$$u(t) = -K\ \hat{x}(t)\ . \tag{2.4}$$

The optimal state estimate $\hat{x}(t)$ is calculated by a Kalman filter to minimize the steady state error covariance. The governing equation of state estimate can be written as,

$$\dot{\hat{x}}(t) = A\hat{x}(t) + Bu(t) + L\left(y(t) - C\hat{x}(t)\right) \tag{2.5}$$

$$\hat{y}(t) = C\hat{x}(t)\,. \tag{2.6}$$

The gain matrices K and L can be calculated by using MATLAB commands “lqr” and “kalman”, respectively. It should be noted that appropriate positive values for matrices Q and R to calculate K, and Q_n and R_n to calculate L must be chosen to get accurate and optimum results.

2.3. Simple Adaptive Control Method (SACM)

An adaptive controller is defined as a controller with adjustable parameters, which enable the adaptive controller to modify its behavior in response to variations in the dynamics of the plant or external disturbances. By continuously comparing its

performance against a desired condition, an adaptive controller can modify its parameters using a closed-loop action to reach a predefined desired behavior. Implementation of an adaptive controller consists of the following steps:

- characterization of the desired behavior of the closed-loop system
- determination of a suitable control law with adjustable parameters
- choosing a mechanism to adjust the parameters
- implementation of the control law

Adaptive control can be divided into two main categories: direct and indirect methods. In the direct method, the identification and control processes are combined into a single system where control gains are determined directly without any explicit identification of the system parameter. In the indirect approach, parameter identification and control are executed separately. Some of the advantages of the direct approach over the indirect method are ease of implementation, speed, and its applicability to multi-input multi-output systems. The Simple Adaptive Control Method (SACM), which is a direct adaptive method is used in this research to control and improve the structural performance.

In SACM, the desired behavior is characterized by a well-defined model. The objective of this method is to force the plant to track the behavior of the model. To make sure that the plant trajectory tracks the model behavior, the system output is compared with the reference model output and necessary parameter adjustments are carried out. The simple adaptive control technique has been successfully applied to various control

problems since 1982 such as flexible structures (Barkana and Kaufman 1993), flight control (Morse and Ossman 1990), power systems (Zhang and Luo 2009), missiles, helicopters (Barkana and Guez 1990) and motor control (Shibata et al. 1996). Sobel, Kaufman and Mabius (1982) introduced the Simple Adaptive Control technique and this method has been developed further by Barkana and Kaufman (1993) and Wen and Balas (1989) to infinite-dimensional systems. This technique can make the performance of the arbitrary system close to the ideal desired performance represented by an ideal model. A system with a large degree of uncertainty in the presence of sudden load changes or with significant variation in its characteristics might benefit from using SACM (Sobel et al. 1982). Yasser et al. (2003; 2007) used SACM with Multiple Neural Networks for SISO and MIMO nonlinear systems.

The simplicity of implementing SACM is specifically appealing to engineers dealing with practical applications. Less demanding conditions in SACM that guarantee asymptotic tracking in comparison with constant controllers in the linear time-invariant (LTI) systems, make this approach superior to constant controllers (Barkana and Kaufman 1993). In particular, asymptotic adaptive tracking with no general LTI tracking solution is possible because the control parameters are fitted to the specific problem by adaptive controllers (Barkana 2005a).

The plant parameters are generally unknown in adaptive methodologies,. Hence, in indirect approaches, both plant parameter identification and control of the plant should be performed separately. In direct methods, the controller parameters are determined directly without explicit plant parameter identification so that the error between plant

and reference model outputs approaches zero. Usually, in SACM, low-order models are used and no observers are needed (Barkana et al. 1991). Furthermore, in most adaptive control techniques, prior knowledge of the controlled plant, such as its order is required but is not readily available (especially in large real systems). In SACM, such prior knowledge is not needed, hence broadening its range of application (Barkana and Kaufman 1993).

Figure 2.2 shows the block diagram of the adaptive control system. In addition to the feedforward of the model states and inputs, the feedback of the error between the plant and model outputs are used in this methodology to control the performance of the controlled system (Barkana 1987).

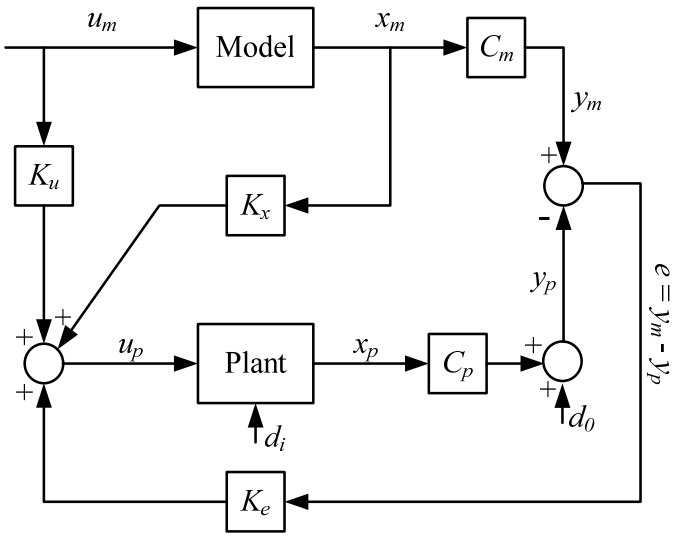

Figure 2.2: Block diagram of adaptive control system.

The governing equations for the plant (the controlled system) and the model (the system with the desired performance) are (Barkana and Kaufman 1993)

$$\dot{x}_p(t) = A_p x_p(t) + B_p u_p(t) + d_i(t) \tag{2.7}$$

$$y_p(t) = C_p x_p(t) + d_0(t) \tag{2.8}$$

$$\dot{x}_m(t) = A_m x_m(t) + B_m u_m(t) \tag{2.9}$$

$$y_m(t) = C_m x_m(t)\,, \tag{2.10}$$

where A_p and A_m are state matrices, B_p and B_m are input matrices and C_p and C_m are output matrices for the plant and the model, respectively. The vectors x_p and x_m are the $n\times1$ plant state vector and $n_m \times1$ model state vector. Also, y_p and y_m denote the plant output vector and the model output vector. The vector u_p is the $m\times1$ input control vector, and u_m is the $m\times1$ input command vector. The plant order is considered to be n, with m inputs and m outputs. The order of the model is n_m, and y_m is an m-order vector. The dimension of the model state may be less than the dimension of the plant state but it should be large enough to create the desired command for the plant. However, the order of model outputs is equal to the order of the plant outputs because y_p tracks y_m. It can be noted that for large structures with large number of states, there is no need to measure all of the states because the order of plant output, m, can be less than the order of the plant state, n. The variables $d_i(t)$ and $d_0(t)$ represent input and output disturbances.

Time-varying adaptive gains are used in the SACM to bring the tracking error to zero. The control command can be calculated by (Barkana and Kaufman 1993).

$$u_p = K(t)\, r(t) \tag{2.11}$$

where

$$K(t) = [K_e(t), K_x(t), K_u(t)] = K_I(t) + K_P(t) \tag{2.12}$$

and

$$r^{\mathrm{T}}(t) = [\, y_m - y_p \quad x_m^{\mathrm{T}}(t) \quad u_m^{\mathrm{T}}(t) \,]. \tag{2.13}$$

The overall gain $K(t)$ is the sum of the integral gain $K_I(t)$ and proportional gain $K_p(t)$ which can be calculated from (Barkana and Kaufman 1993)

$$\dot{K}_I(t) = (y_m(t) - y_p(t))\; r^{\mathrm{T}}(t)\; T - \sigma\, K_I(t) \tag{2.14}$$

$$K_p(t) = (y_m(t) - y_p(t))\; r^{\mathrm{T}}(t)\; \overline{T}\,. \tag{2.15}$$

The scale matrices T and $\overline{T}$ are selected to be positive definite matrices and can control the rate of adaptation. The rate of convergence of the error between the plant and model outputs to zero can be increased by the proportional gain, while the integral gain is required for the stability and tracking of the system. The coefficient σ in Equation (2.14) is used to prevent the integral gain from reaching very high values or diverging in the presence of the disturbance and it can be extremely small (Barkana 2005a).

The stability and robustness issues of SACM were studied by Barkana (2005a). The prior principal condition for asymptotic stability of the adaptive systems is to have a strictly positive real (SPR) plant (Barkana 2005b). If a controlled plant and its transfer function are almost strictly passive (ASP) and almost strictly positive real (ASPR), respectively, then the system would be SPR. If an unreal, unknown constant output feedback gain that is not needed for implementation can stabilize the LTI plant and make it SPR, the LTI plant and its transfer function are called ASP and ASPR, respectively. The ASPR condition guarantees the convergence with the various system identification methods so the plant knowledge level can be upgraded. It can be shown that the ASPR property is the only condition required to guarantee asymptotically perfect tracking with Simple Adaptive Control (Barkana 2005b). However, in reality, most of the plants might

not be ASPR. The ASPR condition could be satisfied by using various forms of parallel feedforward configuration (PFC) (Barkana 1987) or a structural decomposition method (Dosho and Ohmori 1997). It should be noted that the additional output term presented by PFC has to be small in order to have the performance of the actual system close enough to the desired performance. Some basic knowledge like a frequency response plot or an experimental test can be used to test the ASPR properties of the plant and build the proper parallel feedforward configuration to ensure a safe and robust strategy.

Definition 1: A linear time-invariant system with a state space realization (Equation (2.7) and (2.8)) is called "Strictly Passive (SP)" and its transfer function "Strictly Positive Real (SPR)" if there exist two positive definite symmetric (PDS) matrices, *P* and *Q*, such that the following two relations are simultaneously satisfied:

$$PA + A^T P = -Q \tag{2.16}$$

$$PB = C^T . \tag{2.17}$$

Definition 2: A linear time-invariant system with a state space realization (Equation (2.7) and (2.8)) is called "Almost Strictly Passive (ASP)" or "Almost Strictly Positive Real (ASPR)" if there exists a constant output feedback gain, $\tilde{K}_e$ (unknown and not needed for implementation), such that the closed loop system with the system matrix

$$A_K = A - B\tilde{K}_e C \ , \tag{2.18}$$

is SPR. It is known that any minimum-phase system with positive definite symmetric *CB* is ASPR (Barkana 2008). The required symmetry of *CB* is not always satisfied in practice. Barkana et al. (2006) managed to eliminate the symmetry condition of *CB* and showed that the properties of ASPR system can be extended to a new class of systems

called W-ASPR. It can be simply summarized that any minimum-phase LTI systems $\{A,B,C\}$ is ASPR if the product of two matrices B and C (BC) is Positive Definite Symmetric (PDS).

Definition 3: A linear time-invariant system with a state space realization (Equation (2.7) and (2.8)) is called "W-Almost Strictly Passive (WASP)" if there exist three PDS matrices, P, Q and W and a positive definite gain $\tilde{K}_e$ such that the following two conditions are simultaneously satisfied:

$$P(A - B\tilde{K}_e C) + (A - B\tilde{K}_e C)^T P = -Q \tag{2.19}$$

$$PB = C^T W^T . \tag{2.20}$$

2.3. 1. Simple Adaptive Control Method to Mitigate Damage

When damage happens to a structure as a result of earthquakes, strong winds or deterioration, the structure doesn't respond the same way as an undamaged structure with acceptable performance. Figures 2.3 and 2.4 show the difference between the response of the damaged and undamaged three-story structures under the earthquake LA23 (from SAC Phase II Project). 25% stiffness reduction in the columns of the first story of the SAC building is assumed as the potential damage. As shown in these figures, the maximum displacement, drift and acceleration increase when damage occurs in the structure.

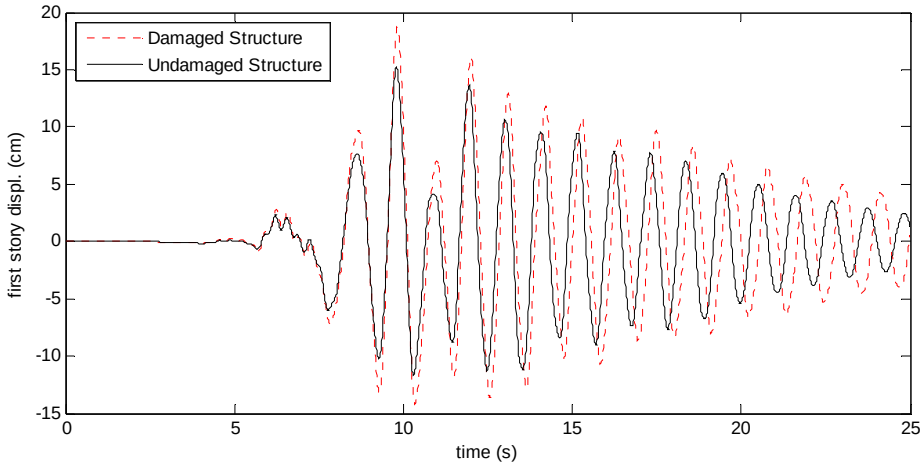

Figure 2.3: First story displacement for the undamaged and damaged structures subjected to earthquake LA23.

An increase in the maximum acceleration of the structure results in a reduction in serviceability and a rise in the maximum inter-story drift causes a safety reduction. SACM can be used to mitigate the impact of the damage on the performance of the damaged structure and make the damaged structure behave like an undamaged structure. To achieve this goal, the reference model of SACM, that behaves desirably, is defined as the undamaged structure. Therefore, the characteristics of the undamaged structure such as stiffness, mass and damping should be known. Additionally, the external load applied to the structure must be known to calculate the response of the undamaged structure. It should be noted that this method can be used to mitigate the damage impact if the damage is not very large and does not cause collapse in the structure. It is obvious that nothing can prevent the damaged structure from collapsing if the percentage of damage is substantial.

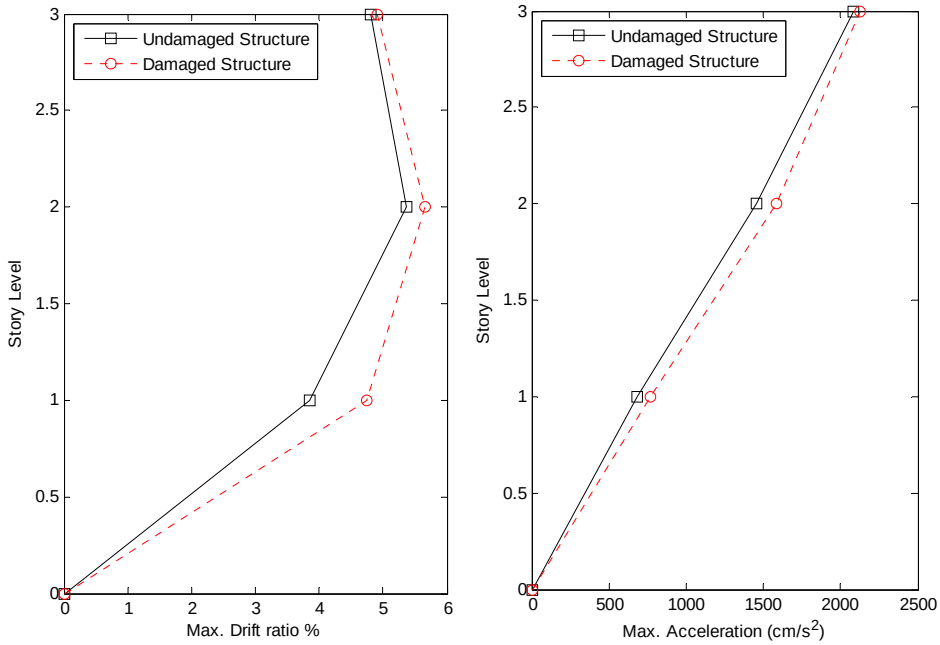

Figure 2.4: Maximum drift ratio and acceleration for the undamaged and damaged 3-story building subjected to earthquake LA24.

Mitigating the damage impact in this study means preventing the structure having large drift or acceleration and forcing the damaged structure to behave like an undamaged structure. Therefore, as damage occurs in the structure and does not cause its collapse, mitigating the damage by the means of active and semi-active control methods could prevent further harm, while helping keep the building residents calm and providing them more time to escape the building.

2.3.2. Simple Adaptive Control Method to Optimize Structural Performance

To define the model with the desired behavior for controlling the performance of the structure, three issues should be considered. The first issue is that it is not always possible to measure the input force to the structure caused by winds or earthquakes.

Besides, the behavior of the model should always outperform the behavior of the controlled system and it should not depend on the input of the structure. Figures 2.5 and 2.6 show the deformation and acceleration response spectrums of an earthquake from the SAC project (LA10). It is assumed that 25% stiffness reduction is the potential damage occurred in columns of the first story of the SAC building. It is shown that the damaged structure displacement and acceleration would be smaller than the undamaged structure response for some earthquakes.

Another important issue to consider is the limitation of control devices. For example, there are upper and lower limits on the amount of force produced by MR dampers and they are also energy-dissipating devices. Taking these factors into account helps designers to better develop the control system and have realistic expectations of results.

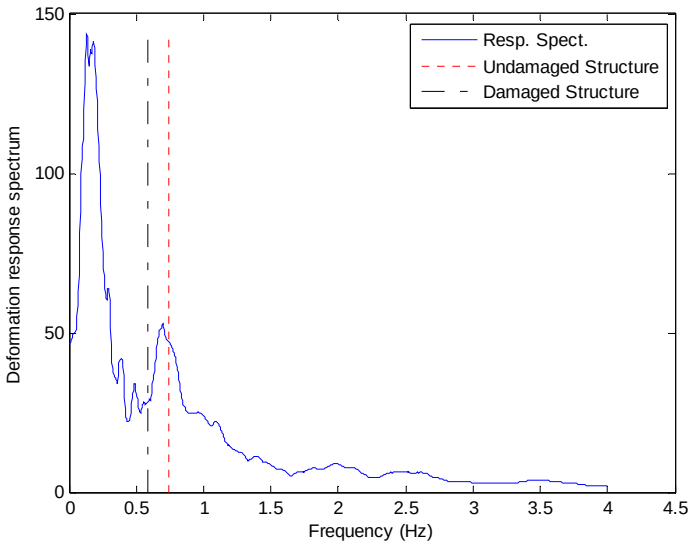

Figure 2.5: Deformation response spectrum (LA10).

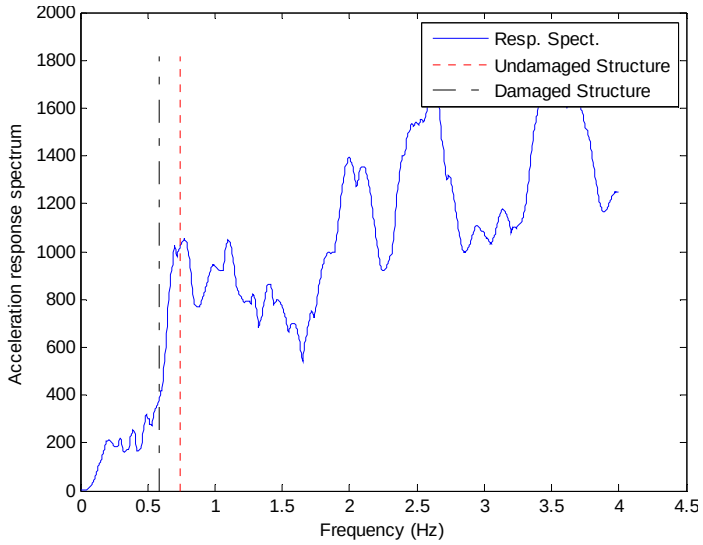

Figure 2.6: Acceleration response spectrum (LA10).

By considering all the noted terms, the model for the SACM in this research is defined as a structure having the output in a specific range, which is explained by

$$y_m = y_p \qquad if \left| y_p \right| < Y_{\max} \tag{2.21}$$

$$y_m = Y_{\max} \qquad if \left| y_p \right| \geq Y_{\max}, \tag{2.22}$$

where $Y_{\max}$ is the vector of the maximum acceptable value for the model output. In this model, it is assumed that all values less than $Y_{\max}$ are acceptable for the model output. Specifically, if the output of the system is less than the $Y_{\max}$, the error between the plant and model output is equal to zero, and if the output of the system is greater than $Y_{\max}$, the goal of the adaptive control method is to decrease the error and make the plant output fall in the range defined by $Y_{\max}$.

Once the model for SACM is defined as described above there is no need to know the input force applied to the structure. It is guaranteed that the SACM never increases the response of the controlled system with respect to the uncontrolled system

and it is not dependent on the characteristics of the input of the controlled system. Finally, it can be seen that the model explained by equations (2.21) and (2.22) fits well in the framework of SAC method to control the structure equipped with the MR damper considering its limitations.

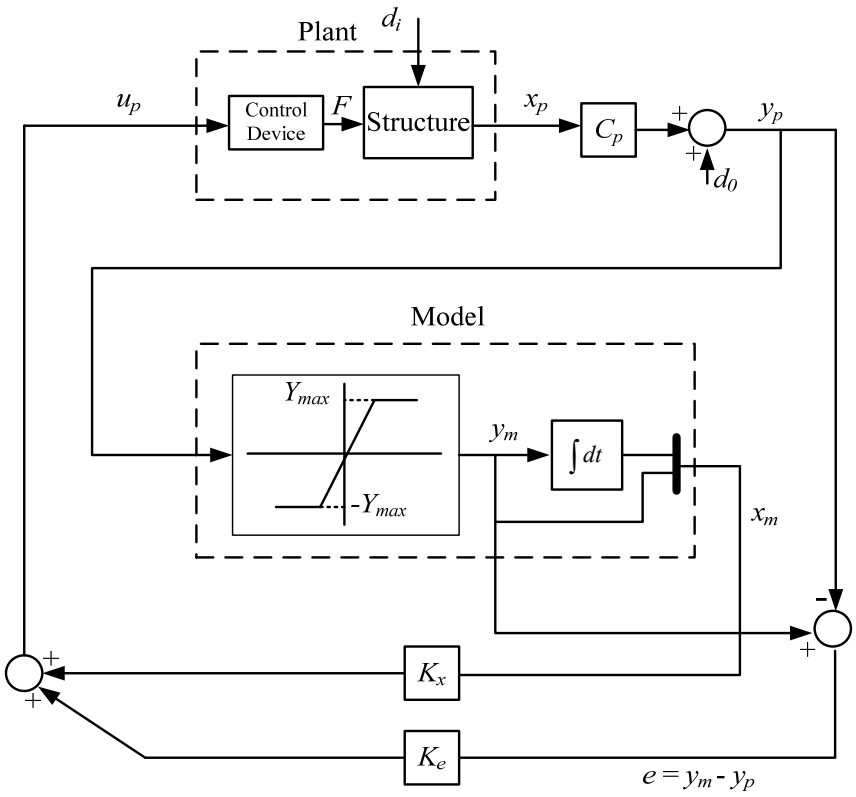

Figure 2.7: Block diagram for SACM to optimize structural performance.

The value for the parameter Y_{max} could be any value equal to or greater than zero. In this study, the minimum values for the drift and displacement can be achieved by choosing Y_{max} equal to zero. However, it should be noted that if Y_{max} is set equal to zero, the values obtained for acceleration response of the structure may not be in the acceptable range. Therefore, selecting the optimum value of Y_{max} depends on the goal of

the study. Also, the input command u_m is assumed to be zero and the model state vector can be calculated from the output model as

$$x_m = \begin{bmatrix} X_m \\ \dot{X}_m \end{bmatrix} = \begin{bmatrix} \int \dot{X}_m \, dt \\ \dot{X}_m \end{bmatrix} = \begin{bmatrix} \int y_m \, dt \\ y_m \end{bmatrix}, \tag{2.23}$$

where X_m and $\dot{X}_m$ are displacement and velocity of the model system. Figure 2.7 shows the block diagram for the SACM if the model is defined in a way to optimize the performance of the structure.

2.3.3. Simple Adaptive Control Method for Nonlinear Problem

As mentioned before, SACM evaluates the system behavior by comparing the system output and the model output, and its goal is to match the response of the controlled system (plant) with the reference model. The equations, which represent the dynamic behavior of a nonlinear plant in state-space form, are (Barkana and Guez 1990)

$$\dot{x}_p(t) = A_p(x_p)x_p(t) + B_p(x_p)u_p(t) + d_i(x_p, t) \tag{2.24}$$

$$y_p(t) = C_p(x_p)x_p(t) + D_p(x_p)u_p(t) + d_0(x_p, t)\,. \tag{2.25}$$

Nonlinearities in structural responses can be result of nonlinearities in the behavior of structure materials. The output of the plant is required to follow the output of the model, which is

$$\dot{x}_m(t) = A_m(x_m)x_m(t) + B_m(x_m)u_m(t) \tag{2.26}$$

$$y_m(t) = C_m(x_m)x_m(t) + D_m(x_m)u_m(t)\,. \tag{2.27}$$

Equations (2.24) and (2.25) show the general nonlinear form of the model but the reference model in SACM can be chosen as a linear time-invariant model. The control command u_p can be calculated in the same way as calculated for the linear system which is explained by equations (2.11) through (2.15) (Figure 2.8). The controlled system is called strictly casual if $D_p(x_p)$ is equal to zero. The parallel term, $D_p(x_p)$, can be very small and may not affect the controlled plant output but it can substantially change the stability properties of the plant. The stability of ASP plant is guaranteed by SACM on the presence of input commands and input or output disturbances (Barkana and Guez 1990).

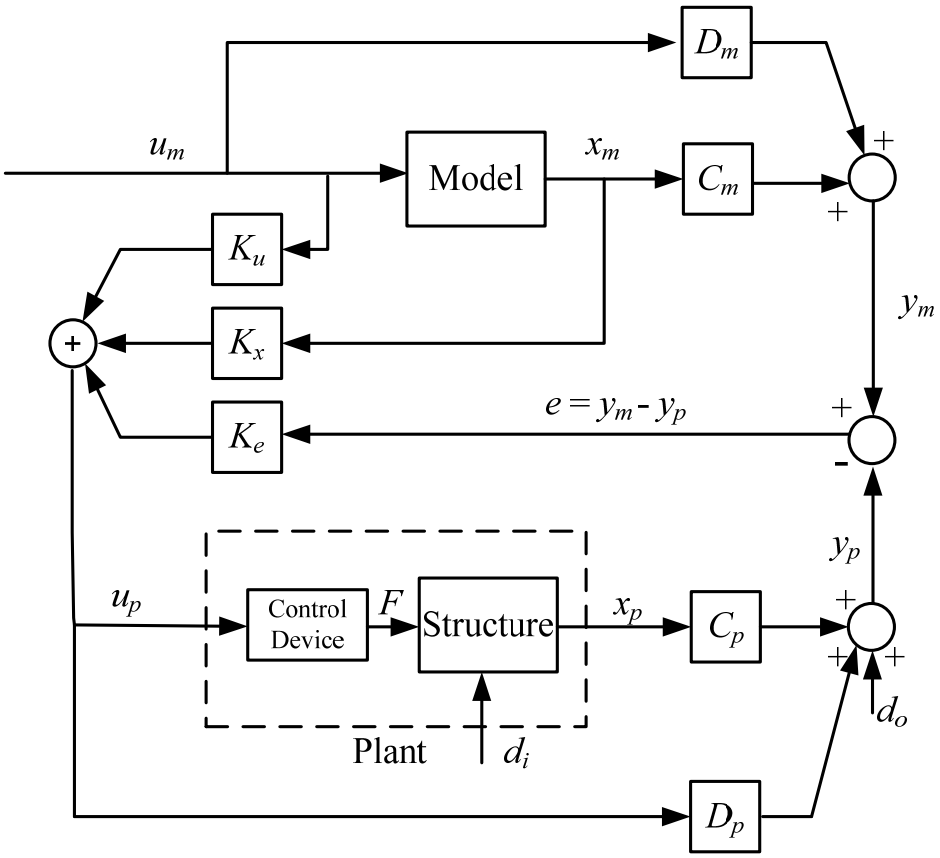

Figure 2.8: Block diagram of adaptive control system for nonlinear problem.

2.3.4. How Can Simple Adaptive Control Method Deal with Uncertainties?

Uncertainties can be aleatory or epistemic. Aleatory uncertainties are inherent in nature and cannot be reduced during the system identification, damage detection methods or control processes. Contrary to aleatory uncertainties, epistemic uncertainties can be reduced and influenced by the observer or the manner of observation (Gardoni et al. 2002).

Different types of uncertainties which have to be accounted in system identification processes or damage detection methods can be enumerated as model errors, measurement errors, statistical uncertainty (Gardoni et al. 2002) and low sensitivity to parameters variation (Vanik 1997).

2.3.4.1. Model Errors

Model error may be caused by using an inaccurate or simplified model form instead of using the accurate one. For example, if a linear model is used to model a system with nonlinear behavior, a model error will arise. This type of error is epistemic uncertainty and can be reduced by using a more exact model. In addition, it is possible that some variables in the model form are missing which is an aleatory uncertainty.

2.3.4.2. Measurement Errors

The model parameters can be updated by comparing the model predictions with measurements of the actual system response. But there are always some errors in

measured data due to the types and locations of sensors. This type of uncertainty is epistemic and can be reduced by using measurement devices with higher accuracy and sensitivity.

2.3.4.3. Statistical Uncertainty

If the amount of data gathered for estimation of the model parameters is not adequate, statistical uncertainty will arise. This type of uncertainty is epistemic because it can be reduced by using a larger amount of data.

2.3.4.4. Low Sensitivity to Parameters Variation

It is possible that the objective function chosen for system identification or damage detection methods is more sensitive to some parameters of the model than other parameters. Therefore, variation of low sensitive parameters may not cause a significant change in the chosen objective function and the model parameters may not be updated properly or the damage cannot be detected.

To consider all the mentioned uncertainties in system identification or damage detection methods, different probabilistic methods have been used by many researchers. The effects of epistemic uncertainties are compensated by using such probabilistic methods and the results are satisfactory.

As mentioned before, SACM is a direct adaptive method which does not need explicit system identification or observation, and control parameters are modified

automatically during the control process. In the direct adaptive method, the identification and control functions are merged into one scheme and control gains are computed directly. Therefore, SACM has the ability to cope with the internal uncertainties and environmental uncertainties and there is no need to worry about the existence of different errors. In the process of the SACM, there is no model error because the reference model is a system with desired behavior which is defined by researchers and the response of the plant is just measured and there is no need to model the behavior of the plant (controlled system). The performance of SACM in the presence of measurement noise is evaluated by some examples (Section 5) and results show that SACM can be effective in improving the structural performance even in the presence of damage or measurement noise.

3. CONTROL DEVICES

Over the past several decades, civil engineers have been using active, semi-active and passive control devices to mitigate the effects of the dynamic loads on the structures. Active control devices (Kerber et al. 2007) are adaptive to any change in the characteristics of structure or external loads, but their stability problems, reliability and large power requirements are still major concerns to engineers. In contrast, passive control devices are reliable but with low adaptability. The semi-active devices are alternative approaches to protect the structures against external loadings such as wind and earthquakes. In this section, characteristics of active and semi-active control devices are briefly explained and different models of dynamic behavior of those control devices are described.

3.1. Semi-Active Control Devices

Semi-active devices can offer the reliability of passive devices and versatility and adaptability of active devices (Gaul et al. 2008). Semi-active devices cannot inherently make the structure unstable. They only need a small amount of external power to be operated. Many semi-active control devices such as stiffness control devices, electrorheological (ER) fluid dampers, magnetorheological (MR) dampers, friction control devices, and fluid viscous dampers have been used to protect civil structures against seismic loads. In this part, two types of semi-active devices, MR dampers and variable friction devices are studied.

3.1.1. Magnetorheological (MR) Dampers

Magnetorheological (MR) dampers are one of the promising semi-active. MR dampers are capable of generating controllable damping forces by using MR fluids. When the magnetic field is applied to the fluid, particles dispersing in the fluid would be aligned, particle chains form and the fluid changes from a free-flowing, linear viscous fluid to a semi-solid and shows viscoplastic behavior in a few milliseconds (Figure 3.1). MR dampers are efficient for vibration suppression in many applications because of their mechanical simplicity, high dynamic range, low power requirements, large force capacity and their high stability, robustness and reliability. Furthermore, they are relatively inexpensive to manufacture and maintain and are insensitive to temperature changes so they can be used for indoor and outdoor applications. They offer rapid variation in damping properties because they have the ability to reversibly change from free-flowing, linear viscous liquids to semisolids having controllable yield strength in milliseconds when exposed to a magnetic field (Jung et al. 2004).

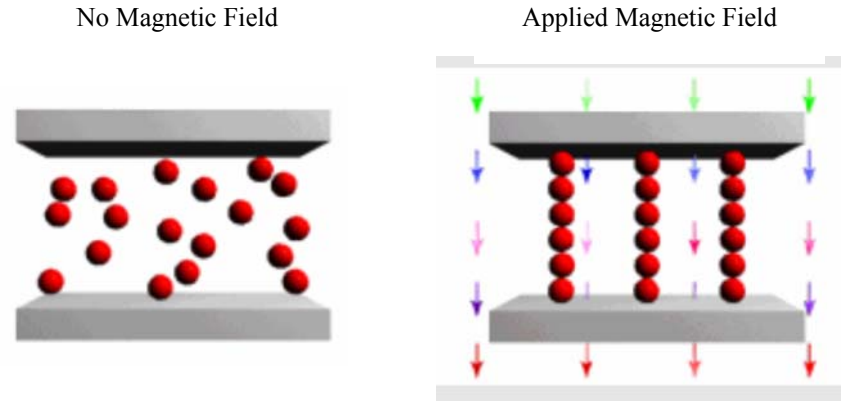

Figure 3.1: Chain-like structures formation in the MR fluid under applied magnetic field (LORD Corporation).

A schematic of the prototype 20-ton large-scale MR fluid damper is shown in Figure 3.2. Due to the mentioned characteristics of MR dampers, they are considered good candidates for reducing the structural vibrations and have been studied by a number of researchers for seismic protection of civil structures (Dyke et al. 1996b; Spencer et al. 1997; Sahasrabudhe and Nagarajaiah 2005a; Jung et al. 2006; Shook et al. 2008).

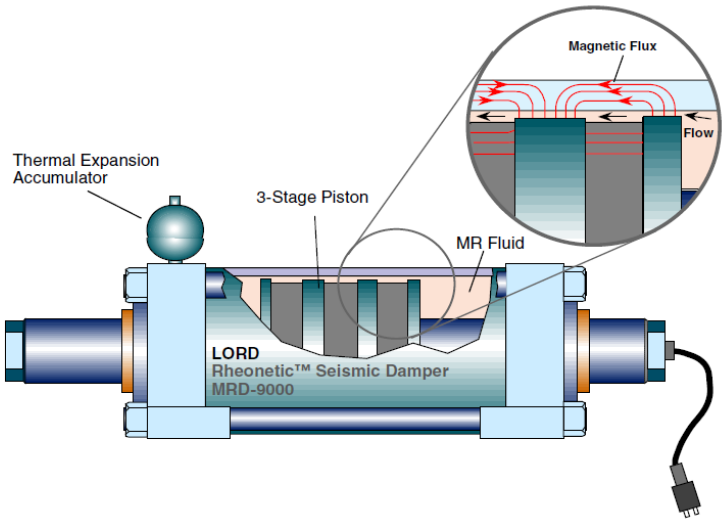

Figure 3.2: Schematic of the prototype 20-ton large-scale MR fluid damper (LORD Corporation).

Because of the inherent nonlinear behavior of MR dampers, modeling their dynamic behavior is a primary challenge. There are two types of dynamic models for the MR dampers: nonparametric models and parametric models. Many nonparametric models have been used to control the dynamic behavior of the MR dampers such as neural network-based models (Chang and Roschke 1998; Wang and Liao 2005) and fuzzy logic-based models (Kim et al. 2008). The Bingham model (Lee and Wereley 2002), nonlinear hysteretic bi-viscous model (Kamath and Wereley 1997), hyperbolic

tangent model (Christenson et al. 2008) and Bouc-Wen hysteresis model (Jansen and Dyke 2000) are some of the parametric models that have been used to model the behavior of MR dampers.

The Bingham model is usually used to design MR dampers because of its simplicity and ease of implementation. However, the fluid's elastic properties at small deformations and low shear rates cannot be described and the observed nonlinear force-velocity response cannot be reproduced by this model (Jung et al. 2004). The nonlinear hysteretic bi-viscous model can predict the MR damper behavior very well, but to meet the practical requirements, it is essential that more extensive research be carried out on this model (Jung et al. 2004). The hyperbolic tangent model can capture the nonlinear force response of large-scale MR dampers but its equations are more complicated than those of other proposed models.

To characterize the behavior of a MR fluid damper, Spencer et al. (1997) introduced the simple Bouc-Wen model. This model can predict the force-displacement and force-velocity behavior well, and results obtained from this model are similar to the experimental data (Spencer et al. 1997). The simple Bouc-Wen model cannot capture the force roll-off when the acceleration and velocity have opposite signs and the magnitude of the velocities is small; so, to overcome this drawback, Spencer et al. (1997) proposed a modified version of the Bouc-Wen model. The accuracy of the modified Bouc-Wen model is very high, but the governing equations are more complicated; also, solving the equations is more time consuming and expensive. To model the MR damper behavior,

both the simple and modified Bouc-Wen models are used in this paper and are described below.

3.1.1.1. Bingham Model

One of the most popular dynamic models for the behavior of MR dampers is the Bingham model. Stanway et al. (1987) suggested the Bingham model to predict the behavior of Electrorheological (ER) fluids, and Spencer et al. (1997) adopted Bingham model for MR dampers. The schematic of the Bingham model is shown in Figure (3.3). In the Bingham model, the force generated by the MR damper is given by

$$f = f_y \operatorname{sgn}(\dot{x}) + c_0 \dot{x} \tag{3.1}$$

$$f_y = f_{ya} + f_{yb} u \tag{3.2}$$

$$c_0 = c_{0a} + c_{0b} u \,, \tag{3.3}$$

where f_y is the yield force, c_0 is the damping coefficient, and $\dot{x}$ is the velocity of the damper. Equations (3.2) and (3.3) show that the parameters f_y and c_0 are functions of applied voltage u.

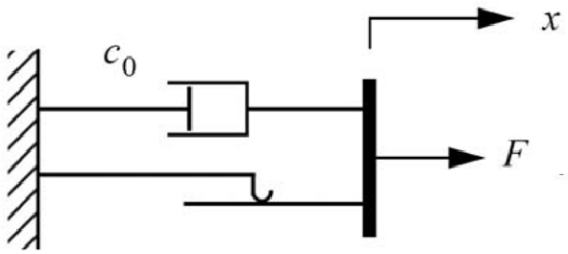

Figure 3.3: Bingham Model of the MR Damper (Jung et al. 2004).

3.1.1.2 Simple Bouc-Wen Model

Figure 3.4 shows the simple mechanical model for the MR dampers based on the Bouc-Wen hysteresis model. The governing equation for the behavior of MR dampers is (Jansen and Dyke 2000)

$$f = c_0 \dot{x} + \alpha z , \tag{3.4}$$

where f and $\dot{x}$ are the MR damper force and velocity, respectively; c_0 is the viscous damping at large velocities. The evolutionary variable z describing the hysteretic behavior of MR dampers is governed by

$$\dot{z} = -\gamma |\dot{x}| z |z|^{n-1} - \beta \dot{x} |z|^n + A \dot{x} , \tag{3.5}$$

where γ, β, n, and A are adjustable shape parameters of the hysteresis loops for the yielding element in the MR damper (Kim et al. 2008). The model parameters of the MR damper governing equation α and c_0 are functions of the applied voltage v (Jansen and Dyke 2000)

$$\alpha = \alpha_a + \alpha_b u \tag{3.6}$$

$$c_0 = c_{0a} + c_{0b} u \tag{3.7}$$

$$\dot{u} = -\eta (u - v) , \tag{3.8}$$

where u and v are the input and output voltages of the first-order filter and η is the time constant of the first order filter. The variables α_a, α_b, c_{0a} and c_{0b} are parameters that account for the dependence of the MR damper force on voltages applied to the current driver and the resulting magnetic current (Spencer et al. 1997). To find the required MR damper voltage that produces the forces calculated from the adaptive control method, the

inverse model of the MR damper is used. The voltage and force are related together in the inverse model by

$$z \cong \text{sign}(\dot{x})\left(\frac{A}{\gamma+\beta}\right)^{1/n} \tag{3.9}$$

$$u = \frac{f - c_{0a}\dot{x} - \alpha_a z}{c_{0b}\dot{x} + \alpha_b z} \tag{3.10}$$

$$v = u + \frac{\dot{u}}{\eta}\ , \tag{3.11}$$

assuming that the evolutionary variable z can be approximated as its ultimate hysteretic strength (Tse and Chang 2004).

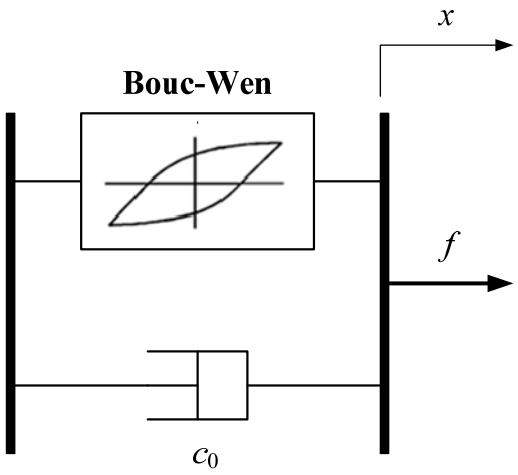

Figure 3.4: Simple Bouc-Wen model of the MR damper (Jung et al. 2004).

3.1.1.3. Modified Bouc-Wen Model

The schematic of the MR damper mechanical model for the modified Bouc-Wen model is shown in Figure 3.5. The force produced by the MR damper is calculated by (Yang et al. 2002)

$$F = \alpha z + c_0(\dot{x} - \dot{y}) + k_0(x - y) + k_1(x - x_0) = c_1\dot{y} + k_1(x - x_0). \tag{3.12}$$

The parameters z and y are defined as

$$y = \frac{1}{c_0 + c_1}\left\{\alpha z + c_0\dot{x} + k_0(x - y)\right\} \tag{3.13}$$

and

$$\dot{z} = -\gamma|\dot{x} - \dot{y}|z|z|^{n-1} - \beta(\dot{x} - \dot{y})|z|^n + A(\dot{x} - \dot{y}), \tag{3.14}$$

where k_0 and c_0 are the stiffness and viscous damping at large velocities. The variable c_1 is the viscous damping for low velocities and k_1 is the accumulator stiffness. For large scale MR dampers, it is assumed that the parameters α, c_0 and c_1 are functions of the input current i in the form of a third-order polynomial (Yang et al. 2002)

$$\alpha(i) = 16566i^3 - 87071i^2 + 168326i + 15114 \tag{3.15}$$

$$c_0(i) = 437097\,i^3 + 1545407\,i^2 + 1641376\,i + 457741 \tag{3.16}$$

$$c_1(i) = -9363108\,i^3 + 5334183\,i^2 + 48788640\,i - 2791630. \tag{3.17}$$

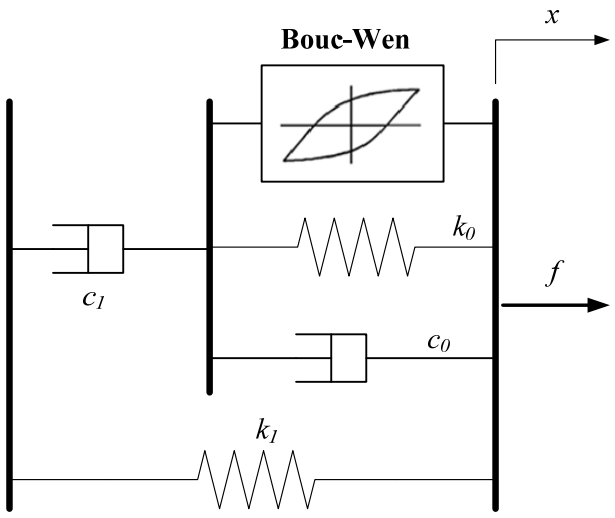

Figure 3.5: Modified Bouc-Wen model of the MR Damper (Jung et al. 2004).

As mentioned before, the inverse model should be used to calculate the required current for producing the desired force F by the MR damper. Tsang et al. (2006) showed how the required current i can be calculated assuming that stiffnesses are negligible and the variable z can be approximated as its ultimate hysteretic strength

$$i(t) = -\frac{2}{3}\ln\left[1 - \frac{-|F| + |\tilde{F}_\eta|}{1.5\times 10^5}\right] \tag{3.18}$$

$$\tilde{F}_\eta(t) = \frac{c_0(t-\Delta t)\,c_1(t-\Delta t)}{c_0(t-\Delta t) + c_1(t-\Delta t)}\dot{x}(t)\,. \tag{3.19}$$

The current and force units in Equations (3.12) through (3.18) are A and N. The parameters for dynamic behavior of a large-scale 200 kN MR damper for the simple Bouc-Wen model (equations (3.3) to (3.8)) are listed in Table 3.1, adopted from Spencer et al. (2002) and Yang (2002). Because some of the values of the simple Bouc-Wen model parameters could not be obtained directly from these references, the least squares method (Crassidis and Junkins 2004) is used to modify the parameters' values. Some values for the force are generated using the equations from the modified Bouc-Wen model (Yang et al. 2002); then, the best value for the parameters c_{0a}, c_{0b}, α_a, α_b are calculated using the general least squares method to minimize the error between the simple Bouc-Wen model and the modified Bouc-Wen model.

Table 3.1: 200 kN MR dampers parameters for simple Bouc-Wen model.

Parameter	Value	Parameter	Value
c_{0a}	137460 (Ns/m)	β	100.1 (m^{-1})
c_{0b}	12553 (Ns/mV)	A	833.45
α_a	103690 (N/m)	n	2.39832
α_b	4904 (N/mV)	η	31.4 (s^{-1})
Γ	3819.4 (m^{-1})		

Table 3.2: 200 kN MR damper parameters for modified Bouc-Wen model.

Parameter	Value	Parameter	Value
k_0	137810 (N/m)	β	647.46 (m^{-1})
x_0	0.18 (m)	A	2679 (m^{-1})
k_1	617.31 (N/m)	n	10
Γ	647.46 (m^{-1})	η	31.4 (s^{-1})

Table 3.3: 1000 kN MR dampers parameters for simple Bouc-Wen model (Yoshida and Dyke, 2005).

Parameter	Value	Parameter	Value
c_{0a}	4.4×10^2 Ns/m	β	300 m^{-1}
c_{0b}	4.4×10^3 Ns/mV	A	1.2
α_a	1.0872×10^7 N/m	n	1
α_b	4.9615×10^7 N/mV	η	50 s^{-1}
γ	300 m^{-1}	V_{max}	10 V

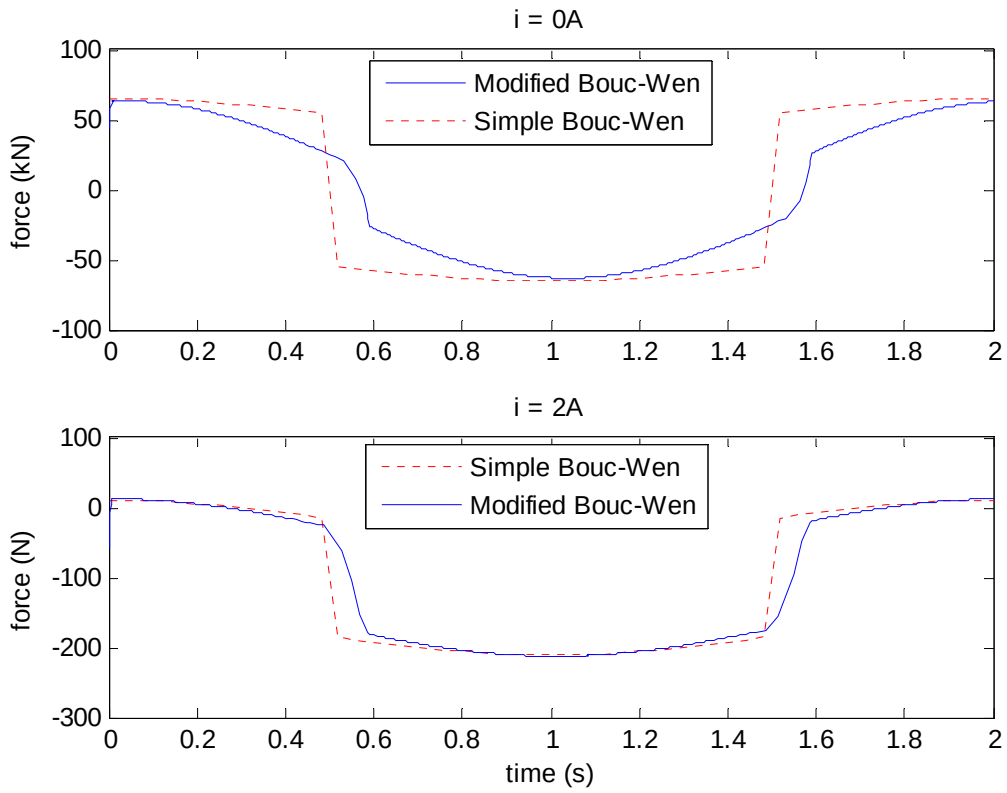

Figure 3.6: Comparison of the MR damper behavior using modified and simple Bouc-Wen model.

The MR damper forces are generated under a sinusoidal displacement excitation with 2.54 cm (1 inch) amplitude and 0.5 Hz. Each MR damper can produce a force equal to 200 kN. Figure 3.6 illustrates the comparison between the large scale MR damper behavior modeled with the modified Bouc-Wen model and the simple Bouc-Wen model. It shows that the simple Bouc-Wen model is acceptable for modeling the MR damper in the simulation files. The MR damper parameters for the modified Bouc-Wen model are presented in Table 3.2.

3.1.1. Variable Friction Device

Over the past few years, friction dampers have been widely investigated as an energy dissipation system to reduce the structural response due to dynamic loading (Cheryy and Filiatrault 1993; Gaul and Nitsche 2001; Gaul et al. 2008). A typical passive friction damper consists of two solid bodies that slide over each other to develop friction, which absorbs energy. As it is the case for other passive devices, the passive friction dampers cannot adjust the slip force in real-time according to the structural response. When the contact force is very large, the damper will not dissipate energy for moderate and weak ground motions since it may not slide. On the other hand, when the contact force is reduced, the damper will have small energy dissipation capacity under strong earthquakes due to its small sliding friction force. Therefore, a controllable normal force is favorable in order to ensure the required amount of energy dissipation for various levels of ground motions. A variable friction damper enables the adaptation of the contact force by an actuator and can effectively suppress the vibrations of a

structure. Several variable friction dampers have been conceptually investigated and some have been implemented (Kannan and Uras 1995; Hirai et al. 1996; Morita et al. 2001; Narasimhan and Nagarajaiah 2006).

In this study, the variable friction damper investigated experimentally and analytically by Lu and Lin (2009) is adopted in numerical simulations (Figure 3.7). This damper employs a piezoelectric actuator to provide a controllable contact force. The friction force of the variable damper is proportional to the normal contact force and the friction coefficient between the friction pad and friction bar of the damper. The contact force of the damper is given as

$$N(t) = N_{pre} + C_{pz}V(t) \tag{3.20}$$

where *N(t)* is the total normal contact force, N_{pre} represents constant preload, C_{pz} is the piezoelectric coefficient of the piezoelectric actuator, and *V(t)* is the applied voltage on the stack actuator. Then, the friction force of the semi-active damper, *f(t)*, is given by

$$f(t) = m\,N(t)\,\mathrm{sgn}(\dot{x}) \qquad \text{if } \dot{x} \neq 0 \tag{3.21}$$

$$-\mu\,N(t) \le f(t) \le \mu\,N(t) \qquad \text{if } \dot{x} = 0 \tag{3.22}$$

where μ is friction coefficient of the damper and $\mathrm{sgn}(\dot{x})$ denotes the sign of the slip rate of the damper. The parameters N_{pre}, C_{pz}, and μ are given as 1000 N, 1.10 N/V and 0.2, respectively. Also, the maximum driving voltage is 1000 V.

During the motion of a structure, a friction damper has two possible states: sticking and slipping phases. A combination of stick and slip phases describes the complete state of the friction force. In the slip phase, the sliding velocity is nonzero and the friction force can be computed by equation (3.21). In the stick phase, the two friction plates are

stuck together, i.e., the sliding velocity equals to zero. The absolute value of the friction force in the sticking phase, f_s, can be approximated for numerical analyses as

$$f_s = \left| f_i + f_r \right| \quad \text{when } \left| f \right| \geq f_s \text{ and } \dot{x} = 0 \tag{3.23}$$

where f_i is the inertial force applied on the mass, and f_r is the restoring force provided by structural stiffness. For a base-isolated building where variable friction dampers are installed between the first floor and the ground, the approximate values of f_i and f_r are given as $f_i = m_t \ddot{u}_g(t)$ and $f_r = k_b x_b(t)$, where m_t is the total mass of the structure, k_b is the isolator stiffness and x_b is the relative displacement of the base isolators (He et al. 2003).

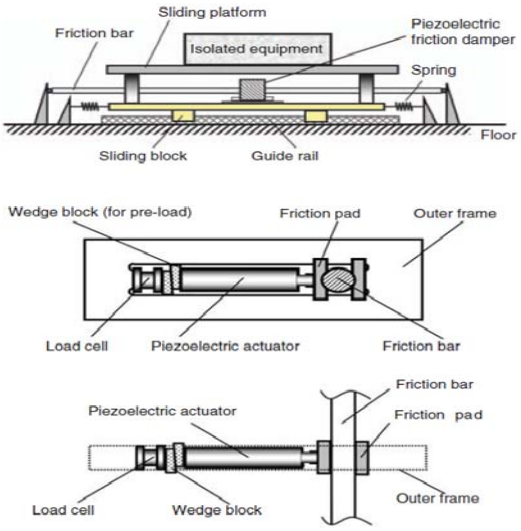

Figure 3.7: Schematic diagram of the piezoelectric smart isolation system and its components (Lu and Lin 2009).

3.2. Active Control Devices

Active control systems are adaptable to any change that may occur in the structure. They can both add and dissipate energy in the structure. Thus, they may make the structure unstable. There are two types of active control systems that have attracted a

lot of interest; the active tuned mass damper and the active tendon system. A typical control device in these active control systems is a hydraulic actuator.

3.2.1. Hydraulic Actuator

Hydraulic actuators can generate very high forces at very high power level. Two important components of a hydraulic actuator are the servo-valve and the actuator (Figures 3.8). An electrical command signal is converted to spool displacement by the servo-valve which results in oil flow into the actuator chamber to enable the motion of the actuator piston (Sivaselvan et al. 2008).

(a)

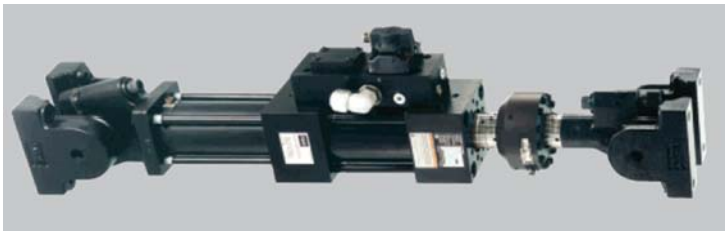

(b)

Figure 3.8: Two important components of a hydraulic actuator, (a) Servo-valve, (b) Actuator (www.mts.com).

3.2.1.1. Dynamic Model of Hydraulic Actuator

The dynamic behavior of the servo-valve can be defined as (DeSilva 1989)

$$q = k_q u_v - k_c \frac{f}{A_{HA}}, \tag{3.24}$$

which is a linearized flow model of the servo-valve. The flow rate and valve input are presented by the variables q and u_v, respectively. The parameters k_q, k_c and A_{HA} are referred to as the flow gain, the flow pressure coefficient, and the cross-sectional area of the actuator, respectively. The variable f is the force generated by the actuator. The dynamic actuator pressure is given by

$$q = A_{HA}\dot{x} + \frac{V_t}{4\beta A_{HA}}\dot{f}\ , \tag{3.25}$$

where β is the bulk modulus of the fluid, V_t is the total chamber volume of the actuator, and $\dot{x}$ is the actuator velocity (Spencer et al. 1999).

By combining and rewriting equations (3.24) and (3.27), the hydraulic actuator equation can be defined as (Dyke et al. 1995)

$$\dot{f} = \frac{4\beta A_{HA} k_q}{V_t}u_v - \frac{4\beta {A_{HA}}^2}{V_t}\dot{x} + \frac{4\beta k_c}{V_t}f = \alpha_1 u_v - \alpha_2 \dot{x} + \alpha_3 f \tag{3.26}$$

$$\dot{f} = \alpha_1 u_v - \alpha_2 \dot{x} + \alpha_3 f \tag{3.27}$$

$$\alpha_1 = \frac{4\beta A_{HA} k_q}{V_t} \tag{3.28}$$

$$\alpha_2 = \frac{4\beta {A_{HA}}^2}{V_t} \tag{3.29}$$

$$\alpha_3 = \frac{4\beta k_c}{V_t}. \tag{3.30}$$

Equation (3.26) shows that to model the dynamic behavior of the hydraulic actuator, a differential equation has to be added to the equations of motion of the controlled structure.

4. SIMPLE ADAPTIVE CONTROL TO MITIGATE DAMAGE IMPACT ON STRUCTURAL RESPONSE

In this section, the undesired response of a 3-story building in the presence of damage is mitigated using SACM. The goal of the adaptive control method in Section 4 is to force the damaged structure to behave like an undamaged structure that has an acceptable performance. This method is used to calculate the required forces for improving the performances of the structures. It is assumed that the undamaged structure responds optimally under external loads and as such the goal is to achieve this optimal behavior. This section focuses on steel moment resisting frames, specifically SAC[2] Phase II structures for the Los Angeles region that are also utilized for the third generation structural control benchmark problem (Barroso et al. 2002), and three types of possible designs: (1) original design with no supplemental control; (2) structure with supplemental active devices governed by an adaptive active control strategy; (3) structure with supplemental semi-active dampers controlled by an adaptive control strategy. Simulations of these systems, both controlled and uncontrolled, are prepared using the three suites of earthquake records from the SAC Phase II project, representing three different return periods for the area.

[2] SAC is a joint venture of three nonprofit organizations: The Structural Engineers Association of California (SEAOC), the Applied Technology Council (ATC), and California Universities for Research in Earthquake Engineering (CUREE) (Ohtori et al., 2004).

4.1. Description of Numerical Example (3-Story Building)

To evaluate the efficiency of the adaptive control strategy for its use with MR dampers, an example is considered in which a model of a three story building is controlled with two MR dampers at each story under several ground motions. Two MR dampers are connected between the ground and first floor, two MR dampers are connected between the first and second floors and two MR dampers are connected between the second and third floors.

The structure analyzed in this study is a steel moment resisting frame building (SMRF), 3-stories tall, and designed as part of a SAC steel project for the Los Angeles area. The building is an office building designed for gravity, wind and seismic loads. As shown in Figure 4.1, the North-South frame of the 3-story structure has three fully moment-resisting bays and one simply connected bay. The floor plan of the structure is shown in Figure 4.2. The mass of the ground, first, and second floors is 9.56×10^5 kg (65.6 kip-s^2/ft) each, and the mass of the roof (3^{rd} floor) is 10.5×10^5 kg (71 kip-s^2/ft). Half of the mass of the structure is considered to be seismically effective for each of the perimeter moment resisting frames in the weak direction. The structure is modeled using two dimensional frames that represent half of the structure in the north-south direction, and it is assumed that the model of the structure has a Rayleigh damping with 2% damping ratio for the first two modes. The schematic diagram of the MR damper implementation in the 3-story building is shown in Figure 4.1.

Three suites of earthquake records with different probability of exceedence, 2% in 50 years, 10% in 50 years and 50% in 50 years, are applied to the SAC building to

study the performance of the structure. The basic characteristics of the LA ground motion records that are used in the analysis of the structure are shown in Table 4.1. Figure 4.3 shows the acceleration time history of those ground motion records.

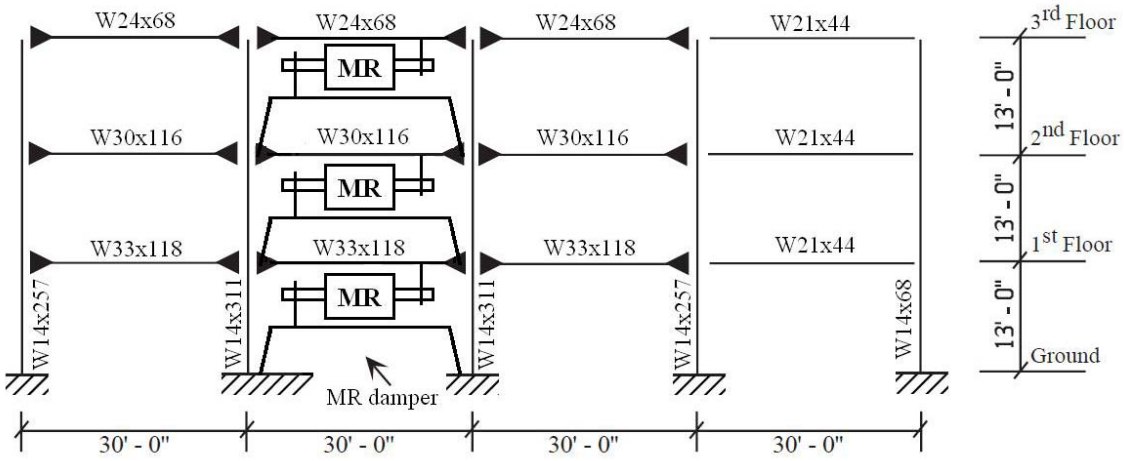

Figure 4.1: 3-story North-South moment resisting frame of SAC building with MR dampers.

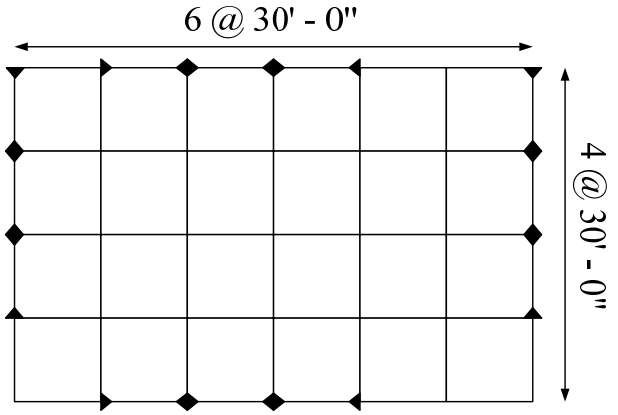

Figure 4.2: Floor plan of the 3-story building.

Table 4.1: Basic characteristics of LA ground motion record.

SAC Name	Probability of exceedence	Record	Earthquake Magnitude	Distance (km)	Duration (s)	PGA (cm/s^2)
LA01	10% in 50 years	Imperial Valley, 1940, El Centro	6.9	10	39.38	452.03
LA23	2% in 50 years	1989 Loma Prieta	7	3.5	24.99	409.95
LA44	50% in 50 years	Imperial Valley, 1979	6.5	1.2	39.08	109.45

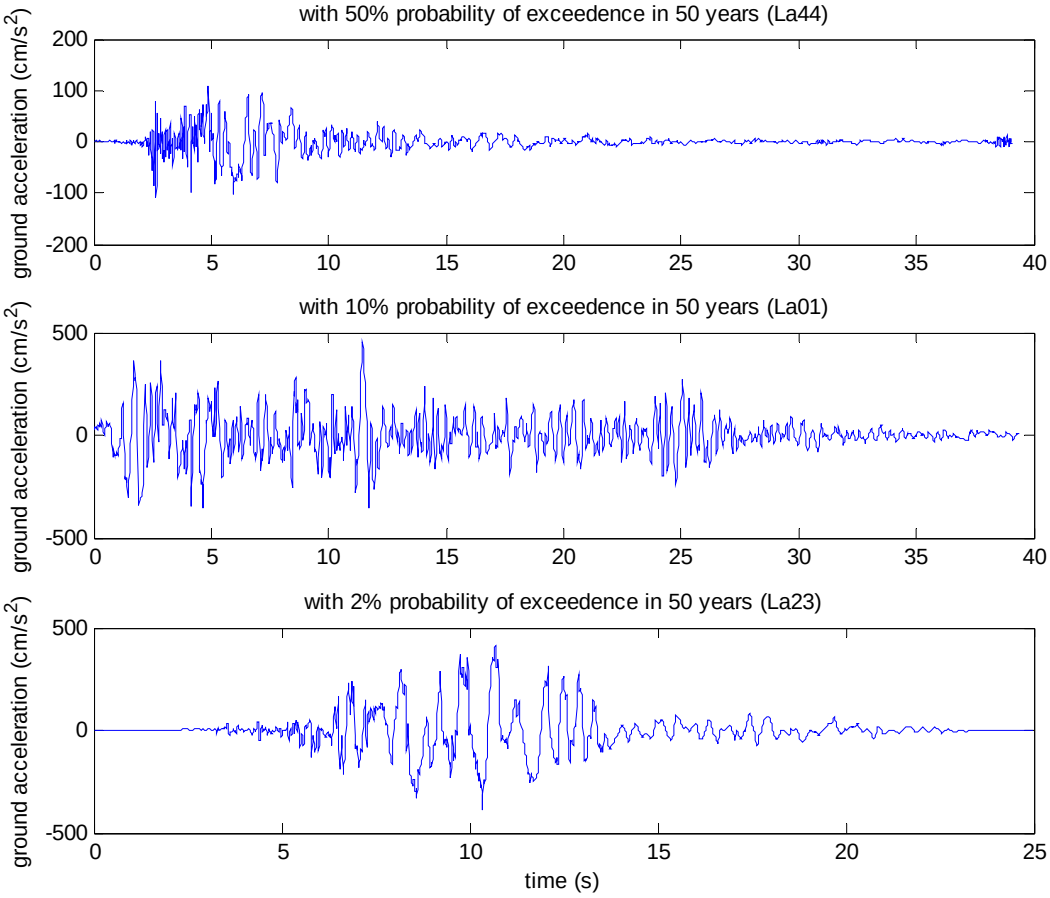

Figure 4.3: Acceleration-time-history of ground motions with different probability of exceedence.

To simulate potential damage during a seismic event, it is assumed that 10%, 25% or 50% stiffness reduction occurred in the first, second or third story of the building. The goal is to make the damaged structure behave like the undamaged building using adaptive control. The plant refers to the damaged SAC building and the model is the undamaged SAC building. To calculate the response of the undamaged structure under earthquake loading, it is assumed that a sensor is located on the ground floor of the controlled structure which can measure the ground acceleration. Also, the characteristics of the undamaged structure such as the stiffness matrix, mass matrix and damping are known. Therefore, the behavior of the undamaged structure can be calculated using the specifications of the undamaged structure and the excitation applied to the structure.

In this simulation the matrices A_p, A_m, B_p and B_m (for the SACM) are defined as

$$A_p = \begin{bmatrix} 0 & I \\ -M_P^{-1}K_P & -M_P^{-1}C_{dP} \end{bmatrix} \tag{4.1}$$

$$A_m = \begin{bmatrix} 0 & I \\ -M_m^{-1}K_m & -M_m^{-1}C_{dm} \end{bmatrix} \tag{4.2}$$

$$B_p = B_m = \begin{bmatrix} 0 \\ I \end{bmatrix}, \tag{4.3}$$

where M_P and M_m are the mass matrices, K_P and K_m are the stiffness matrices, and C_{dP} and C_{dm} are the damping matrices for the plant and the model, respectively.

The mass and stiffness matrices of half of the undamaged 3-story building are

$$M_{und} = \left(\frac{10^5}{2}\right)\begin{bmatrix} 9.56 & 0 & 0 \\ 0 & 9.56 & 0 \\ 0 & 0 & 10.5 \end{bmatrix}(kg), \tag{4.4}$$

and

$$K_{und} = 10^8 \times \begin{bmatrix} 3.7281 & -2.0298 & 0.3512 \\ -2.0298 & 2.7478 & -1.1457 \\ 0.3512 & -1.1457 & 0.8383 \end{bmatrix} (N/m) . \quad (4.5)$$

It is assumed that the story velocities are the outputs of the plant and the model, y_p and y_m, where the former is measured by sensors, so the plant and the model outputs are of 3rd order. Since the sensors measuring the velocities are usually more expensive than the sensors measuring the accelerations, acceleration of each story could be measured by some common sensors and velocities would be calculated using the acceleration data.

The goal of the adaptive control method, forcing the controlled system to follow the response of the system with desired behavior, would be achievable if the controlled system is controllable. Observability of a system shows that the internal states of the system can be inferred by knowledge of its external outputs. The controllability and observability of the system with the governing equation represented by Equation (2.7) and (2.8) is checked using the Gilbert Method (Gilbert 1963). If it is assumed that matrix P is the matrix of eigenvectors of the matrix A_p, then matrix P can diagonalize A_p,

$$P^{-1} A_p P = \text{diag}\{\lambda_1, \lambda_2, ..., \lambda_6\} = \Lambda , \quad (4.6)$$

where Λ is the diagonal matrix of the eigenvalues of A_p.

The controllability and observability of the system can be assessed by calculating two matrices $P^{-1}B_p$ and C_pP, respectively. There will be an element of x_p which is unaffected by any of the inputs, u_p if all elements of any row of $P^{-1}B_p$ are zero. In this

case, there will be state variables that cannot be controlled by the inputs. Each mode of the system can be independently controlled and the system is controllable if none of the rows of the matrix $P^{-1}B_p$ has all zero elements. Existence of any column in C_pP with all of its elements equal to zero will result in an unobservable system and there will be an element of x_p which does not affect any element of the output.

In the studied case, the matrix $P^{-1}B_p$ has no zero rows, therefore the system is controllable. By assuming that there is one sensor at each story to measure the response of the controlled structure, it can be concluded that the system is observable because matrix C_pP has no columns which are zero.

Equation (4.7) shows how the control command u_p and MR damper forces are related together,

$$u_p(t) = \begin{bmatrix} 1 & -1 & 0 \\ 0 & 1 & -1 \\ 0 & 0 & 1 \end{bmatrix} \begin{bmatrix} F_1(t) \\ F_2(t) \\ F_3(t) \end{bmatrix}, \tag{4.7}$$

where $F_1(t)$, $F_2(t)$ and $F_3(t)$ are the total forces generated by the MR dampers connected between the ground and first floor, the MR dampers connected between the first and second floors and the MR dampers connected between the second and third floors. At each time step, the value of the control command u_p is calculated by the adaptive control method, and then the required MR damper forces and the needed voltage to generate these forces are obtained using Equation (4.7) and the equations of the inverse method for the simple or modified Bouc-Wen model, respectively. It should be mentioned that the control force provided by the MR dampers is a function of the relative responses between two successive stories and the input voltage. The relative displacements and

velocities of the stories are calculated using the outputs of the controlled structure, and then, the MR damper forces are obtained by Equations (3.4) and (3.5) for the simple and the modified Bouc-Wen model, respectively. To find the optimum value for the adaptive parameters, an impulse input is applied to the plant and the model in the simulation file, and responses of the structure and model are calculated for several different values of σ, T and $\overline{T}$. Figure 4.4 illustrates how accurately the plant response can track the model response using different values of σ. Considering the results of Table 4.2 and Figure 4.4, the value of σ, T and $\overline{T}$ are chosen to be 0.1, 1000 and 1000, respectively. The error indicated in Figure 4.4 and Table 4.2 is defined as:

$$error = \frac{\sum \left| \text{response}_{\text{plant}} - \text{response}_{\text{model}} \right|}{\sum \left| \text{response}_{\text{model}} \right|} \times 100\% \tag{4.8}$$

Table 4.2: First story displacement error when an impulse input is applied to the system for different values of T.

T	100 $I_{12\times12}$	1000 $I_{12\times12}$	10000 $I_{12\times12}$	100000 $I_{12\times12}$
error %	9.67	2.99	0.94	0.05368

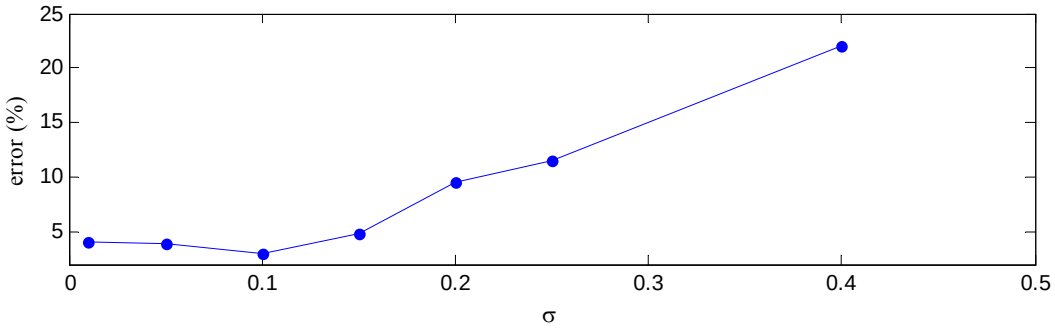

Figure 4.4: First story displacement error respect to σ when an impulse input is applied to the system.

4.2. Results and Discussions

In this section, the performance of the three-story building controlled by SACM and equipped with ideal active devices is studied. Also, the structural response of the building equipped with MR dampers and controlled by SACM is presented and compared with response of the building controlled with ideal active devices.

4.2.1 Ideal Active Device

First, to prove that the SACM is fully capable of mitigating the damage impact on structural response, ideal active devices (as a theoretical example) are used as control devices. It is assumed that the structure is controlled with the ideal active devices located at each story without any limitation in producing the force. The first, second and third story displacements of the controlled damaged structure, the model (undamaged structure) and the uncontrolled damaged structure subjected to the earthquake load (LA01) are shown in Figures 4.5 to 4.7. The figures show that the controlled structure with 50% stiffness reduction in the first story can track the model response very well. The errors obtained from Equation (4.8) for the first, second and third story displacements are 0.1102%, 0.0071% and 0.0007%, respectively.

Tables 4.3, 4.4 and 4.5 show the error between the controlled structure response with different percentages of damage at different locations and the undamaged structure response under different ground motion. e1, e2 and e3 are displacement errors and e4, e5 and e6 are velocity errors for 1st, 2nd and 3rd story, respectively. The results from different ground motion records indicate that the adaptive control strategy is very

effective as the behavior of the controlled structure with ideal active devices is very close to the behavior of the model (undamaged structure).

4.2.2. MR Damper

For the results presented by Figures 4.5 to 4.7 and Tables 4.3 to 4.5, it is assumed that ideal active actuators which can produce any needed force without any limitation are used in the structure. When semi-active devices such as MR dampers are used to control the structure, inherent limitations of these devices in producing the forces should be considered. The restriction of the MR dampers is that there is an upper and lower limit on the force produced (Tsang et al. 2006). As a result of this constraint, MR dampers cannot produce the exact forces calculated by adaptive control method.

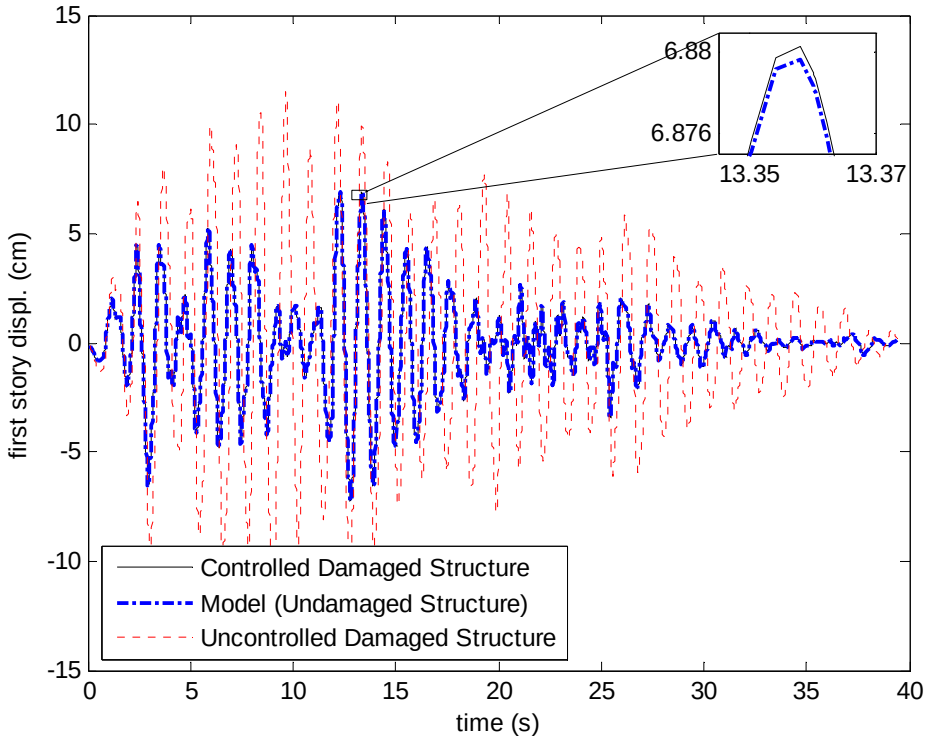

Figure 4.5: First story displacement for the structure (with 50% damage in the 1st story) subjected to earthquake LA01 and controlled by ideal active devices.

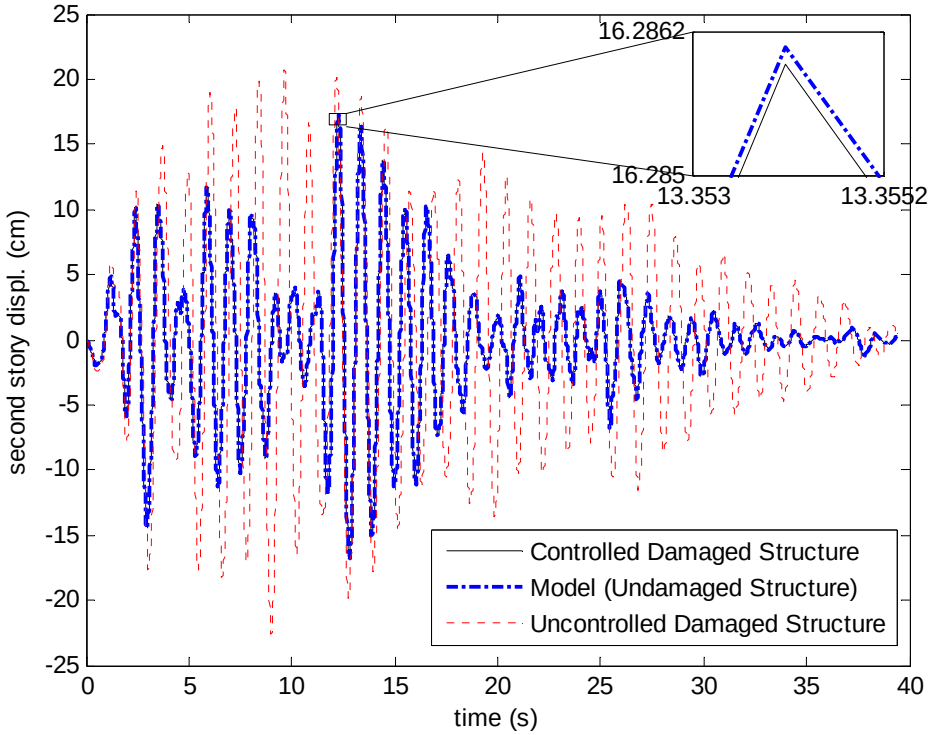

Figure 4.6: Second story displacement for the structure (with 50% damage in the 1st story) subjected to earthquake LA01 and controlled by ideal active devices.

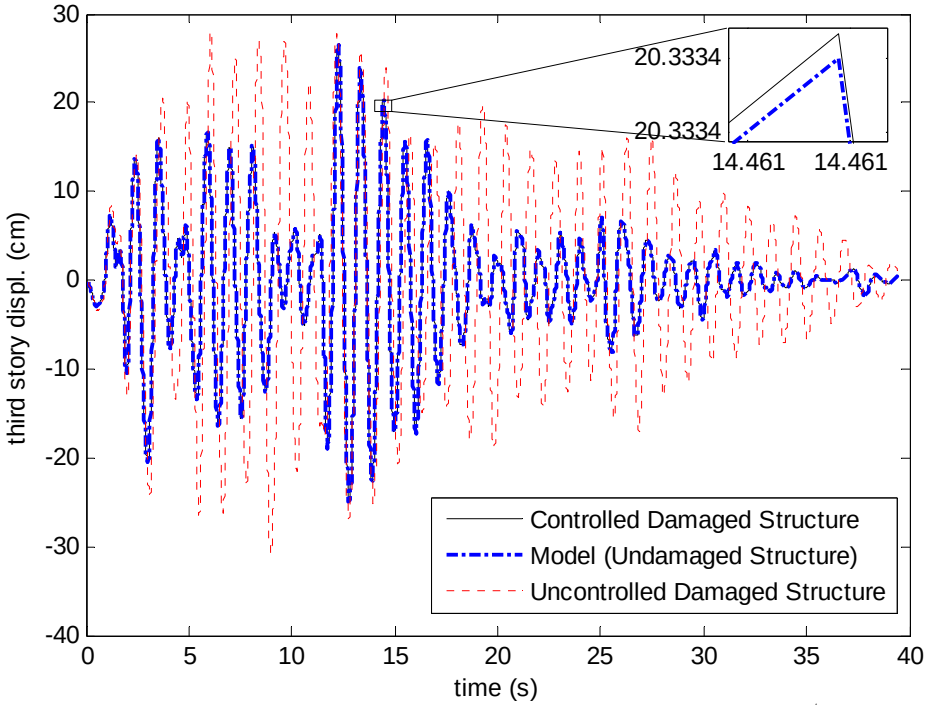

Figure 4.7: Third story displacement for the structure (with 50% damage in the 1st story) subjected to earthquake LA01 and controlled by ideal active devices.

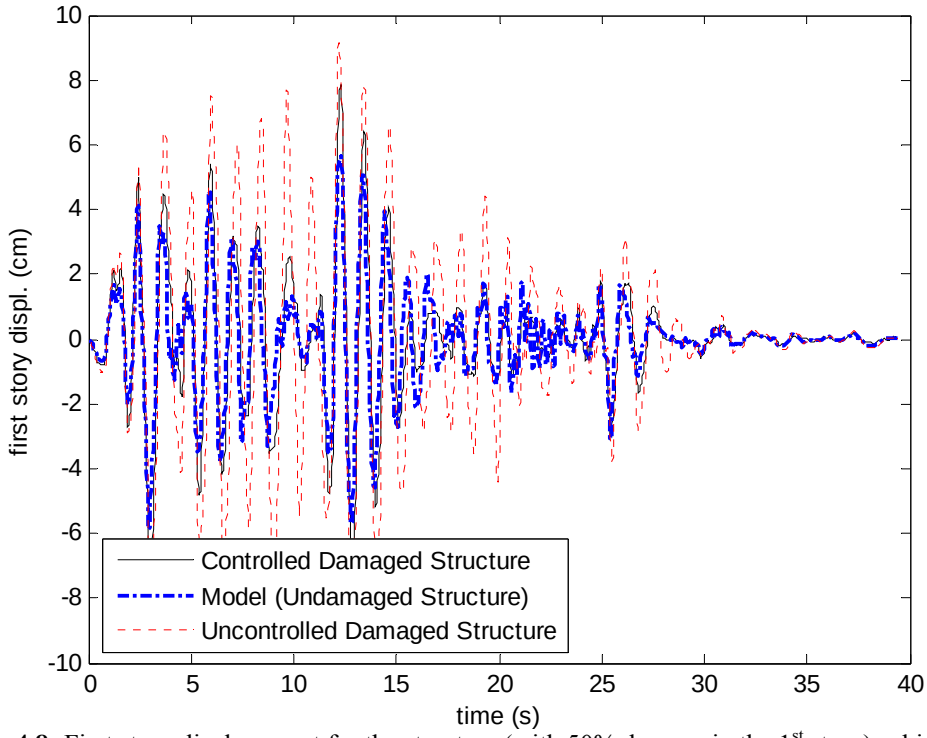

Figure 4.8: First story displacement for the structure (with 50% damage in the 1st story) subjected to earthquake LA01 and controlled by MR dampers with Simple Bouc-Wen Model.

The first story displacement of the damaged structure controlled by the MR damper modeled with the simple and modified Bouc-Wen model subjected to earthquake LA01 is shown in Figures 4.8 and 4.9. It is found that the MR damper modeled with the modified Bouc-Wen model can improve the behavior of the structure more than the MR damper modeled with the simple Bouc-Wen model. Therefore, the result of the simulations for different percentages of damage and several locations of damage are only done for the structure controlled by the MR damper modeled with the modified Bouc-Wen model.

Figures 4.10 and 4.11 illustrate the second and third story displacement for the controlled damaged structure compared with the uncontrolled damaged structure and undamaged structure. As shown in Figures 4.9 to 4.11 the behavior of the controlled

structure with MR dampers is better than the uncontrolled damaged structure and uncontrolled undamaged structures. The figures show that by using two MR dampers at each story, the performance of the structure is close to the performance of the undamaged structure and the controlled system can track the behavior of the model acceptably. The results show that this control method is a suitable method for controlling the structure with MR dampers.

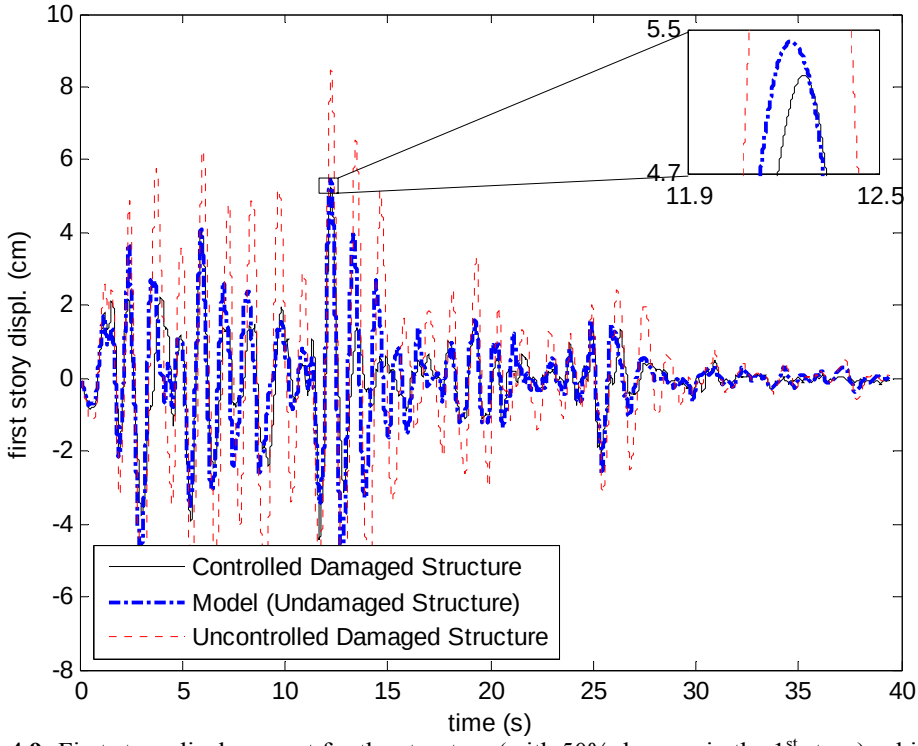

Figure 4.9: First story displacement for the structure (with 50% damage in the 1st story) subjected to earthquake LA01 and controlled by MR dampers with Modified Bouc-Wen Model.

Table 4.6 represents the maximum drift ratio of the controlled and uncontrolled damaged structure and undamaged structure subjected to earthquake LA01 using MR dampers as controllers and assuming different percentages of damage at different locations. Tables 4.7 and 4.8 show the same results when earthquakes LA23 and LA44

are applied to the structure. In all the cases, the maximum drift ratio of the controlled damaged structure is less than or equal to the undamaged structure's drift ratio and the uncontrolled damaged structure's drift ratio. Figures 4.5 to 4.7 and 4.9 to 4.11 show that the response of the undamaged structure (model) when MR dampers are used is different from the undamaged structure response when active devices are used. The reason is that the MR damper is a semi-active device and it always has the passive effect on the structure when no power is used to activate the active part of the MR damper.

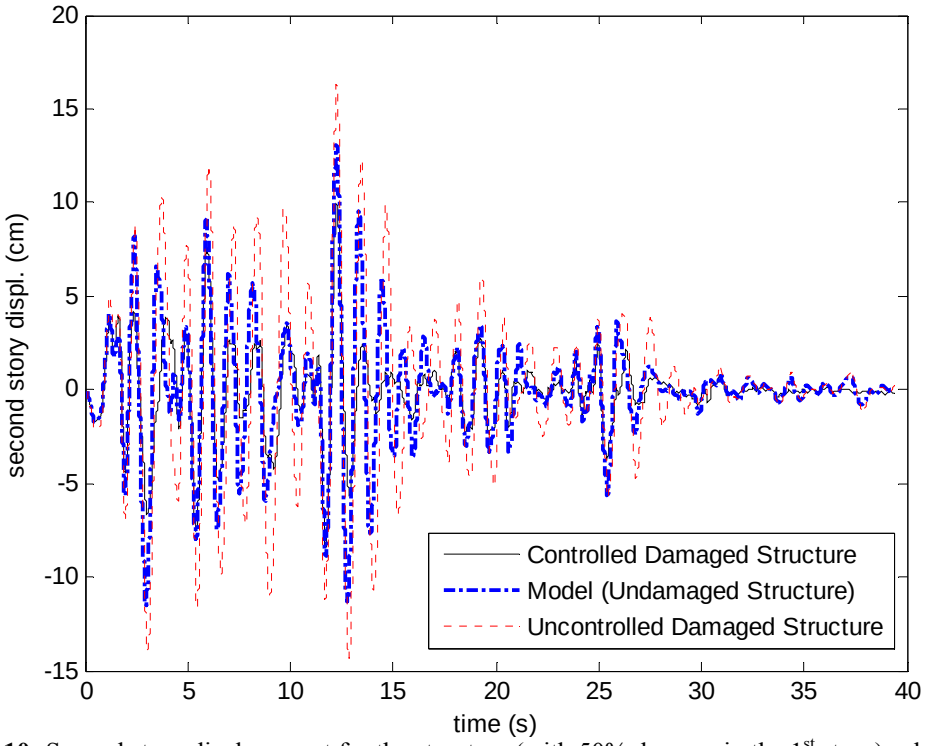

Figure 4.10: Second story displacement for the structure (with 50% damage in the 1st story) subjected to the earthquake LA01 and controlled by MR dampers with modified Bouc-Wen model.

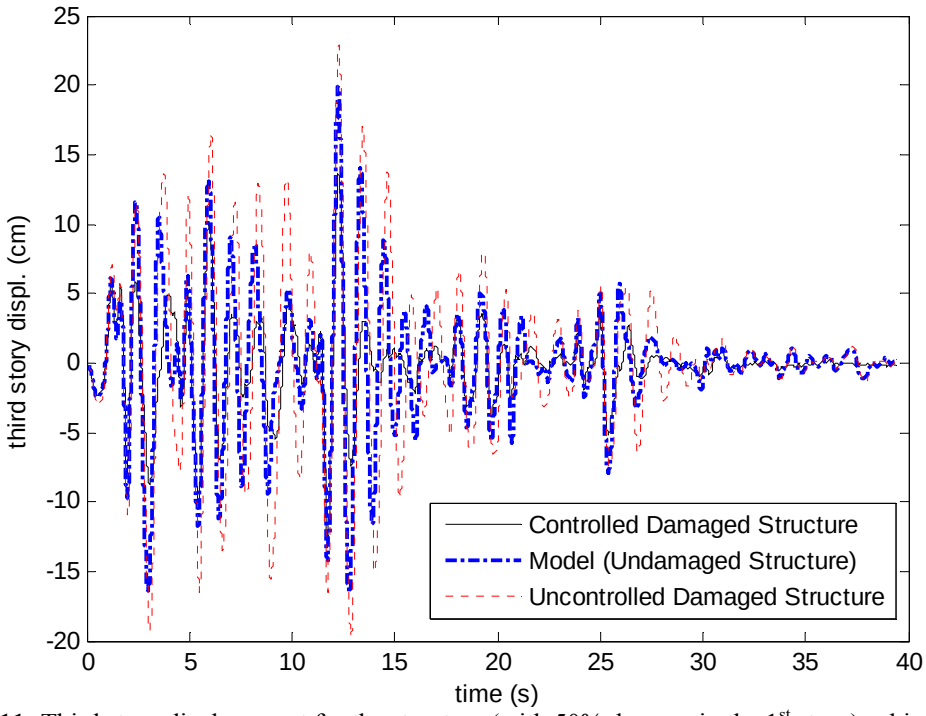

Figure 4.11: Third story displacement for the structure (with 50% damage in the 1st story) subjected to the earthquake LA01 and controlled by MR dampers with modified Bouc-Wen model.

Table 4.3: Error between the response of the controlled damaged structure and model (undamaged structure) when structure is subjected to LA01.

LA01		50% Damage	25% Damage	10% Damage
Damaged @ 1st story	e1 %	0.1102	0.0568	0.0193
	e2 %	0.0071	0.0039	0.0013
	e3 %	0.0007	0.0006	0.0005
	e4 %	0.0585	0.0776	0.0123
	e5 %	0.0043	0.0054	0.0010
	e6 %	0.0002	0.0004	0.0002
Damaged @ 2nd story	e1 %	0.0670	0.0316	0.0266
	e2 %	0.0296	0.0135	0.0111
	e3 %	0.0031	0.0016	0.0020
	e4 %	0.0459	0.0355	0.0203
	e5 %	0.0214	0.0163	0.0094
	e6 %	0.0027	0.0023	0.0017
Damaged @ 3rd story	e1 %	0.0147	0.0062	0.0053
	e2 %	0.0223	0.0086	0.0065
	e3 %	0.0112	0.0041	0.0024
	e4 %	0.0083	0.0061	0.0040
	e5 %	0.0132	0.0075	0.0052
	e6 %	0.0058	0.0031	0.0016

Table 4.4: Error between the response of the controlled damaged structure and model (undamaged structure) when structure is subjected to LA23.

LA23		50% Damage	25% Damage	10% Damage
Damaged @ 1st story	e1 %	0.1854	0.0615	0.0236
	e2 %	0.1281	0.0488	0.0161
	e3 %	0.0242	0.0084	0.0011
	e4 %	0.0696	0.0293	0.0114
	e5 %	0.0053	0.0021	0.0008
	e6 %	0.0007	0.0004	0.0003
Damaged @ 2nd story	e1 %	0.1344	0.0597	0.0215
	e2 %	0.0390	0.0149	0.0062
	e3 %	0.0416	0.0137	0.0027
	e4 %	0.0467	0.0185	0.0068
	e5 %	0.0195	0.0077	0.0028
	e6 %	0.0025	0.0011	0.0005
Damaged @ 3rd story	e1 %	0.0336	0.0145	0.0063
	e2 %	0.0283	0.0113	0.0055
	e3 %	0.0375	0.0108	0.0015
	e4 %	0.0092	0.0041	0.0017
	e5 %	0.0122	0.0051	0.0018
	e6 %	0.0053	0.0020	0.0006

Table 4.5: Error between the response of the controlled damaged structure and model (undamaged structure) when structure is subjected to LA44.

LA44		50% Damage	25% Damage	10% Damage
Damaged @ 1st story	e1 %	0.2992	0.2789	0.1016
	e2 %	0.0285	0.0202	0.0070
	e3 %	0.0040	0.0037	0.0024
	e4 %	0.1413	0.0553	0.0177
	e5 %	0.0086	0.0032	0.0011
	e6 %	0.0003	0.0003	0.0003
Damaged @ 2nd story	e1 %	0.5954	0.2372	0.0819
	e2 %	0.2407	0.0972	0.0332
	e3 %	0.0291	0.0127	0.0059
	e4 %	0.0866	0.0341	0.0126
	e5 %	0.0392	0.0152	0.0056
	e6 %	0.0048	0.0021	0.0010
Damaged @ 3rd story	e1 %	0.0394	0.0125	0.0061
	e2 %	0.0677	0.0214	0.0098
	e3 %	0.0298	0.0087	0.0030
	e4 %	0.0187	0.0159	0.0010
	e5 %	0.0301	0.0229	0.0013
	e6 %	0.0134	0.0091	0.0004

Table 4.6: Maximum drift ratio when structure is subjected to earthquake LA01 and controlled by MR dampers.

LA01	Max. drift ratio %	Damaged controlled structure	Model (undamaged structure)	Damaged uncontrolled structure
50% Damaged @ 1st story	1st Story	2.4761	2.4777	3.9338
	2nd Story	1.1587	2.3920	1.5567
	3rd Story	0.2528	0.5235	0.3185
25% Damaged @ 1st story	1st Story	2.3883	2.4777	3.1455
	2nd Story	1.6760	2.3920	1.9741
	3rd Story	0.3636	0.5235	0.4042
10% Damaged @ 1st story	1st Story	2.3883	2.4777	2.7672
	2nd Story	1.9889	2.3920	2.1424
	3rd Story	0.4218	0.5235	0.4664
50% Damaged @ 2nd story	1st Story	1.6387	2.4777	1.8641
	2nd Story	2.4013	2.3920	3.3232
	3rd Story	0.2724	0.5235	0.3472
25% Damaged @ 2nd story	1st Story	2.0840	2.4777	2.3203
	2nd Story	2.3103	2.3920	2.7230
	3rd Story	0.4026	0.5235	0.4316
10% Damaged @ 2nd story	1st Story	2.3413	2.4777	2.4483
	2nd Story	2.1423	2.3920	2.3960
	3rd Story	0.4382	0.5235	0.4814
50% Damaged @ 3rd story	1st Story	1.2815	2.4777	2.4400
	2nd Story	0.9579	2.3920	2.1549
	3rd Story	0.4542	0.5235	1.1002
25% Damaged @ 3rd story	1st Story	1.4741	2.4777	2.4691
	2nd Story	1.3905	2.3920	2.3134
	3rd Story	0.3742	0.5235	0.7148
10% Damaged @ 3rd story	1st Story	2.3470	2.4777	2.4756
	2nd Story	1.7867	2.3920	2.3675
	3rd Story	0.4180	0.5235	0.5864

Table 4.7: Maximum drift ratio when structure is subjected to earthquake LA23 and controlled by MR dampers.

LA23	Max. drift ratio %	Damaged controlled structure	Model (undamaged structure)	Damaged uncontrolled structure
50% Damaged @ 1st story	1st Story	2.6618	4.0006	4.5763
	2nd Story	1.2157	3.4187	2.0442
	3rd Story	0.2854	0.7174	0.4496
25% Damaged @ 1st story	1st Story	2.6612	4.0006	5.1489
	2nd Story	1.3611	3.4187	3.4272
	3rd Story	0.3115	0.7174	0.7268
10% Damaged @ 1st story	1st Story	2.0826	4.0006	4.5246
	2nd Story	1.9277	3.4187	3.5224
	3rd Story	0.3355	0.7174	0.7415
50% Damaged @ 2nd story	1st Story	1.4774	4.0006	2.4707
	2nd Story	2.1846	3.4187	5.1215
	3rd Story	0.3101	0.7174	0.5671
25% Damaged @ 2nd story	1st Story	1.5089	4.0006	3.8379
	2nd Story	2.0318	3.4187	4.6293
	3rd Story	0.3454	0.7174	0.7388
10% Damaged @ 2nd story	1st Story	1.7599	4.0006	4.0117
	2nd Story	2.0457	3.4187	3.8791
	3rd Story	0.4565	0.7174	0.7362
50% Damaged @ 3rd story	1st Story	1.4904	4.0006	4.0327
	2nd Story	1.3210	3.4187	3.5164
	3rd Story	0.7131	0.7174	1.5204
25% Damaged @ 3rd story	1st Story	2.0991	4.0006	4.0260
	2nd Story	2.0515	3.4187	3.4601
	3rd Story	0.4968	0.7174	0.9786
10% Damaged @ 3rd story	1st Story	2.2629	4.0006	4.0100
	2nd Story	2.2377	3.4187	3.4334
	3rd Story	0.4969	0.7174	0.8036

Table 4.8: Maximum drift ratio when structure is subjected to earthquake LA44 and controlled by MR dampers.

LA44	Max. drift %	Damaged controlled structure	Model (undamaged structure)	Damaged uncontrolled structure
50% Damaged @ 1st story	1st Story	0.5268	0.5437	1.2057
	2nd Story	0.3077	0.4313	0.4731
	3rd Story	0.0560	0.0903	0.0948
25% Damaged @ 1st story	1st Story	0.4988	0.5437	0.7231
	2nd Story	0.3081	0.4313	0.4256
	3rd Story	0.0842	0.0903	0.0901
10% Damaged @ 1st story	1st Story	0.4866	0.5437	0.5937
	2nd Story	0.3349	0.4313	0.4303
	3rd Story	0.0645	0.0903	0.0904
50% Damaged @ 2nd story	1st Story	0.4372	0.5437	0.5400
	2nd Story	0.3528	0.4313	0.8766
	3rd Story	0.0726	0.0903	0.0909
25% Damaged @ 2nd story	1st Story	0.4583	0.5437	0.5301
	2nd Story	0.3389	0.4313	0.5639
	3rd Story	0.0884	0.0903	0.0907
10% Damaged @ 2nd story	1st Story	0.4958	0.5437	0.5349
	2nd Story	0.3853	0.4313	0.4774
	3rd Story	0.0900	0.0903	0.0906
50% Damaged @ 3rd story	1st Story	0.4586	0.5437	0.5285
	2nd Story	0.2778	0.4313	0.4340
	3rd Story	0.0827	0.0903	0.1849
25% Damaged @ 3rd story	1st Story	0.4664	0.5437	0.5395
	2nd Story	0.3026	0.4312	0.4317
	3rd Story	0.0601	0.0903	0.1215
10% Damaged @ 3rd story	1st Story	0.5067	0.5437	0.5425
	2nd Story	0.3830	0.4313	0.4310
	3rd Story	0.0740	0.0903	0.1009

5. ACTIVE AND SEMI-ACTIVE ADAPTIVE CONTROL TO OPTIMIZE THE STRUCTURAL PERFORMANCE

In Section 5, the SACM is used to optimize the response of the undamaged structure and mitigate the undesired behavior of the damaged structure subjected to the earthquake. The damaged structure may result from extreme earthquakes, wind loads, and deterioration caused by corrosion or fatigue. The MR damper and hydraulic actuator are used to generate the required force to control the performance of the structure. Using the adaptive methodology, the force required for the desired performance of the structure is calculated. Then, the required voltage to generate the force in the MR damper is obtained. For the hydraulic actuator, PID control is designed to calculate the input command for the active device.

To evaluate the effectiveness of the SACM in controlling the structure, it is used to control the performance of a 3-story building from the SAC Phase II structures for the Los Angeles region (Barroso et al. 2002). The structure is assumed to be equipped with two types of control device either active or semi-active. The effectiveness of using the SACM to control the behavior of the structure in the presence of noise in the output measurement is studied. The model is the structure which exhibits the desired behavior and the controlled structure is forced to behave like the model. The model in this research is defined as a structure having velocities in a specific range. By using this model, the response of the controlled structure is always reduced, and the model output is independent of the characteristic of the earthquake which is applied to the structure.

In Section 4, the effectiveness of using SACM to mitigate the impact of damage in the performance of a 3-story building equipped with MR dampers was studied. The objective of Section 4 was to force the damaged structure to behave like the undamaged structure. However, in this Section, a different model with desired behavior which can optimize the performance of the structure in addition to mitigate the impact of damage in the structural response is defined. Also, it can be guaranteed that the response of the controlled structure would always be better than the response of the uncontrolled structure in the presence or absence of damage and noise. More details about defining a SACM model with desired performance to optimize the structural responses were discussed in Section 2.3.2.

5.1. Case Study

The 3-story building from the SAC Phase II project for the Los Angeles region is used to study the effectiveness of using the SACM to optimize the behavior of the structure subjected to the seismic excitations. More details about the characteristics of the building can be found in Section 4. Three suites of ground motions with different probability of exceedence, 2%, 10% and 50% in 50 years, developed for the SAC steel project, are applied to the 3-story building to study the performance of the structure (Somerville 1997).

It is assumed that the structure in the simulation would be controlled by a control device (MR damper or hydraulic actuator) at each story. One control device is connected

between the ground and first story, one is connected between the first and second, and one is connected between the second and third stories as shown in Figure 4.3. It can be noted that effective locations for the control devices installed in the buildings should be studied to improve the structural performance (Barroso et al. 2003). For the SAC 3-story building, the best performance is obtained when one MR damper is installed at each story instead of using just one MR damper in the first story. The values for the MR damper parameters are presented in Table 3.3 (Yoshida and Dyke 2005). The maximum capacity of this MR damper is 1000 kN. The hydraulic actuator parameters are adopted from Spencer et al. (1999) and the rounded up parameters, α_1, α_2 and α_3 are 5.81×10^6 kN/m-s, 5.46×10^4 kN/m and 1.62×10^3 s^{-1}, respectively. The maximum valve input displacement, u_v, is scaled up to 0.28 m, therefore the capacity of the hydraulic actuator is 1000 kN. The maximum accepted velocity for the model in SACM is assumed to be zero. The simulation is done for different values of Y_{max} and it is concluded that zero is the optimum value for Y_{max} for this example.

For the structure controlled with MR dampers, at each time step the values of the required forces to control the behavior of the structure are calculated using the SACM. Then using the inverse method, the required voltage is obtained, and finally the forces applied to the structure are calculated. As mentioned before, PID control is used for the hydraulic actuator to calculate the input command. Figure 5.1 shows the block diagram, which explains how the input command to generate the desired force is calculated. The PID control parameters, k_P, k_I and k_D, are chosen as 1, 100, and 0, respectively. Figures 5.2 and 5.3 show that the designed PID control works very well for the hydraulic

actuator. Since accelerometers are more commonly used than sensors measuring velocity, velocities are obtained by numerical integration of the accelerations (Bitaraf et al. 2010a). It should be noted that the measured data become smoother and have offset by passing through the integrator.

There are different sets of evaluation criteria used in the benchmark problem in structural control to evaluate the performance of the buildings (Spencer et al. 1998). The set of evaluation criteria used in this study to compare the performance of the structure controlled with different methods is

$$J_1 = \frac{\max\left(\left|x_i(t)\right|\right)}{x_{\text{unctrl}}} \tag{5.1}$$

$$J_2 = \frac{\max\left(\left|d_i(t)\right|\right)}{d_{\text{unctrl}}} \tag{5.2}$$

$$J_3 = \frac{\max\left(\left|\ddot{x}_i(t)\right|\right)}{\ddot{x}_{\text{unctrl}}} \tag{5.3}$$

$$J_4 = \frac{\max\left(\left|f_i(t)\right|\right)}{W}, \tag{5.4}$$

where $x_i(t)$, $\ddot{x}_i(t)$ and $d_i(t)$ are the relative displacement, acceleration, and drift of the ith floor. The variables x_{unctrl}, $\ddot{x}_{\text{unctrl}}$ and d_{unctrl} are the maximum absolute displacement, acceleration, and drift of the uncontrolled structure. The maximum control force per device and total weight of the structure are denoted by f_i and W, respectively, in Equation (5.4).

The structural response of the SAC building is evaluated for the undamaged and damaged structures. To investigate the effectiveness of the SACM in the presence of changes, a Gaussian noise in the output measurement and stiffness reduction as a potential damage are applied to the structure and the structural response is evaluated. Different control algorithms are used for the structure controlled by MR dampers such as passive control methods (passive-on and passive-off), the LQR, and the SACM, and the structure with hydraulic actuators is controlled by the SACM and the LQR. Passive-off refers to the case when MR dampers are operated with zero voltage and passive-on is the operational case in which MR dampers are operated with a constant maximum voltage.

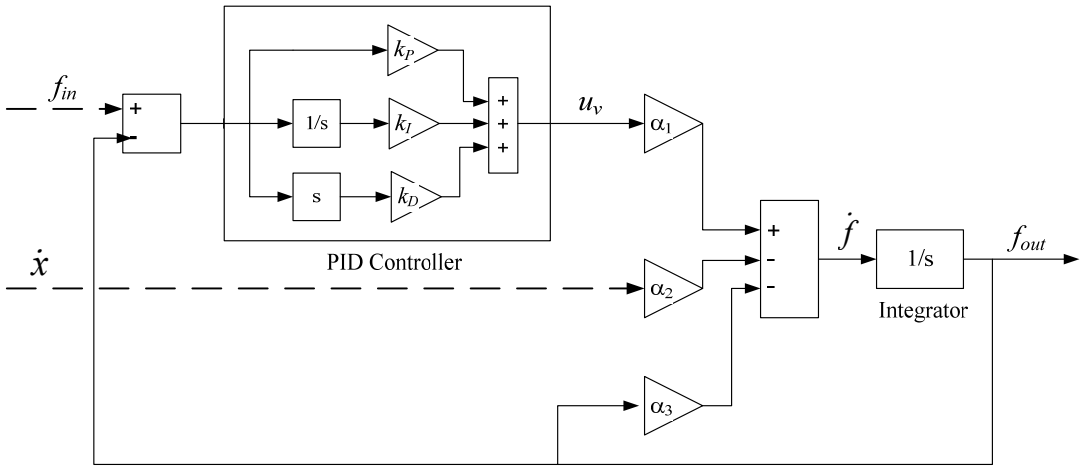

Figure 5.1: Block diagram of the hydraulic actuator showing that PID control is used to calculate the input command.

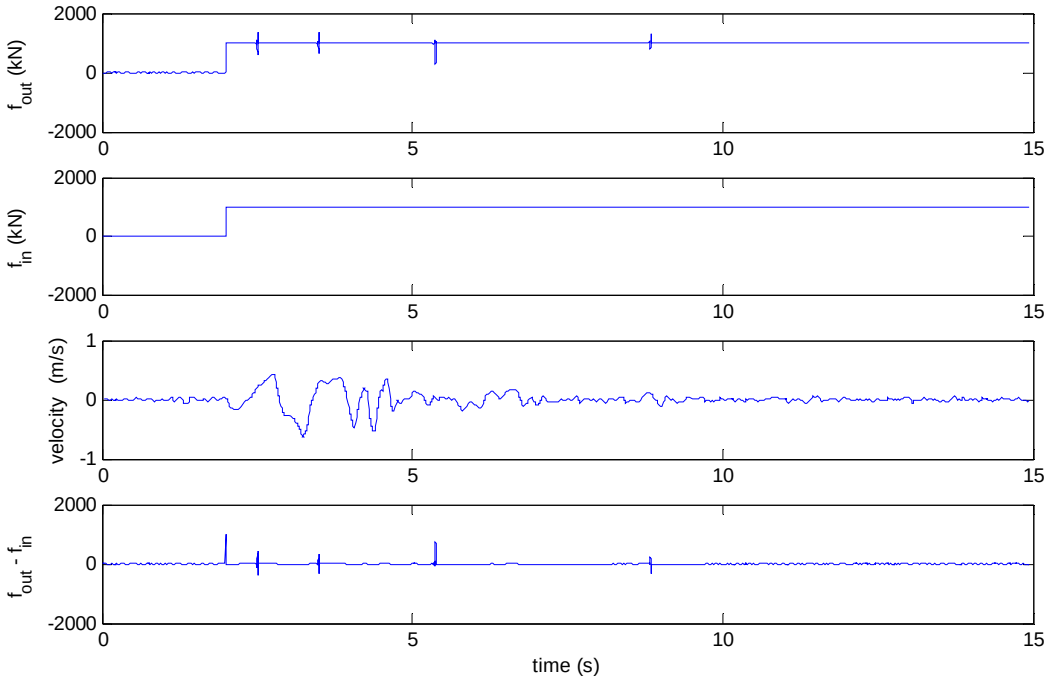

Figure 5.2: Performance of hydraulic actuator while the input force is step function.

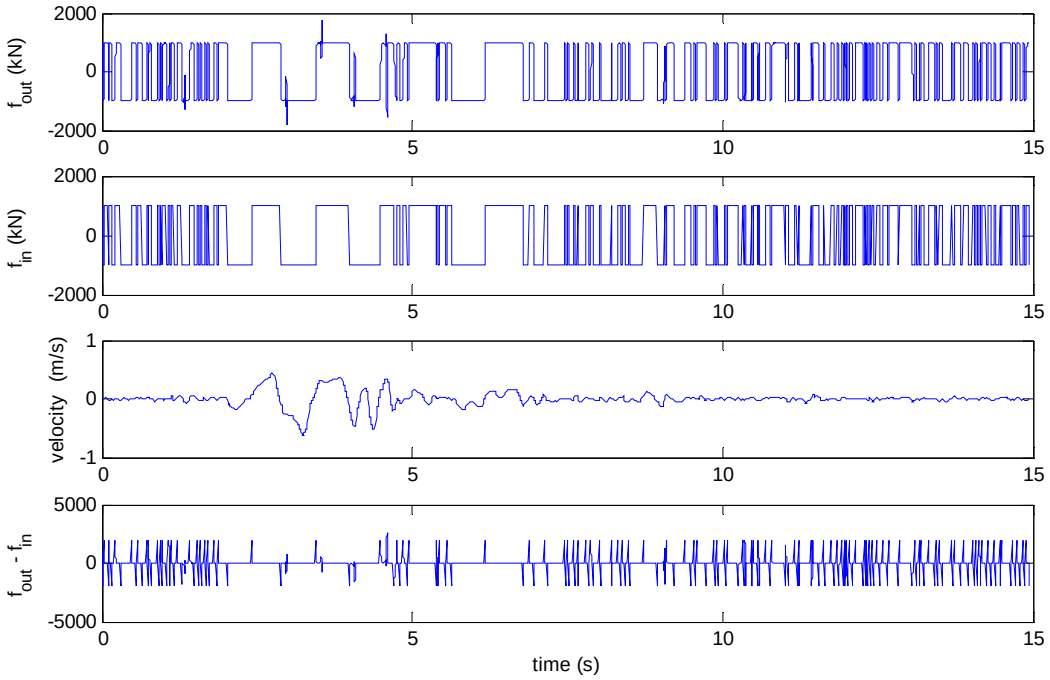

Figure 5.3: Performance of hydraulic actuator while the input force is obtained by SACM.

The weighting matrices, R and Q, for the LQR for both the active and semi-active devices are chosen as

$$Q = \frac{1}{2}\begin{bmatrix} K & 0 \\ 0 & M \end{bmatrix} \tag{5.6}$$

$$R = 100 I_{3\times 3}\,. \tag{5.7}$$

This choice of Q minimizes the total energy of the structure (Loh et al. 1999) and also the choice of R results in the best structural performance when some random earthquakes are applied to the structure.

5.2. Results and Discussion

Table 5.1 shows the ratio of the base shear of the undamaged controlled structure equipped with MR damper to the uncontrolled structure base shear. Figure 5.4 compares the first-story displacements of the uncontrolled and controlled undamaged structure with MR dampers under earthquake LA25. The results show that SACM is very effective in reducing the displacement and can improve the performance of the structure. Figure 5.5 shows the maximum drift ratios and accelerations for each story, when 25% stiffness reduction as a potential damage is assumed for the first story and the structure is controlled by the SACM with active and semi-active devices. It should be noted that no noise is added to the output measurement for the results of this figure. As shown in Figure 5.5, the SACM with MR dampers reduces the maximum drift by 21.6% as compared to the uncontrolled damaged case, while the SACM with hydraulic actuators

provides a 34% reduction in the maximum drift of the structure. The maximum acceleration of the controlled damaged structure with MR dampers and hydraulic actuators are reduced by 11% and 7% of the uncontrolled value, respectively. From Figure 5.5, it can be concluded that the SACM can improve the performance of the controlled damaged structure significantly.

Table 5.1: The ratio of the base shear of undamaged controlled structure equipped with MR damper to the uncontrolled structure base shear (without noise).

Base shear	LA53	LA55	LA59	LA08	LA11	LA16	LA22	LA29	LA36
Adaptive	0.84	0.70	0.84	0.62	0.75	0.74	0.97	1.01	0.75
LQR	0.83	0.83	0.86	0.69	0.77	0.76	0.97	1.01	0.77
On	0.70	0.86	0.83	0.71	0.78	0.72	0.96	1.02	0.74
Off	1.00	1.01	0.99	0.99	1.00	1.00	1.00	0.97	1.00

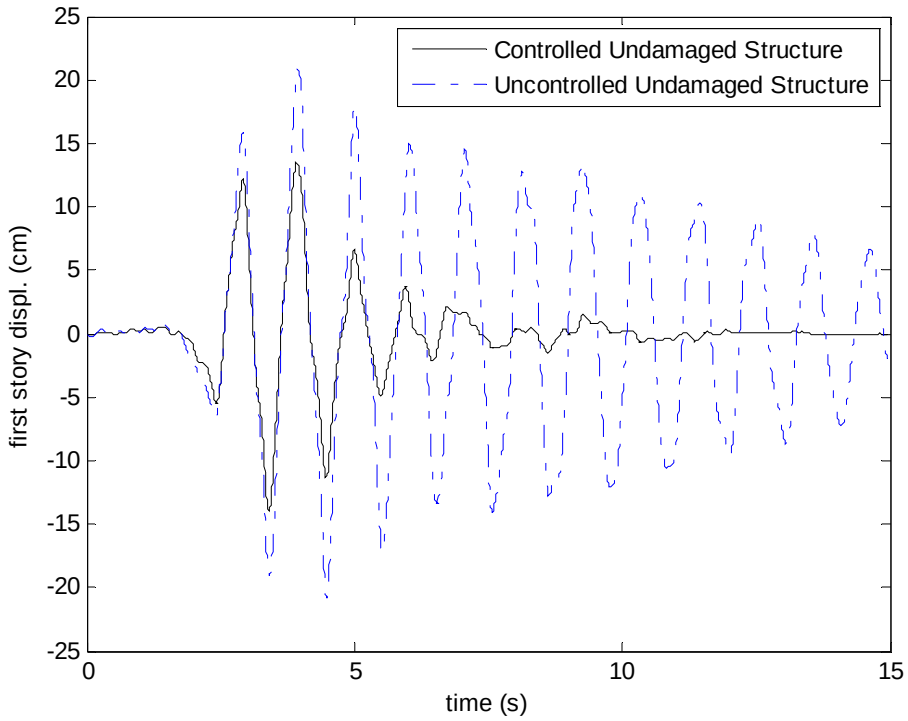

Figure 5.4: First story displacement of the undamaged 3-story building controlled with SACM and MR dampers and subjected to earthquake LA25.

To allow a more comprehensive comparison between different control methods, various ground motions from SAC project II (Somerville 1997) are used. Three ground motion records are chosen randomly from each suite of ground motions with three different probabilities of occurrence. From the earthquake ground motions with 50% probability of exceedence in 50 years, earthquakes LA53, LA55, and LA59 are chosen. LA08, LA11, and LA16 from the suite of ground motions with 10% probability of exceedence in 50 years and LA22, LA29, LA36 from the earthquake ground motions with 2% probability of exceedence in 50 years are selected to apply to the 3-story building.

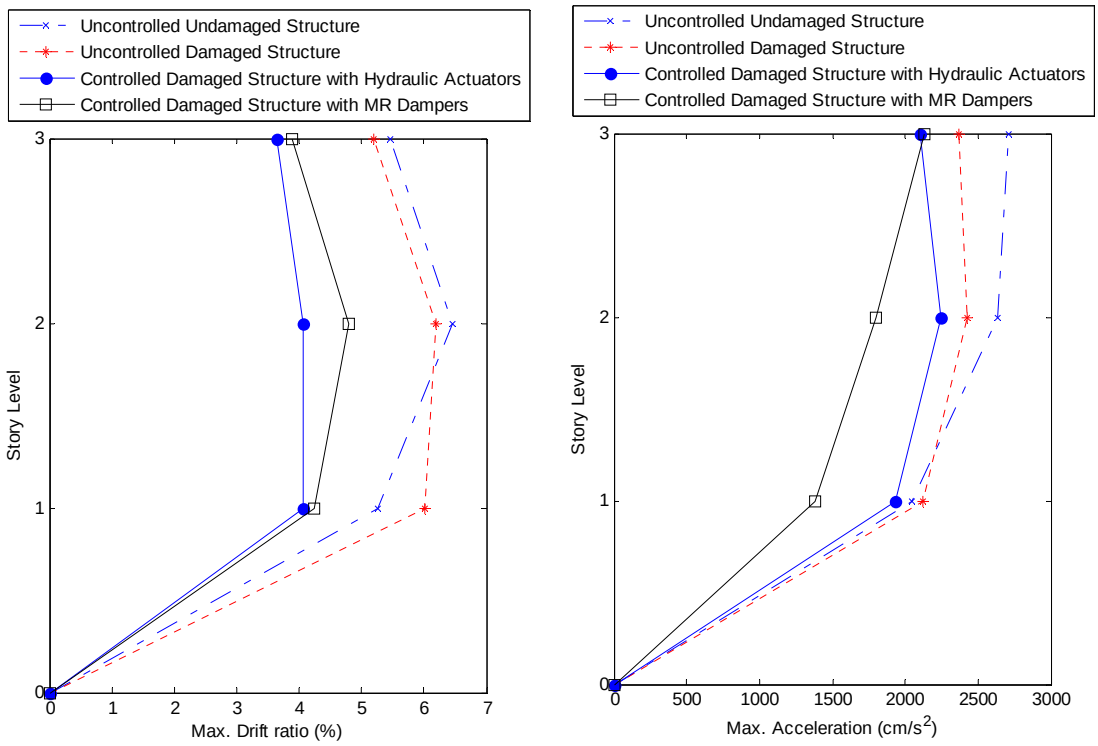

Figure 5.5: Maximum drift ratio and acceleration for the damaged 3-story building subjected to earthquake LA25 and controlled with SACM.

Figure 5.6 shows the values of the evaluation criteria for the undamaged structure and Figure 5.7 illustrates the results for the damaged structure. Figure 5.6 indicates that the maximum acceleration of the structure controlled with passive-on exceeds that of uncontrolled structure in LA53 and LA55 for the damaged and undamaged structures. All the control methods have used the maximum capacity of the control devices to improve the performance of the structure except the passive-off control method. The values of J_1 for the SACM with hydraulic actuator are slightly better than the results for the SACM with MR damper, however, Figures 5.6 and 5.7 show that using the SACM and active devices may increase the acceleration of the controlled structure in comparison with the uncontrolled structure. Figures 5.8 to 5.9 show the effectiveness of using the SACM in controlling the undamaged and damaged structure in the presence of noise for output measurements. The results show that in terms of reducing drift and acceleration response of the structure, the SACM with MR dampers is the most effective control method for both damaged and undamaged cases in the presence and absence of the noise. The structure controlled with the SACM and hydraulic actuators has the maximum displacement reduction in comparison with the uncontrolled case.

By comparing the evaluation criteria obtained for the undamaged case (Figure 5.6) with the evaluation criteria for the damaged and noisy measurement cases (Figures 5.7-5.9), it can be concluded that passive control can improve the performance of the structure but it cannot be as effective as other control methods in the presence of any change such as damage or noise. Additionally, significant reduction in the evaluation criteria can be obtained using semi-active adaptive control. Although, using an active

device can reduce the response of the structure, it cannot guarantee to always provide stable and reliable results. By comparing the performance of the SACM and the LQR, it can be concluded that using the SACM to control the response of the structure results in smaller values for evaluation criteria than the LQR for both active and semi-active devices.

For some cases when hydraulic actuators are used, the structure becomes unstable, while the structure with MR dampers never experience stability problem because semi-active devices do not destabilize the structure. The instability in the response of the structure controlled with hydraulic actuator and the LQR is shown in Figure 5.10. In the SACM, a system is stable if it can satisfy two conditions (Kaufman et al. 1994). The first one is

$$C_p B_p > 0 . \tag{5.8}$$

For the second condition, the roots of

$$\det \begin{bmatrix} sI - A_p & B_p \\ C_p & 0 \end{bmatrix} = 0 \tag{5.9}$$

should be in the open left hand plane which means that the real part of the roots has to be negative. The governing equations of the controlled structure with MR dampers satisfy the conditions for stability, but when hydraulic actuators are used to control the structure, three more differential equations would be added to the governing equations of the structure for the dynamic behavior of hydraulic actuators. These additional equations cause instability because Equations (5.8) cannot be satisfied.

From the previously mentioned results, it can be concluded that using the SACM and MR dampers to control the behavior of a structure allows the possibility of effective response reduction during both the moderate earthquake (earthquake with 10% and 50% probability of exceedence in 50 years) and the strong seismic activity (earthquake with 2% probability of exceedence in 50 years).

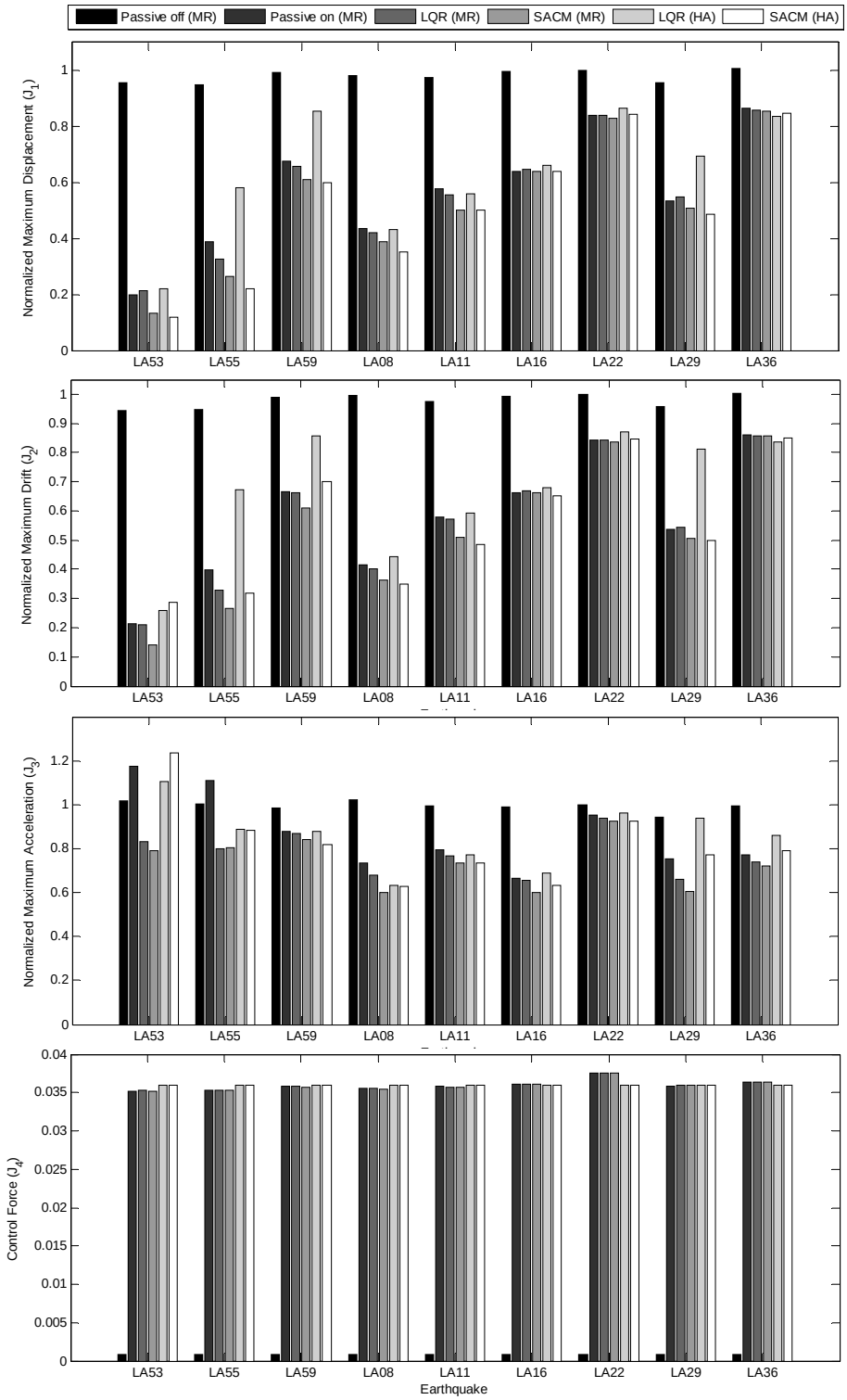

Figure 5.6: Evaluation criteria for the undamaged structure controlled with different control algorithms and different control devices, MR: MR damper, HA: Hydraulic Actuator (without noise).

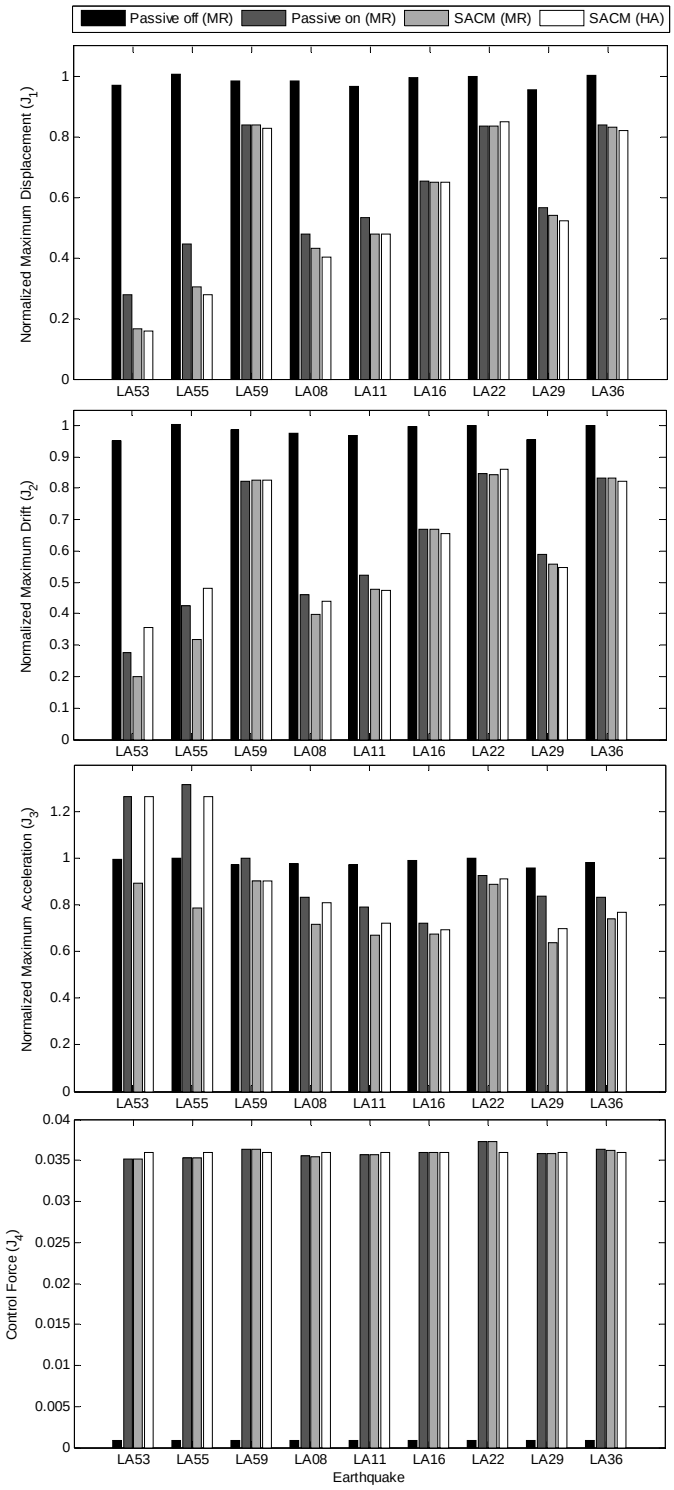

Figure 5.7: Evaluation criteria for the damaged structure controlled with different control algorithms and different control devices, MR: MR damper, HA: Hydraulic Actuator (without noise).

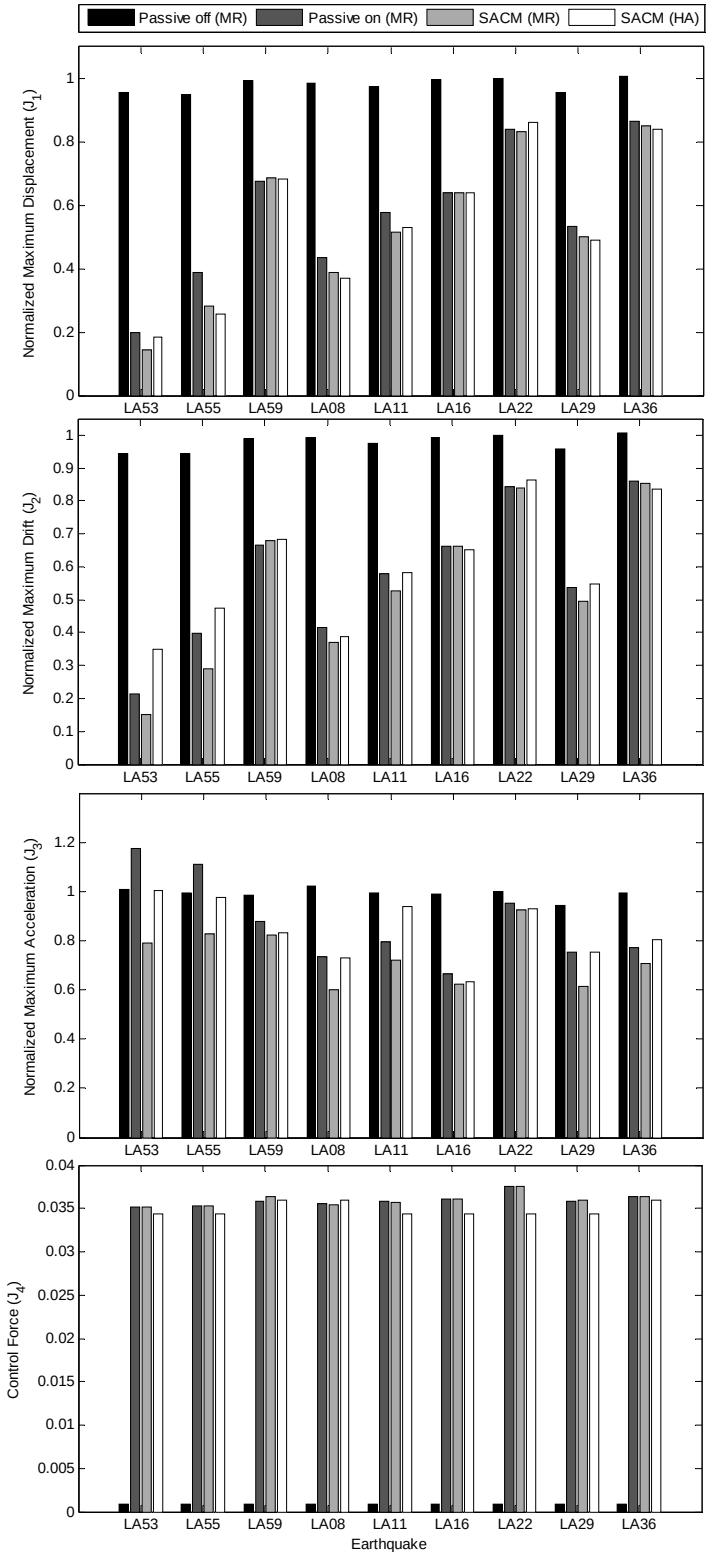

Figure 5.8: Evaluation criteria for the undamaged structure controlled with different control algorithms and different control devices (in the presence of the noise for output measurement).

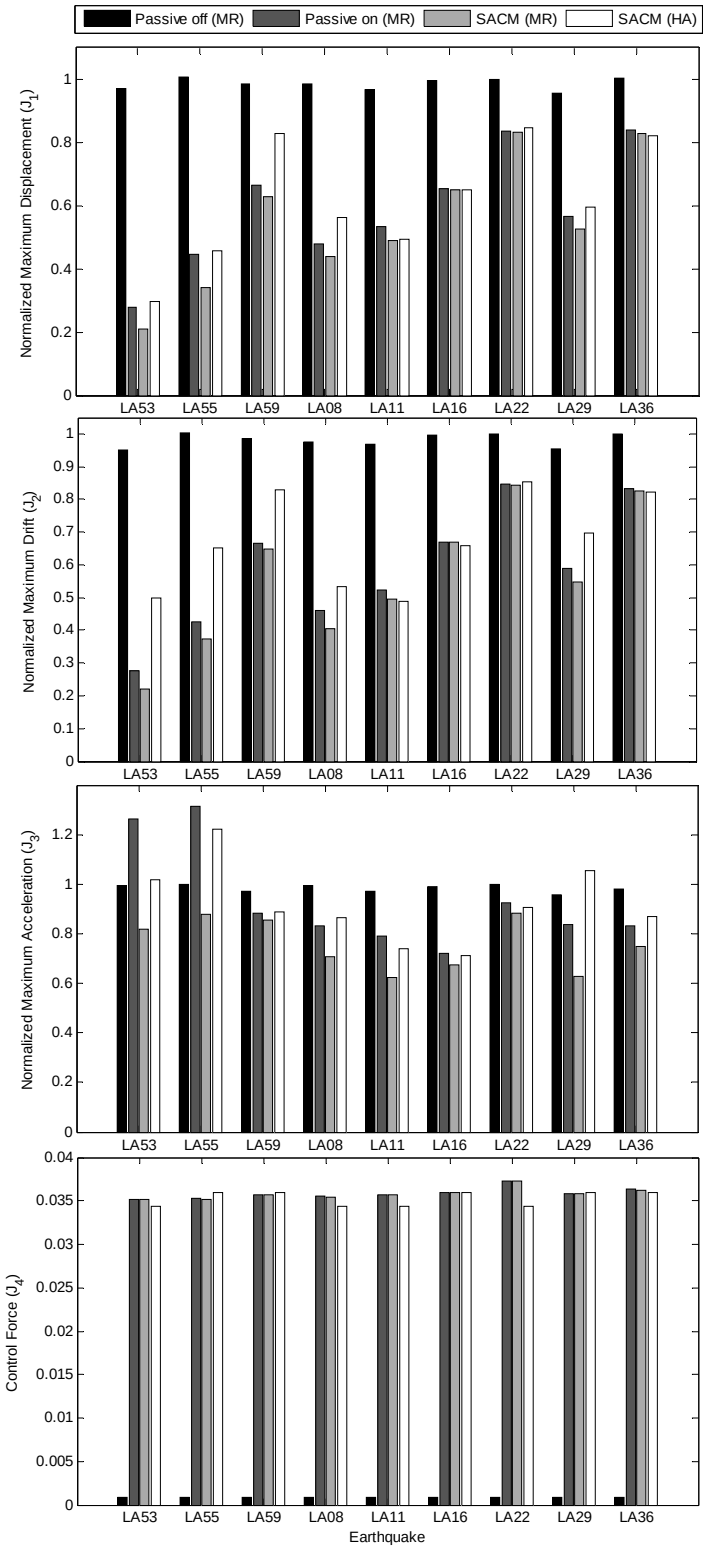

Figure 5.9: Evaluation criteria for the damaged structure controlled with different control algorithms and different control devices (in the presence of the noise for output measurement).

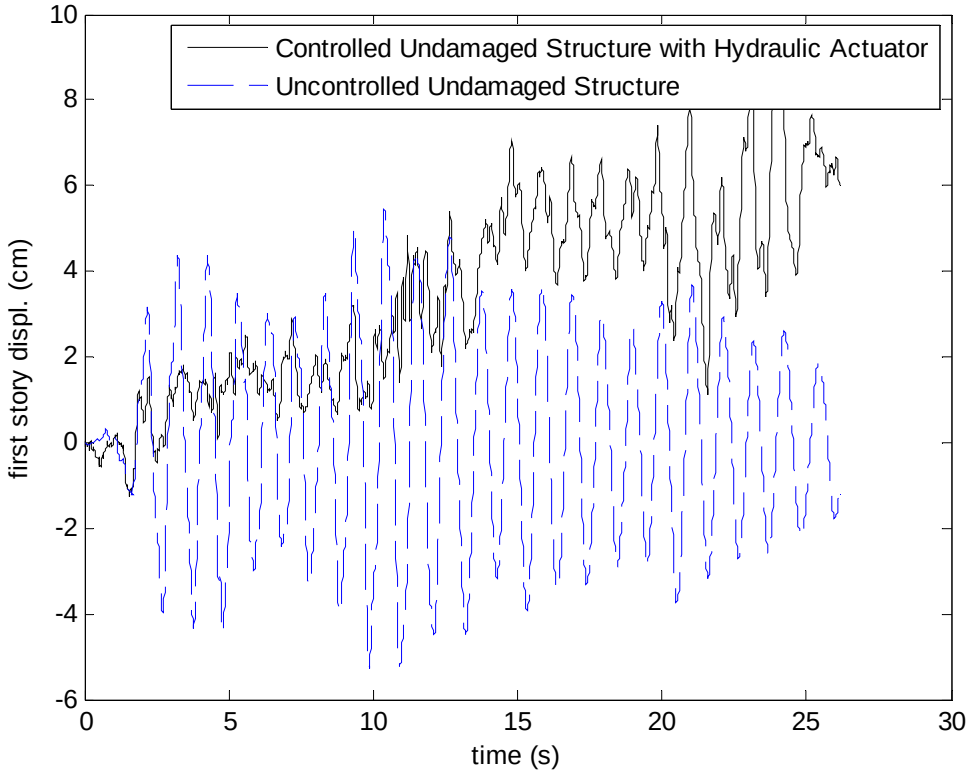

Figure 5.10: Instability for the response of the undamaged structure controlled by LQR with hydraulic actuators.

6. COMPARISON OF SACM WITH OTHER CONTROL METHODS

In this section, two semi-active control strategies, which can compensate the effect of any change like damage in the structure, are employed to control the behavior of the structure equipped with MR dampers. The first method is the SACM (Barkana and Kaufman 1993) which is a type of direct adaptive control approach and the second method is based on fuzzy control theory. Here, a fuzzy logic controller which utilizes a genetic algorithm (GA) as the adaptation engine is developed. In particular, a multi-objective genetic algorithm is used to tune the membership functions and generate the rule base of a Mamdani type fuzzy controller.

To evaluate the performance of the proposed control methods, a numerical example which has been studied by Jansen and Dyke (2000) and Williams (2004) is used. It should be noted that the results of this numerical example were also experimentally verified by Yi et al. (2001) (Figure 6.1).

The numerical example consists of a 6-story building with two MR dampers connected between the ground and first floors and two MR dampers connected between the first and second floors. A set of time-history analyses are performed to investigate the effectiveness of each control method in reducing the displacement and acceleration responses of the structure. Also, the results obtained using the developed controllers in this study are compared with those of the semi-active control strategies studied in Jansen and Dyke (2000).

Figure 6.1: Photograph of test structure (Yi et al. 2001).

6.1. Case Study

The numerical example is a six story building where the mass is equal to 0.227 N/(cm/s^2) for each floor, the stiffness of each floor equals 297 N/cm and the damping ratio for each mode is considered to be 0.5%. The MR damper parameters used in this simulation are c_{0a}=0.0064 N s/cm, c_{0b}=0.0052 N/(cm V), α_a=8.66 N/cm, α_b=8.86 N/(cm V), γ =300 cm^{-2}, β =300 cm^{-2}, A_0=120 and n=2 (Williams 2004). The structure is subjected to the N-S component of the 1940 El Centro earthquake with its amplitude scaled to 10% of the full scale earthquake to represent the magnitude of the displacements that would be observed in laboratory experiments with this structure. It is assumed that two MR dampers are connected between the ground and first floors and

two MR dampers are connected between the first and second floors. Figure 6.2 shows the schematic diagram of the MR damper implementation.

6.2. Results and Discussions

The results for the control method based on Lyapunov theory, the clipped-optimal control, decentralized bang-bang control, maximum energy dissipation and modulated homogeneous friction methods are adopted from Jansen and Dyke (Jansen and Dyke 2000). Clipped-optimal controller A and B are designed to have the moderate weighting (840 cm^{-2}) and higher weighting (9000 cm^{-2}) on relative displacements of all floors, respectively (Jansen and Dyke 2000). Also, Lyapunov controller A and B use different semi-definite matrices (Q_P) for Lyapunov equation (Jansen and Dyke 2000). In addition, two passive operation cases in which MR dampers are operated with zero voltage (passive-off) and with a constant voltage of 5V (passive-on) are considered.

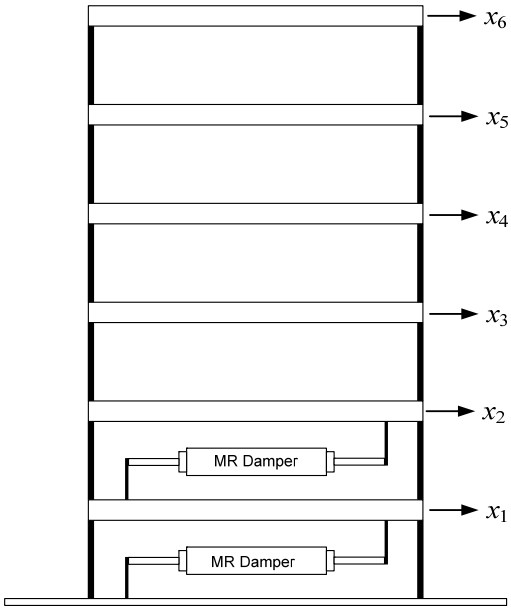

Figure 6.2: Schematic diagram of the MR damper implementation.

In Simple Adaptive Control, the plant and model outputs are velocities of the first and second stories. The maximum value for the velocity of the first and second story is defined to be 0.5 cm/s. By choosing a smaller value for the maximum velocity, a smaller value for J_1 and J_2 would be obtained, but the value for J_3 would increase. By using the SACM method, at each time step the control command vector u_p is calculated and then the values of the required forces to control the behavior of the structure are calculated by

$$\begin{bmatrix} f_1(t) \\ f_2(t) \end{bmatrix} = \begin{bmatrix} 1 & -1 \\ 0 & 1 \end{bmatrix}^{-1} u_p(t), \tag{6.1}$$

where $f_1(t)$ and $f_2(t)$ are the total forces generated by the MR dampers connected between the ground and first floors and the MR dampers connected between the first and second floors. The voltage to be supplied to the MR damper to generate the desired force is obtained by Equations (3.9) to (3.11). Finally, the damper forces applied to the structure are calculated using the obtained voltage. In the calculations, the scale matrix T is chosen to be 100 $I_{7\times7}$ and the numerical value for σ is selected as 0.01.

The design of fuzzy control rules to drive the MR damper voltage is challenging since it requires a good understanding of the dynamic response of the structure with the MR damper which has highly nonlinear behavior. In particular, it is challenging to establish a correlation between structural response and command voltage of the MR dampers in a multi-story building where MR dampers are installed on multiple floors. An eloquent approach to find the optimum parameters of a classical FLC is to employ computation search techniques. Genetic algorithm (GA) is one of such search techniques

based on the mechanics of natural genetics. GA searches large spaces without the need of derivative information (Sanchez et al. 1997). Here, GA is used to generate the rule base of a FLC that specify the command voltage of MR dampers installed on a structure. With its robust nature, GA can efficiently search for effective rules in the FLC. Additionally, it is possible to design a controller that is capable of optimizing both displacement and acceleration response of a building simultaneously using a multi-objective genetic optimization algorithm. In this study, a multi-objective optimization method, namely the Non-dominated Sorting Genetic Algorithm version II (NSGA-II), is employed to determine the rule set of the FLC. NSGA-II has been demonstrated to be one of the most efficient algorithms for multi-objective optimization problems on a number of benchmarks. A detailed description of NSGA-II can be found in Deb et al. (2002).

In order to develop a fuzzy logic controller using NSGA-II, a chromosome is created to obtain the genetic representation of a single FLC. Here, the FLC is designed to have two input variables which can be selected among measured responses of the structure and one output which is the command voltage of the MR damper. Gaussian membership functions are assigned to both inputs and the output. A Gaussian membership function can be defined using two parameters as follows:

$$\mu_{gauss} = -\frac{\exp(x-c)^2}{2\sigma^2}, \tag{6.2}$$

where c is the location of the center and σ is the width of the function.

A typical rule in the fuzzy controller has the form:

Rule i: IF X_1 is A_{i1} and X_2 is A_{i2} then Y is C_i, $i=1,2, ...M$,

where M is the number of fuzzy rules, X_j are the input variables, Y is the output variable, and A_{ij} and C_i are fuzzy sets characterized by membership functions, $\mu_{Aij}(x_j)$ and $\mu_{Ci}(y)$. Each rule maps two input variables to a single output by relating corresponding membership functions. Therefore, to describe a single rule, three Gaussian membership functions are defined by using two parameters (σ_i and c_i) for each membership functions. A random rule base with a total of ten rules is created to define the inference system of the initial FLC. Since each rule requires six parameters, there are a total of 60 parameters which are to be optimized are encoded into the GA chromosome. In order to evaluate each chromosome, four performance indices, which are peak and root-mean-square (RMS) base displacement in the controlled structure normalized by corresponding values in the uncontrolled structure and peak and RMS absolute floor acceleration in the controlled structure normalized by corresponding values in the uncontrolled structure, are defined and calculated. Also, the population size is set to 100 and the GA is run for a total of 200 generations.

For the fuzzy logic controller, the absolute accelerations of the top and second floors are selected as input variables, and the command voltage of the damper is specified as single output. Note that both MR dampers are operated by a centralized fuzzy controller, i.e. the same voltage is applied to both dampers. The development of a relationship between floor accelerations and the command voltages of MR damper in a multi-story building is not straightforward due to highly nonlinear behavior of the MR

dampers and uncertainties in the seismic events. Yet, the use of genetic algorithms to establish the rule base of the fuzzy controllers eliminates the need of well-defined fuzzy rules based on human knowledge. After performing GA-optimization for the knowledge base of the fuzzy controller, two fuzzy logic controllers are selected based on desired performance objectives. The first controller named FLC-1 can achieve higher displacement reductions while the second controller named FLC-2 performs better in controlling acceleration response.

Table 6.1 presents the structural response of the six-story building that is evaluated for the uncontrolled case, passive operation cases of MR dampers, and the cases in which MR dampers are controlled with different semi-active control strategies. The results show that in terms of reducing both displacement and acceleration response of the structure, the SACM and the FLC-2 are the most effective control methods. The clipped-optimal controller-A has the closest performance to the controller developed by the SACM method and the controller the FLC-2; however, both the SACM and the FLC2 provide better results especially for J_1 and J_2 evaluation criteria. Also, note that the smallest value for J_3 is obtained using the SACM method which provides 37% reduction in the maximum absolute acceleration of the structure. Using this method, the maximum displacement and interstory drift are also reduced by 48% and 38%, respectively in comparison with the uncontrolled structural response.

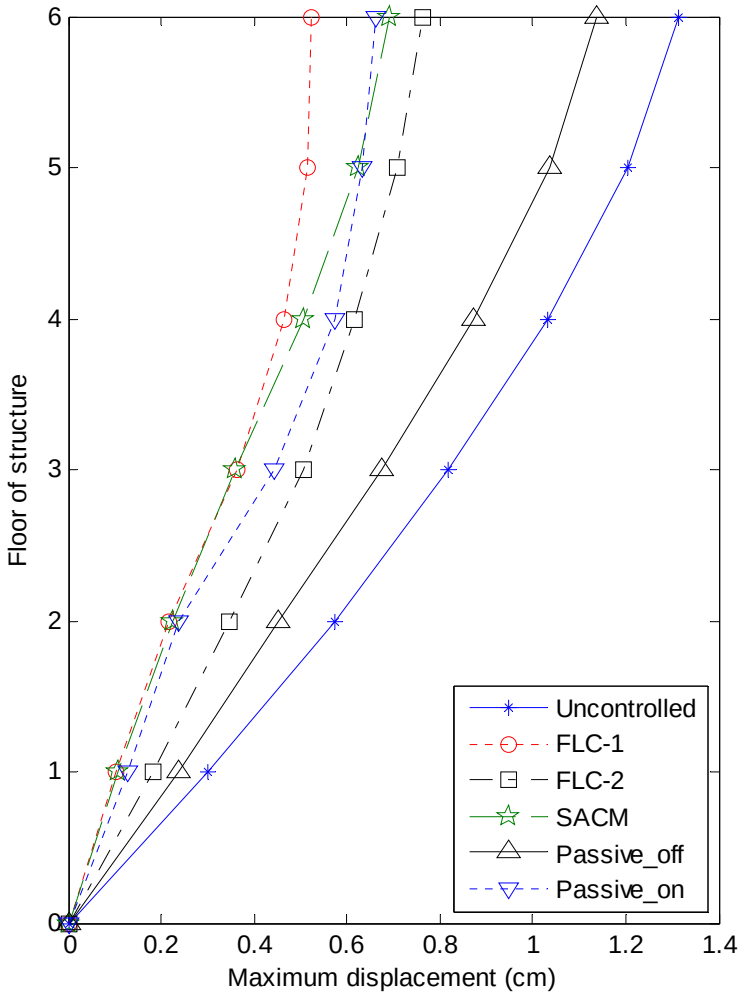

Figure 6.3: Maximum displacement for each floor of the undamaged structure.

Similarly, there is a 36% reduction in the peak absolute acceleration along with 42% and 38% reductions in the peak absolute displacement and interstory drift for the controller FLC-2. In addition, the controller FLC-1 achieves the maximum reduction in absolute displacement of the structure. Note that in terms of displacement reduction the results of the clipped-optimal controller B are very close to the results of the FLC-1, yet; the clipped-optimal controller B increases the acceleration of the structure about 25%. On the other hand, FLC-1 does not increase the maximum acceleration compared to the

result of the uncontrolled structure. In fact, as shown in Table 6.1, the controllers developed in this study, namely the SACM, the FLC-1 and the FLC-2, do not increase the structural dynamic response in comparison with the uncontrolled structure.

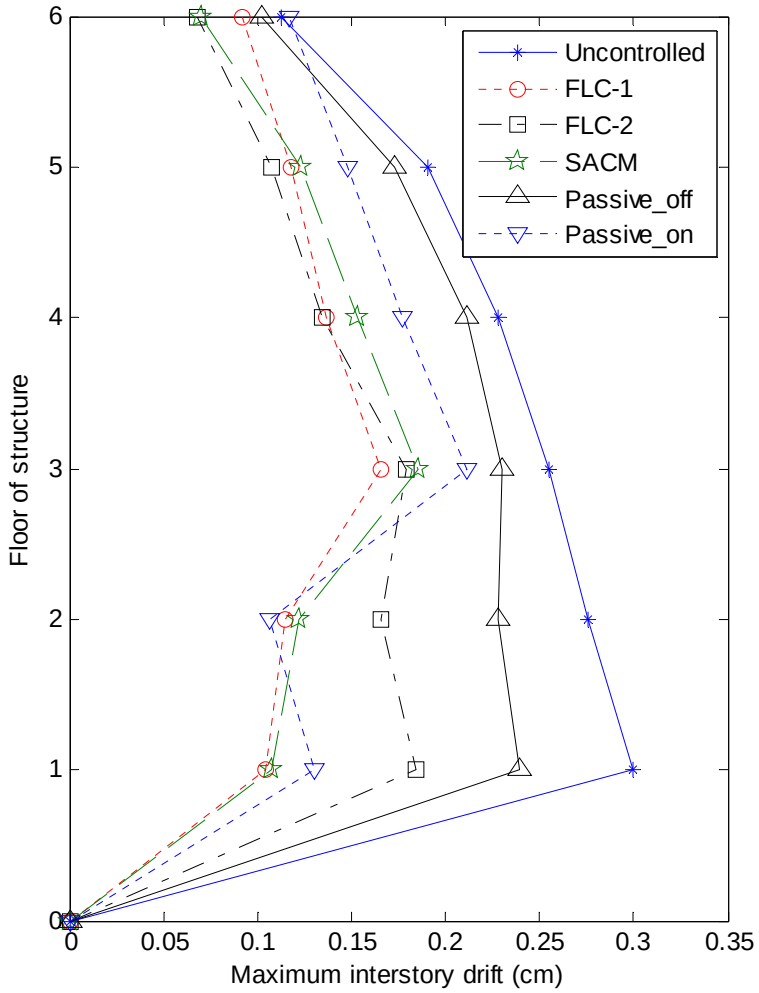

Figure 6.4: Maximum interstory drift for each floor of the undamaged structure.

The profiles of maximum story displacement and drift are shown in Figures 6.3 and 6.4. Figure 6.5 illustrates the maximum acceleration responses for all floors of the 6-story building controlled by different methods. It can be seen that the SACM method

could decrease the maximum acceleration of each floor more than the other methods except for the fifth and sixth floors for which the FLC-2 has the better result.

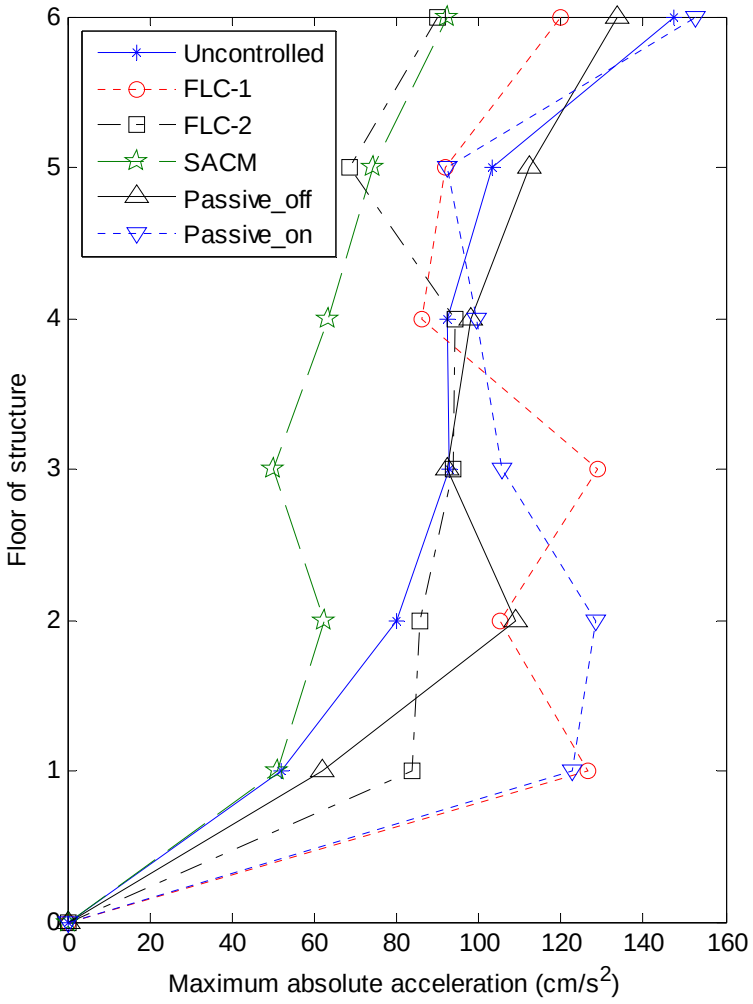

Figure 6.5: Maximum absolute acceleration for each floor of the undamaged structure.

To study whether the SACM and fuzzy logic control method can compensate for the damage that may occur in the structure, it is assumed that 25% stiffness reduction as the potential damage happened in the first story of the building. The results for the damaged structure controlled with different methods are shown in Figures 6.6 to 6.8. Also, Table 6.2 lists the resulting evaluation criteria for the damaged structure. The

results demonstrate that the developed methods can deal with uncertainty or changes in the structural parameters. In particular, the FLC-1 has the minimum value for evaluation criteria J_1 and J_2 and the FLC-2 has the minimum value for J_3 for the damaged structure.

As indicated in Table 6.2, the results for the damaged structure controlled with the SACM are satisfactory and very close to the results with the fuzzy logic control method. Figure 6.8 shows that the minimum acceleration for each story is obtained for the structure controlled with the SACM except for fifth and sixth floors. Moreover, it can be seen from Figures 6.6 through 6.8 that the peak displacement, drift and acceleration responses are significantly decreased especially for the lower floors using the SACM.

Table 6.1: Evaluated performance indices due to El Centro earthquake.

Control Method	J_1	J_2	J_3	J_4
SACM	0.525	0.619	0.627	0.0178
FLC-1	0.397	0.554	0.874	0.0176
FLC-2	0.581	0.615	0.640	0.0119
Passive-Off	0.865	0.814	0.909	0.0029
Passive-On	0.504	0.719	1.040	0.0178
Lyapunov Controller A[a]	0.686	0.788	0.756	0.0178
Lyapunov Controller B[a]	0.326	0.548	1.390	0.0178
Decentralized Bang-Bang[a]	0.449	0.791	1.000	0.0178
Maximum Energy Dissipation[a]	0.548	0.620	1.060	0.0121
Clipped-Optimal-A[a]	0.631	0.640	0.636	0.0110
Clipped-Optimal-B[a]	0.405	0.547	1.250	0.0178
Modulated Homogeneous Friction[a]	0.421	0.559	1.060	0.0178

[a] Ref. (Jansen and Dyke 2000)

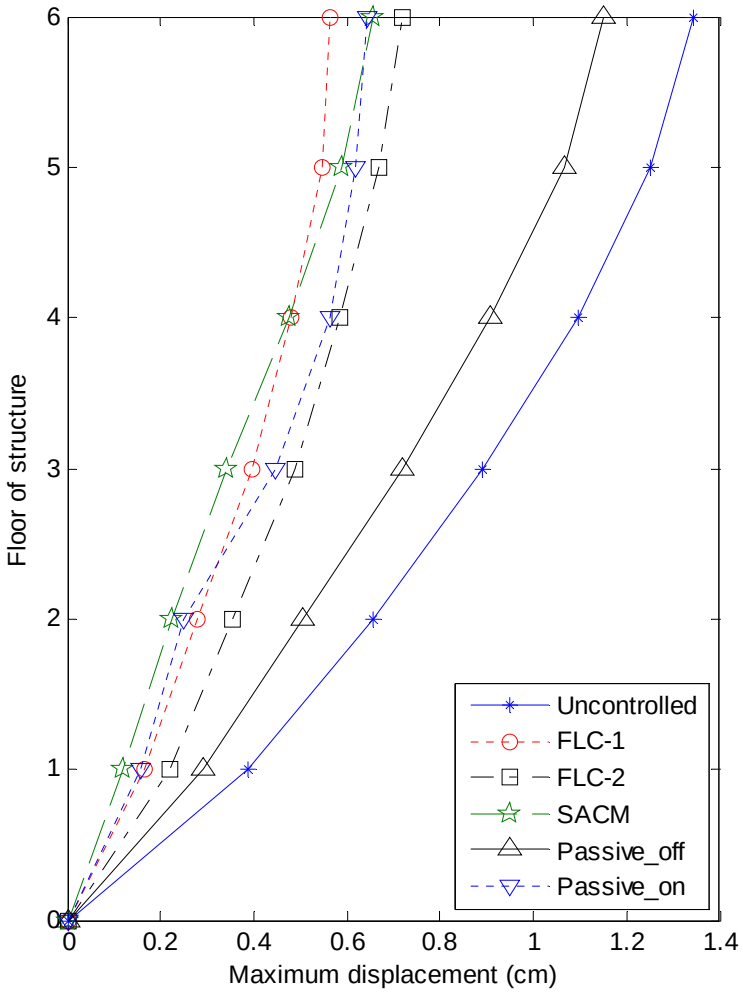

Figure 6.6: Maximum displacement for each floor of the damaged structure.

Finally, to assess the robustness of the proposed controllers with regard to uncertainties in the seismic excitation, simulations of the six-story building are performed under two far-field earthquakes (1968 Hachinohe and 1989 Loma Prieta earthquakes) and two near-field earthquakes (1994 Kobe and 1995 Northridge earthquakes). Again, since the building system studied here is a scaled model, the selected ground motion records are scaled to have a peak ground acceleration of 50 cm/s2.

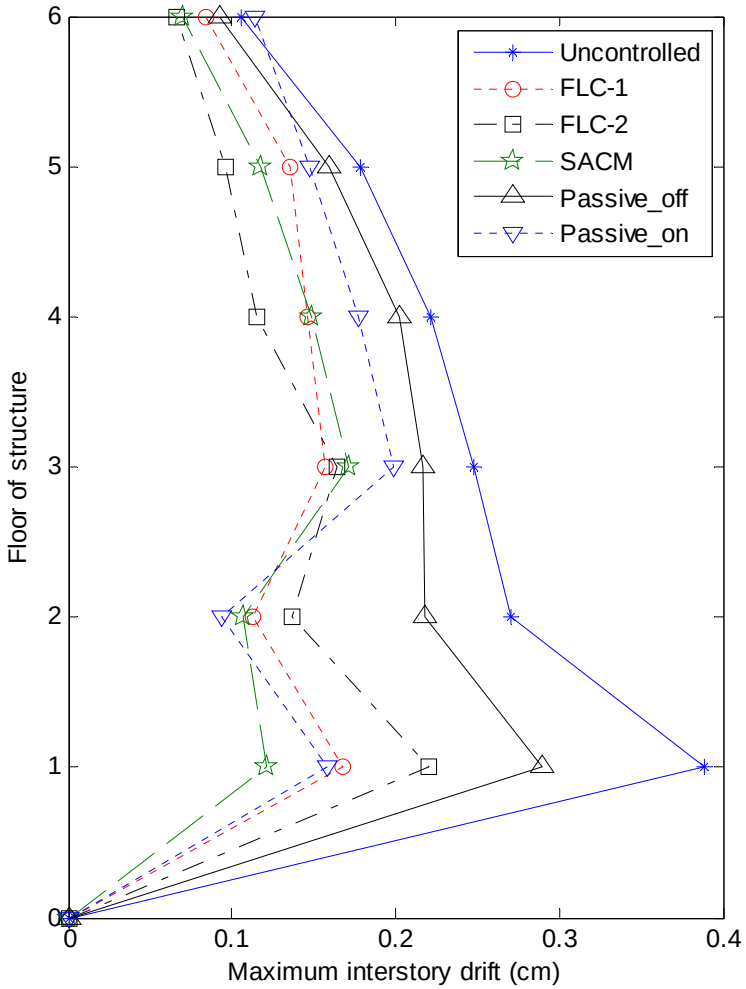

Figure 6.7: Maximum interstory drift for each floor of the damaged structure.

The evaluated performance indices are listed in Table 6.3 for the various control cases. It can be seen that the developed controllers satisfactorily decrease the response of the building under various excitations. In particular, the SACM yields the largest reductions in acceleration response for all excitation cases. Although passive operation of the dampers with a maximum voltage of 5V offers comparable displacement response reductions as semi-active operation of the damper, it produces larger results for peak acceleration response. Also, note that although the parameters of the fuzzy controllers

are optimized under El Centro earthquake, they satisfactorily perform under other external excitations as well.

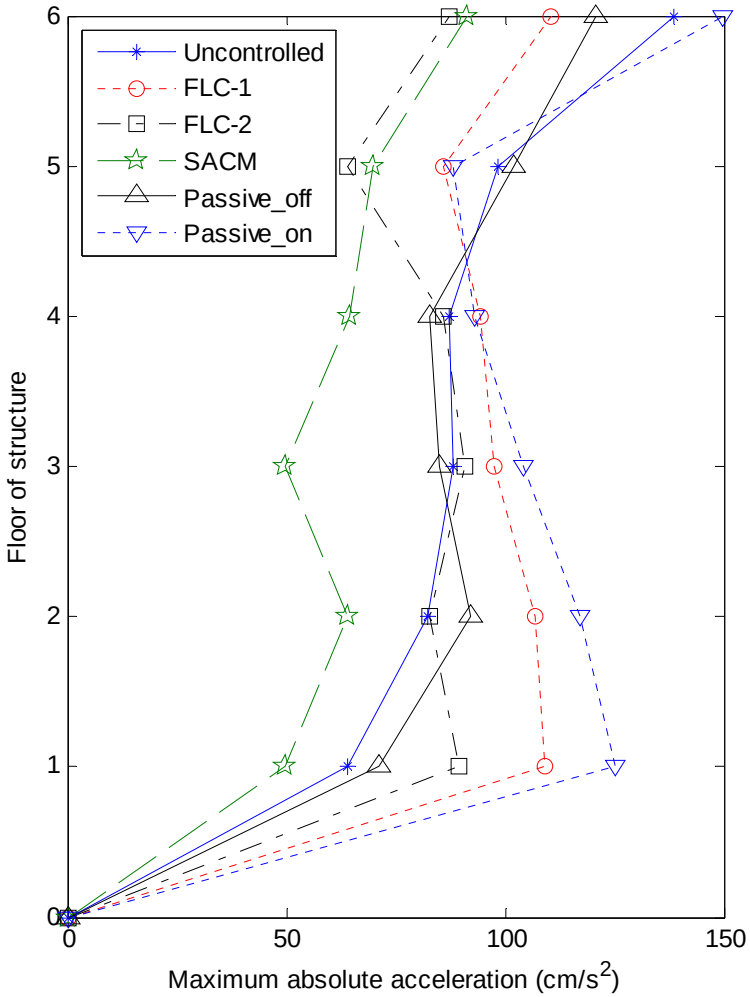

Figure 6.8: Maximum absolute acceleration for each floor of the damaged structure.

Table 6.2: Evaluated performance indices for damaged structure due to El Centro earthquake.

Control Method	J_1	J_2	J_3	J_4
SACM	0.489	0.439	0.661	0.0178
FLC-1	0.421	0.431	0.798	0.0176
FLC-2	0.535	0.568	0.655	0.0127
Passive-Off	0.876	0.986	0.821	0.0029
Passive-On	0.491	0.677	1.018	0.0178

Table 6.3: Evaluated performance indices due to various earthquake excitations.

Control Method	J_1	J_2	J_3	J_4
Hachinohe Earthquake				
SACM	0.36	0.33	0.78	0.0178
FLC-1	0.32	0.41	0.90	0.0176
FLC-2	0.43	0.40	0.75	0.0137
Passive-Off	0.67	0.70	0.91	0.0029
Passive-On	0.37	0.40	0.89	0.0178
Loma Prieta Earthquake				
SACM	0.41	0.47	0.85	0.0178
FLC-1	0.44	0.48	0.95	0.0176
FLC-2	0.59	0.53	0.99	0.0155
Passive-Off	0.96	0.92	1.00	0.0029
Passive-On	0.46	0.52	1.07	0.0178
Kobe Earthquake				
SACM	0.24	0.27	0.33	0.0178
FLC-1	0.24	0.25	0.50	0.0176
FLC-2	0.31	0.30	0.41	0.0152
Passive-Off	0.60	0.59	0.74	0.0029
Passive-On	0.21	0.29	0.46	0.0177
Northridge Earthquake				
SACM	0.28	0.28	0.40	0.0121
FLC-1	0.29	0.39	0.55	0.0176
FLC-2	0.28	0.34	0.47	0.0155
Passive-Off	0.52	0.46	0.62	0.0029
Passive-On	0.33	0.40	0.59	0.0177

7. ADAPTIVE CONTROL OF BASE-ISOLATED STRUCTURES

In this section, two adaptive control strategies are developed to adjust the contact force of variable friction dampers (VFD) used in a smart isolation system. The first control method that is used to improve the performance of a base-isolated structure is the SACM. Here, the required force to optimize the performance of a base-isolated structure against different earthquakes is obtained using the SACM and then, the command voltage of the VFD is determined to generate the required force. The second controller is based on an intelligent control strategy. In particular, fuzzy logic control theory is used to design an adaptive controller whose input and output scaling factors are tuned by a simple neural network according to current level of ground motion. The adaptive fuzzy neural controller (AFNC) determines the command voltage by using isolation displacement and velocity as the two input variables. More details about how this method is used to control the behavior of based-isolated structures is presented in Section 7.1. Also, a linear quadratic Gaussian (LQG) controller is designed and considered in the simulations together with maximum passive operation of the variable friction damper for comparison purposes. A five-story building isolated by laminated rubber bearings is modeled together with variable friction dampers that are installed at the base of the building. Numerical simulations of the base-isolated building are performed and various response quantities are evaluated in order to assess the performance of the controllers.

7.1. Adaptive Fuzzy Neural Control Strategy

Here, neural networks are employed to modify the input and output scaling factors of a fuzzy controller to ensure satisfactory controller performance for both near-field and far-field ground motions. By tuning the scaling factors of input and output variables, the corresponding universe of discourse of the variable will enlarge or reduce, resulting in better specification of fuzzy parameters. The block diagram of the adaptive fuzzy neural controller is shown in Figure 7.1.

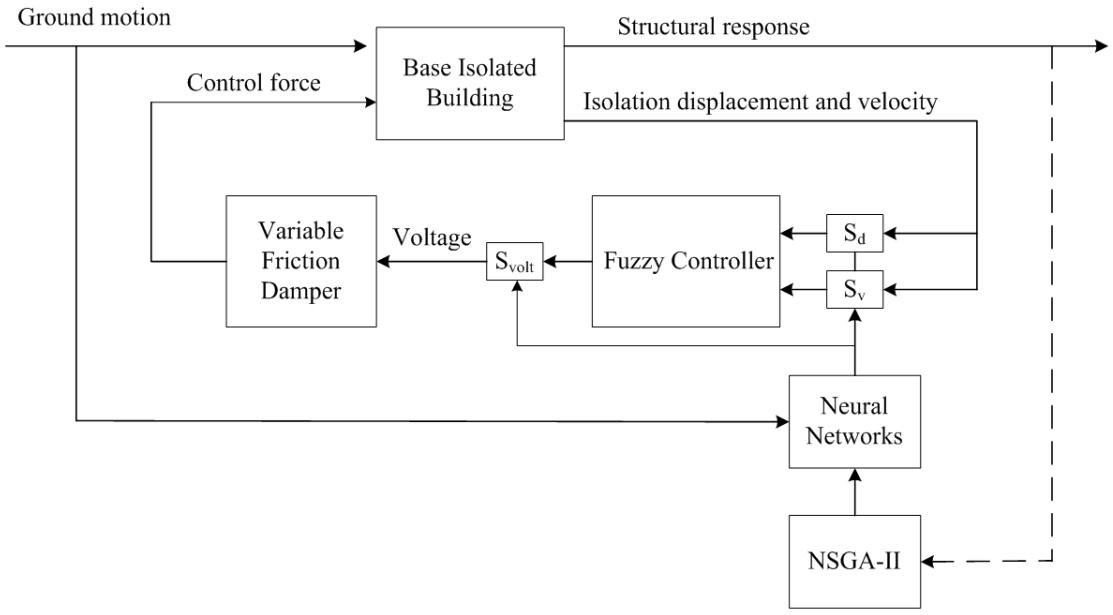

Figure 7.1: Block diagram of adaptive fuzzy neural controller.

The fuzzy logic controller developed in this study employs the isolation system displacement and velocity as two input variables and provides the command voltage of the damper. Seven triangular membership functions are defined for each input variable as shown in Figure 7.2. The fuzzy sets for input variables are NL = negative large, NM =

negative medium, NS = negative small, ZE = zero, PS = positive small, PM = positive medium, and PL = positive large. Note that the universe of discourse for each input variable is defined from -1 to 1. Scaling factors are used to keep the input variables in the range of the universe of discourse. For each input, a reasonable scaling factor should be selected because if the inputs are scaled to the values such that they become too small, then the innermost membership functions will be used frequently. On the other hand, if they become too big after being scaled, the outermost membership function will be mostly employed, and this limits the effectiveness of the controller. Since the amplitudes of isolation deformation and velocity differ greatly for near-field and far-field ground motions, the decision on the scaling factors is done by a simple feedforward neural network introduced later in this section.

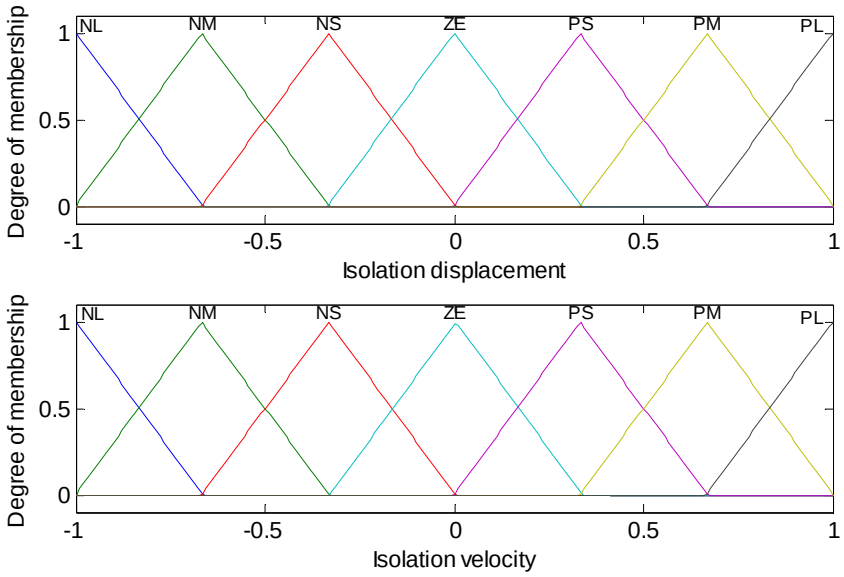

Figure 7.2: Input membership functions for sub-level FLC.

Five triangular membership functions are defined to cover the universe of discourse of the output variable voltage. The maximum driving voltage for the VFD is 1000V. Yet, if the damper is operated at its full capacity during far-field earthquake, the normal contact force of the damper will be too large and the damper will not dissipate much energy since it will not slide as expected. Therefore, a lower command voltage, i.e. a normal contact force, is desirable for moderate and weak earthquakes for effective energy dissipation. On the other hand, when the contact force is reduced too much, there will not be enough energy dissipation for strong earthquakes due to small sliding friction force of the damper. To overcome this difficulty, an output scaling factor that varies in the range of 0 to 1 is used to scale the command voltage of the damper. The output membership functions are equally-spaced over output domain as shown in Figure 7.3. The fuzzy sets for output variables are VL = very large, L = large, M = medium, S = small, and ZE = zero.

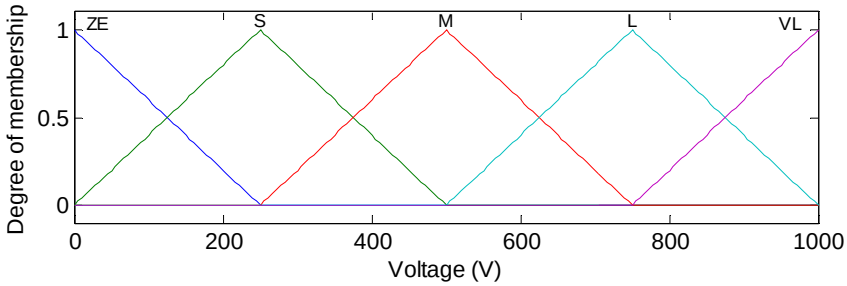

Figure 7.3: Output membership functions for sub-level FLC.

After the fuzzification of the input and output variables, a fuzzy rule base is defined for the FLC. The rule bases adopted for the developed fuzzy controller are given in Table 7.1. The control rules are in the form of if-then statements and map the link

between the input and output membership functions. Since the rules are words instead of mathematical equations, it is easy to interpret and modify the rules. For example, a rule in the Table 7.1 can be read as "if the isolation displacement is negative large and the isolation velocity is negative large, then the voltage is very large."

The rationale used to form to rule bases is as follows: if the displacement velocity of the isolation system is of opposite sign (i.e., the isolation system returns to its original position), then the output voltage is small, and if the isolation displacement and velocity have the same sign, then the output voltage is large. The magnitude of the output (the degree of being "small" or "large") is linearly proportional to the magnitude of the input variables. When the displacement and velocity are almost zero or small, the command voltage is about zero; that means that the variable friction damper acts against motion as a passive Coulomb damper. The center of area method is used as a defuzzification method for the FLC to get a crisp output value.

Table 7.1: Fuzzy rule base for sub-level FLC.

		Isolation Displacement						
	Voltage	**NL**	**NM**	**NS**	**ZE**	**PS**	**PM**	**PL**
Isolation Velocity	NL	VL	VL	L	L	M	S	ZE
	NM	VL	L	L	M	S	ZE	S
	NS	L	L	M	S	ZE	S	M
	ZE	L	M	S	ZE	S	M	L
	PS	M	S	ZE	S	M	L	L
	PM	S	ZE	S	M	L	L	VL
	PL	ZE	S	M	L	L	VL	VL

Neural networks have been used widely for adaptive control of uncertain systems (Zbikowski and Hunt 1996). An artificial neural network consists of a number of simple artificial neurons that are usually organized into three layers, namely, an input layer, a

hidden layer and an output layer, with random connections between the layers. Figure 7.4 shows the schematic representation of an artificial neuron. The input signals, represented by $x_1, x_2, \ldots, x_n$, are modified by synaptic weights. The output of a neuron is specified by an activation function whose input is the sum of weighted inputs.

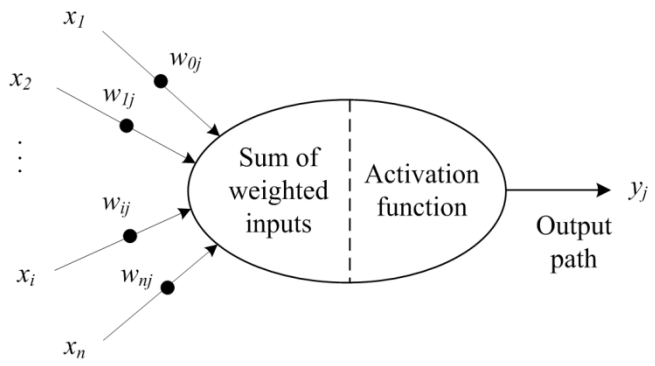

Figure 7.4: Schematic representation of an artificial neuron.

A simple neural network that consists of three artificial neurons as shown in Figure 7.5 is constructed to specify the input and output scaling factors of the fuzzy controller. As discussed earlier, near-field earthquakes usually possess long duration pulses with peak velocities. Therefore, the ground velocity $\dot{x}_g$ is selected as input of each neuron in order to determine the characteristics of the ground motion. The range of the input $\dot{x}_g$ is defined to be [-100, 100] cm/s, where the upper limit of $|100|$ cm/s is set as saturation point and seismic records with ground velocities beyond this value are directly classified as near-field earthquakes. The outputs of the network are scaling factors for isolation displacement S_d, isolation velocity S_v, and command voltage S_{volt}. The activation functions for artificial neurons that produce scaling factors S_d and $S_{v,}$ are

selected to be triangular basis functions, while a bipolar sigmoid function is chosen for S_{volt}. These functions are defined as

$$F_1(x) = c_1 - (c_2 - c_1)\dot{x}_g \tag{7.1}$$

$$F_2(x) = c_3 - (c_4 - c_3)\dot{x}_g \tag{7.2}$$

$$F_3(x) = \frac{1 - \exp(-\alpha \dot{x}_g)}{1 + \exp(-\alpha \dot{x}_g)}, \tag{7.3}$$

where c_1, c_2, c_3, c_4 and α are the constants that define the shape of the activation functions. The shapes of these functions are illustrated in Figure 7.6. Note that the activation functions F_1 and F_2 produce maximum values c_1 and c_3 for the scaling factors S_d and S_v, respectively and the magnitude of the scaling factors decreases when the absolute value of ground velocity increases. On the other hand, the activation function F_3 yields an output scaling factor S_{volt} that increases with the magnitude of the ground velocity and changes in the range of [-1, 1]. However, the absolute value of S_{volt} is used as the scaling factor and, therefore, the output of the fuzzy controller, i.e. the command voltage of the damper, is scaled by a number between 0 and 1. The variation of the output activation function F_3 with the constant α is shown in Figure 7.6. Note that this function is highly nonlinear and the value of α significantly affects the output of the function.

A genetic algorithm (GA) is a search technique that emulates biological evolutionary theories for optimization and search. The method has been successfully applied to a wide range of optimization problems. In recent years, the use of genetic algorithms for training neural networks has been explored in several studies (Whiteley et

al. 1990; Kitano 1994). During training of a neural network, the genetic algorithm can be used to determine the network topology and/or weights and/or transfer functions. In this study, a multi-objective genetic algorithm optimizer, namely NSGA-II, is implemented to search the optimum activation function parameters of the neural network that generate the input and output scaling factors of the fuzzy controller. NSGA-II is a computationally fast and elitist evolutionary algorithm based on a non-dominated sorting approach. Among a pool of initial random candidate values that reside within a user-defined range, NSGA-II generates a set of Pareto-optimal solutions through an iterative process. In particular, it compares each solution with every other solution in the population to determine if it is dominated, and then evaluates the solutions in accordance with given performance objectives. The detailed description of NSGA-II algorithm can be found in (Deb et al. 2002).

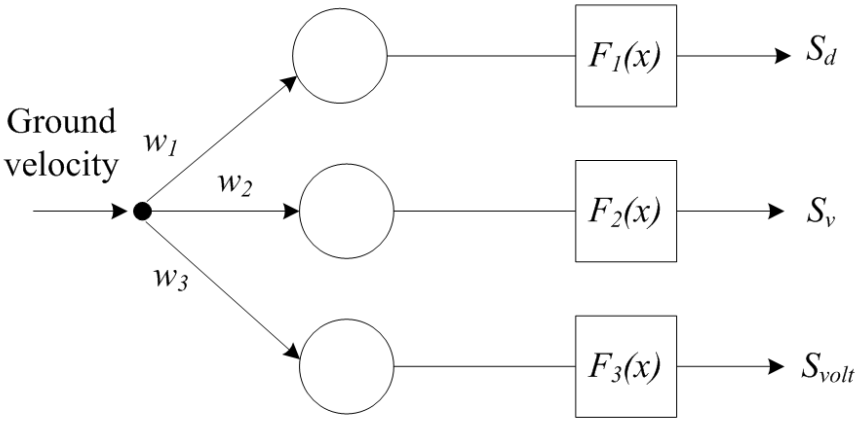

Figure 7.5: Neural network architecture.

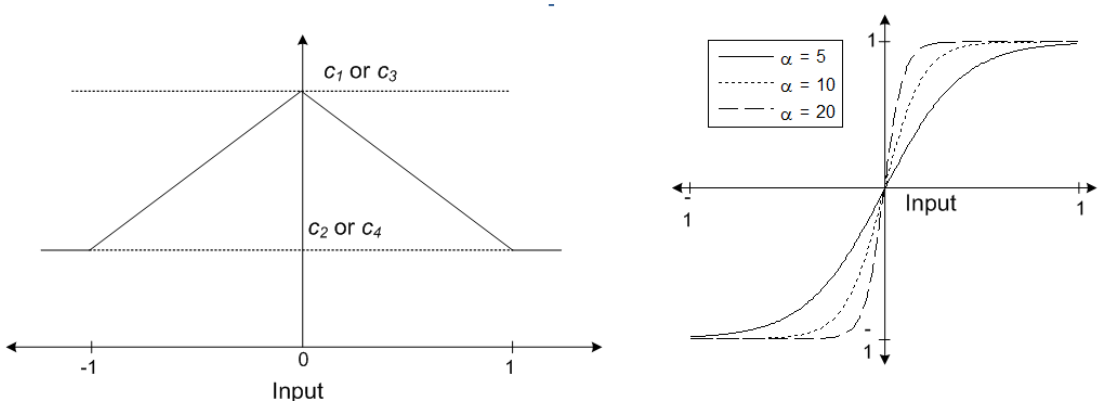

Figure 7.6: Shapes of activation functions.

To determine optimal activation functions using NSGA-II, five parameters, namely, c_1, c_2, c_3, c_4 and α are encoded into a GA chromosome as shown in Figure 7.7. From preliminary simulations, it is found that the parameters c_1 (maximum value) and c_2 (minimum value) of the input scaling factor S_d are within the ranges [7.0, 12.0] and [1.5, 3.0], respectively. Similarly, the ranges for the parameters c_3 and c_4 of the input scaling factor S_v are within the ranges [1.5, 4.0] and [0.5, 1.5], respectively and the parameter α for output scaling factor S_{volt} is varied in the range of [3.0, 20.0].

c_1	c_2	c_3	c_4	α

Figure 7.7: Chromosome representation of neural network.

For evaluation of candidate solutions during NSGA-II optimization, a seismic excitation is required. Since here the goal is to have a single controller that is effective against both far-field and near-field earthquakes, the 1940 El Centro and the 1999 Chi-Chi earthquakes are used to represent far-field and near-field excitations respectively during the GA simulations. To evaluate each chromosome, four objective functions are defined and computed as

$$J_{1F} = \frac{\max_{t(FF)} \left\| x_b(t) \right\|}{\max_{t(FF)} \left\| \hat{x}_b(t) \right\|} \tag{7.4}$$

$$J_{2F} = \frac{\max_{t(FF),f} \left\| \ddot{x}_f(t) \right\|}{\max_{t(FF),f} \left\| \hat{\ddot{x}}_f(t) \right\|} \tag{7.5}$$

$$J_{3F} = \frac{\max_{t(NF)} \left\| x_b(t) \right\|}{\max_{t(NF)} \left\| \hat{x}_b(t) \right\|} \tag{7.6}$$

$$J_{4F} = \frac{\max_{t(NF),f} \left\| \ddot{x}_f(t) \right\|}{\max_{t(NF),f} \left\| \hat{\ddot{x}}_f(t) \right\|} \tag{7.7}$$

where x_b and $\hat{\ddot{x}}_f$ denote base displacement and absolute floor acceleration, respectively; t is time; and f represents the story that is considered. The objective functions J_{1F} and J_{3F} evaluate peak base displacement in the controlled structure normalized by corresponding displacement in the uncontrolled structure during far-field (FF) and near-field (NF) earthquakes, respectively; the objective functions J_{2F} and J_{4F} compute peak absolute floor acceleration in the controlled structure normalized by corresponding acceleration in the uncontrolled structure during far-field and near-field earthquakes, respectively. Here, the term 'uncontrolled' refers to the isolated building without any semi-active dampers. With the above-described settings, a population of 50 chromosomes is initialized for a total of 100 GA runs.

7.2. Numerical Study

A five-story base-isolated building, as studied in Johnson et al. (1998) is selected to investigate the performance of the developed adaptive controllers. A lumped-mass

structure model with one degree of freedom per floor is used in the numerical simulations. The model of the smart base-isolated structure with variable friction dampers is shown in Figure 7.8. The fundamental period of the building is 0.3 s, with a damping of 2% in the first mode. The mass of each floor is equal to 5,897 kg. The damping coefficients for the five floors are 67, 58, 57, 50 and 38 kNs/m, and the stiffness of the five floors are 33732, 29093, 28621, 24954 and 19059 kN/m, respectively. The isolation system consists of low-damping rubber bearings with a base mass of 6,800 kg and assumed to have linear force deformation behavior with viscous damping. The total damping coefficient and the stiffness of the rubber bearings are 7.45 kNs/m and 232 kN, respectively. For the given isolation parameters, the base-isolated building has a period of 2.5 s and a damping ratio of 4% in the fundamental mode. In order to improve the performance of the base-isolated building against different earthquakes, variable friction dampers with a total force capacity of 16.8 kN are installed to the base of the structure. A total of six historical earthquake records that are commonly used in structural control research are employed as external excitation in the numerical simulations. The characteristics of selected ground motions are given in Table 7.2.

Time history analyses of the base-isolated building are performed in MATLAB/Simulink for the six historical earthquakes. For the adaptive fuzzy neural controller, the optimum values of the parameters c_1, c_2, c_3, c_4 and α are found to be 9.3, 2.1, 3.3, 1.1 and 3.4, respectively. For SACM, the value of σ, T and $\overline{T}$ are chosen to be 0.01, 1 $I_{4\times4}$ and 100 $I_{4\times4}$, respectively. The model reference is defined as a structure

having the output equal to zero. In this study, the output is the velocity of the basement, and a velocity equaling zero results in the minimum displacement and drift for the controlled structure.

Table 7.2: Characteristics of the ground motions used in the analyses.

Earthquake	Magnitude (M_w)	PGA (g)	PGV (cm/s)
1940 El Centro	7.2	0.31	29.8
1971 San Fernando	6.6	1.22	112.5
1989 Loma Prieta	6.9	0.37	62.4
1994 Northridge	6.7	0.90	102.8
1995 Kobe	7.2	0.63	76.6
1999 Chi-Chi	7.6	0.36	292.2

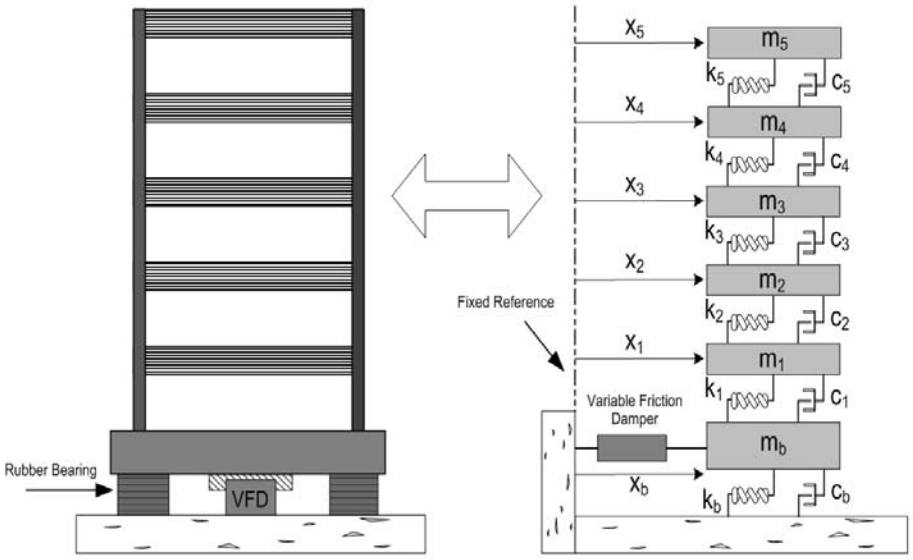

Figure 7.8: Model of smart base-isolated building.

The results of two proposed adaptive control methods for the applied ground motions are presented in Table 7.3. The evaluated response quantities are maximum isolator displacement, $x_{b,\max}$, maximum interstory drift, $d_{s,\max}$, maximum floor

acceleration, $\ddot{x}_{s,\max}$, and maximum damper force, $F_{d,\max}$. The results for the base-isolated building without any damper (uncontrolled structure), for the maximum passive operation of the variable friction dampers, and for the modified clipped-optimal controller, are also given in Table 7.3 for comparison purposes.

It can be seen that passive operation of VFDs with maximum voltage significantly reduces the peak isolation deformation for all considered excitations without an increase in interstory drifts, except in the case of the San Fernando earthquake. The reduction of the maximum base displacement is of the order of 32% to 76%. However, there is a significant amplification in the maximum floor acceleration for most cases. In particular, the maximum floor acceleration increases 306%, 156%, 131% and 23% for San Fernando, Kobe, El Centro and Loma Prieta earthquakes, respectively.

The semi-active control of VFDs notably improves the performance of the base-isolated building, concerning the peak acceleration response at the cost of slight deterioration in the peak isolation deformation. When the performances of three control strategies are compared, it can be seen that developed adaptive control methods are more effective than the clipped-optimal controller, especially in controlling the acceleration response of the base-isolated building. For example, there are 80%, 95% and 109% increases in the peak floor accelerations compared to the uncontrolled cases for El Centro, Kobe, and San Fernando earthquakes respectively, when VFDs are modulated by a clipped-optimal controller, while the same increases are only 30%, 47%, and 58% for the AFNC case and 30%, 28%, and 78% for the SACM.

Table 7.3: Maximum responses of base-isolated building to various seismic excitations.

Earthquake	Response	Uncontrolled	Passive-max	Optimal	AFNC	SACM
El Centro	$x_{b,\max}$ (cm)	20.37	4.95	10.45	10.40	10.69
	$d_{s,\max}$ (cm)	0.12	0.12	0.09	0.08	0.08
	$\ddot{x}_{s,\max}$ (m/s^2)	1.32	3.05	2.37	1.71	1.71
	$F_{d,\max}$ (kN)	-	16.80	16.80	9.28	16.80
San Fernando	$x_{b,\max}$ (cm)	20.57	10.28	11.50	11.36	10.49
	$d_{s,\max}$ (cm)	0.12	0.18	0.10	0.09	0.12
	$\ddot{x}_{s,\max}$ (m/s^2)	1.47	5.97	3.07	2.32	2.62
	$F_{d,\max}$ (kN)	-	16.80	16.80	8.97	16.80
Loma Prieta	$x_{b,\max}$ (cm)	35.75	24.24	30.14	29.71	26.59
	$d_{s,\max}$ (cm)	0.20	0.19	0.20	0.20	0.19
	$\ddot{x}_{s,\max}$ (m/s^2)	2.36	2.91	2.91	2.81	2.49
	$F_{d,\max}$ (kN)	-	16.80	16.80	12.43	16.80
Northridge	$x_{b,\max}$ (cm)	82.17	49.46	60.20	56.37	51.18
	$d_{s,\max}$ (cm)	0.46	0.33	0.36	0.35	0.33
	$\ddot{x}_{s,\max}$ (m/s^2)	5.34	4.11	4.76	4.17	4.24
	$F_{d,\max}$ (kN)	-	16.80	16.80	13.60	16.80
Kobe	$x_{b,\max}$ (cm)	27.94	13.68	18.14	17.16	15.60
	$d_{s,\max}$ (cm)	0.16	0.15	0.18	0.15	0.12
	$\ddot{x}_{s,\max}$ (m/s^2)	1.89	4.84	3.70	2.79	2.42
	$F_{d,\max}$ (kN)	-	16.80	16.80	10.70	16.80
Chi-Chi	$x_{b,\max}$ (cm)	60.19	32.96	39.27	35.05	34.72
	$d_{s,\max}$ (cm)	0.34	0.23	0.24	0.24	0.22
	$\ddot{x}_{s,\max}$ (m/s^2)	3.88	3.14	3.57	2.97	2.67
	$F_{d,\max}$ (kN)	-	16.80	16.80	16.79	16.80

Also, when the performances of adaptive controllers are compared, it is observed that the results of the AFNC and SACM are mostly close to each other; however, the SACM produces slightly better results for the structural response of the base-isolated building while the AFNC commands smaller control forces for most of the excitation cases.

Figures 7.9 and 7.10 show the time histories of the isolator displacement and top floor acceleration for the semi-active control of the base-isolated building with AFNC and SACM subjected to the El Centro and the Chi-Chi earthquakes, respectively. The results of the uncontrolled structure are also provided as a measure of performance evaluation of the semi-active controllers. Also, the force-displacement diagram of the VFDs and the time history of the command voltage for the AFNC and SACM are presented in Figure 7.11 and 7.12 for the same excitation cases. As shown in Figure 7.11, in case of a far-field earthquake such as the El Centro excitation, both adaptive controllers operate the VFDs as passive Coulomb dampers with nearly zero voltage. Therefore, the structural responses for both controllers are very close as illustrated in Figure 7.9.

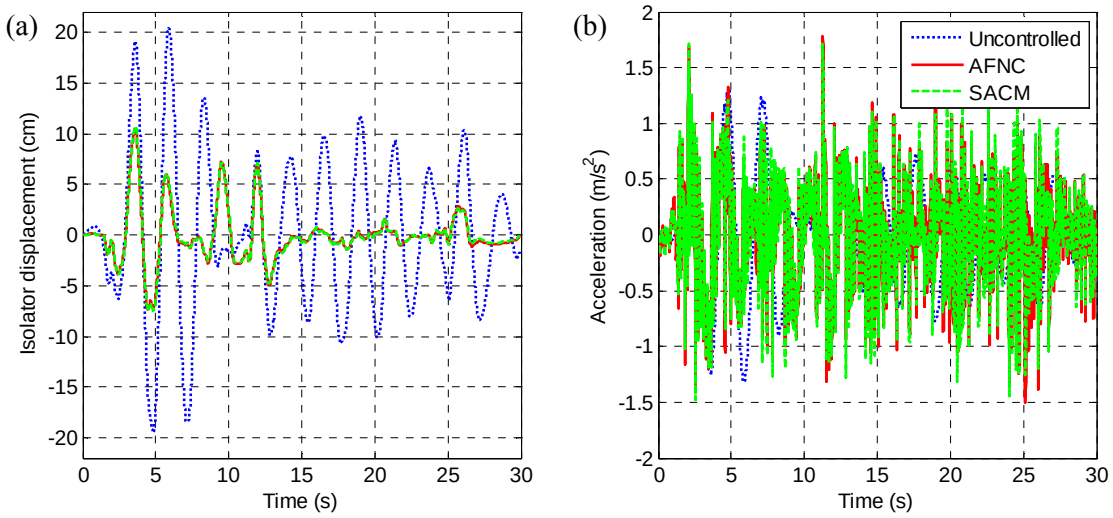

Figure 7.9: Time histories of (a) isolator displacement and (b) top floor acceleration of uncontrolled and semi-active systems subjected to El Centro earthquake.

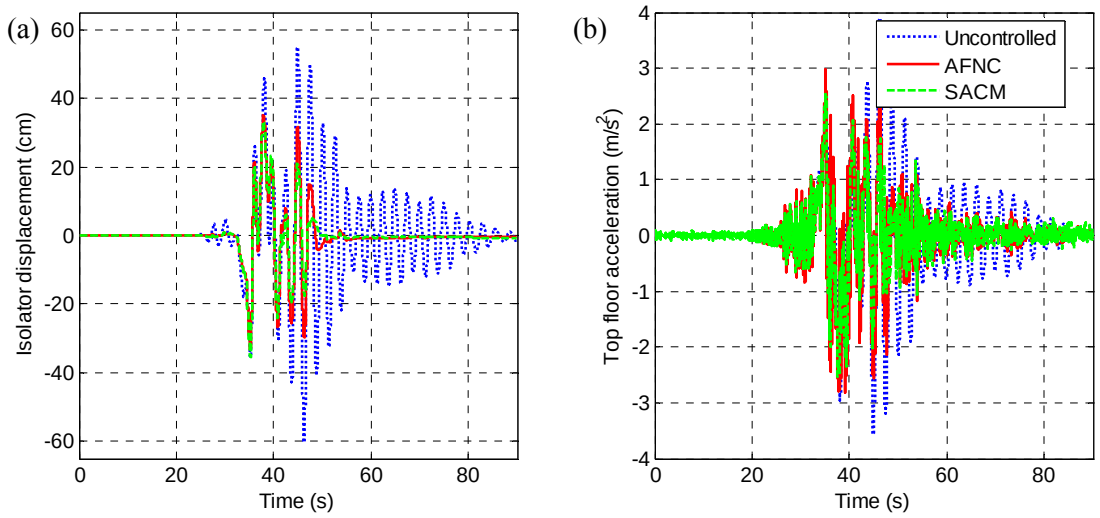

Figure 7.10: Time histories of (a) isolator displacement and (b) top floor acceleration of uncontrolled and semi-active systems subjected to Chi-Chi earthquake.

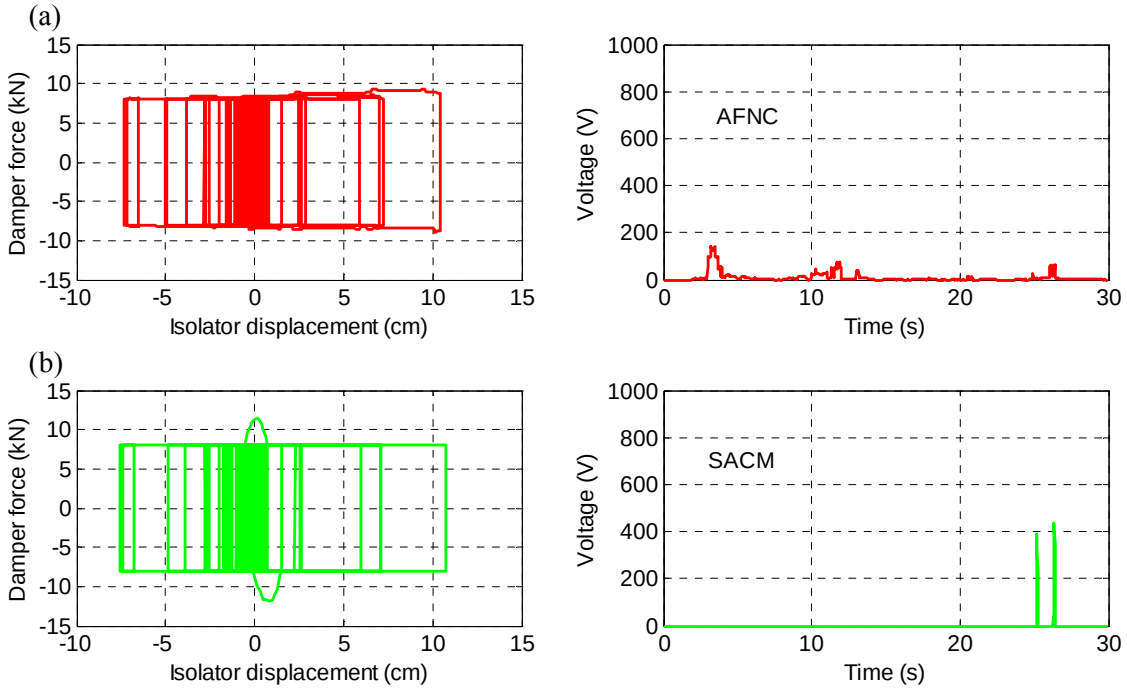

Figure 7.11: Force-displacement diagram of VFDs and time history of command voltage for (a) AFNC and (b) SACM subjected to El Centro earthquake.

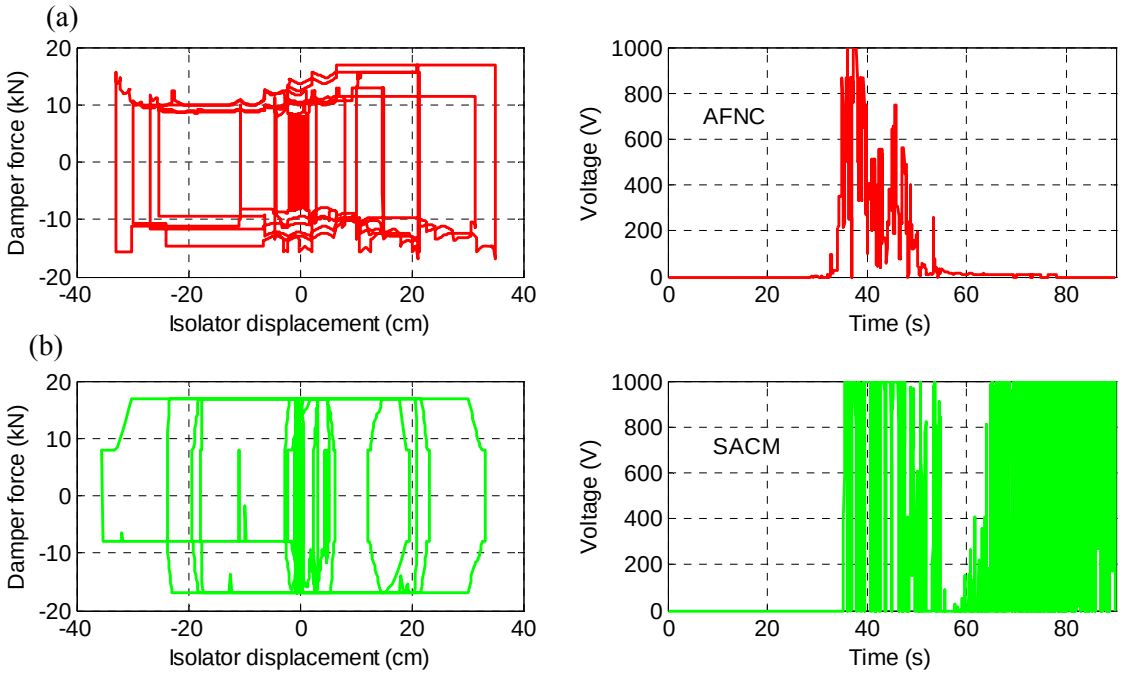

Figure 7.12: Force-displacement diagram of VFDs and time history of command voltage for (a) AFNC and (b) SACM subjected to Chi-Chi earthquake.

When the responses of the base-isolated building subjected to the Chi-Chi earthquake (which has near-field characteristics) are compared for developed adaptive controllers, it can be seen that the peak isolator displacement and top floor acceleration are close to each other. However, the structural response ceases earlier when the dampers are controlled with the SACM. Also, as it is shown in Figure 7.12, the controller developed using the SACM is more aggressive and commands higher voltage values. Overall, both controllers reduce both the displacement and acceleration response of the base isolated building when it is subjected to the Chi-Chi earthquake.

To further assess the performance of the developed controller, the energy balance equations of the base-isolated structure are established. Energy concepts can be used to evaluate the performance of seismically-excited structures since vibrations of structures due to an earthquake can be described as an energy transfer process. For a linear base-isolated structure with an installed variable friction damper, the seismic input energy is the sum of the kinetic energy, the strain energy, the energy dissipated by structural damping, and the energy dissipated by the VFD.

The energy balance equations of the base-isolated structure can be expressed as

$$E_K + E_\xi + E_S + E_H = E_I \tag{7.8}$$

where each term in equation (7.8) can be obtained by integrating individual force terms over the entire relative displacement history and are given as

$$E_K = \frac{1}{2}\dot{x}_t^T M \dot{x}_t \tag{7.9}$$

$$E_{\xi} = \int_0^t \dot{x}^T C \mathrm{d}x = \int_0^t \dot{x}^T C \dot{x} \mathrm{d}t \tag{7.10}$$

$$E_S = \int_0^t x^T K \mathrm{d}x \tag{7.11}$$

$$E_H = -\int_0^t u^T D^T \mathrm{d}x \tag{7.12}$$

$$E_I = -\int_0^t \ddot{x}_g M I \mathrm{d}x \tag{7.13}$$

In the above equations, E_K is the absolute kinetic energy, E_{ξ} is the damping energy, E_S is the elastic strain energy, E_H is the hysteretic energy provided by the VFD, and E_I represents the absolute input energy. Note that E_H is zero for the base-isolated building without any damper. Figure 7.13 shows the time histories of the input energy E_I, the viscous damped energy of the building and rubber bearings E_{ξ}, and the energy dissipated by the VFD E_H, if it is present, for the uncontrolled base-isolated building and the semi-active control of the base-isolated building with the AFNC and the SACM for El Centro earthquake. It can be seen that although input energy somewhat increases when the VFD is installed to the structure, the VFD successfully dissipates most of the input energy. Also, Figure 7.14 illustrates the sum of the kinetic energy and strain energy ($E_K + E_S$) that is known as the total energy of the system or the damage energy. It should be also noted that the maximum damage energy of base-isolated building with the VFD is 60% smaller than without any damper.

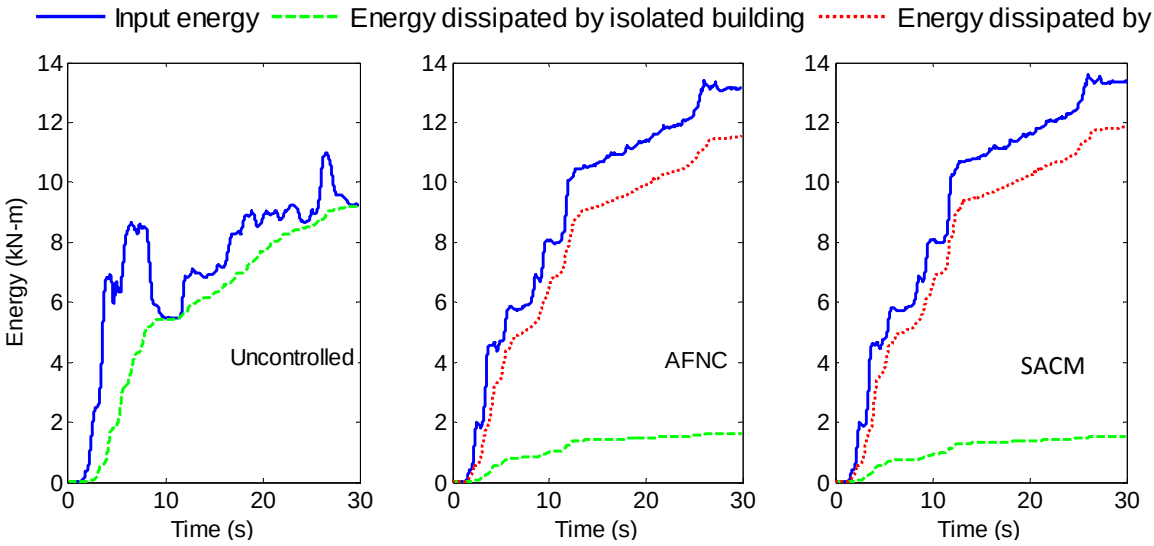

Figure 7.13: Energy time histories for uncontrolled and controlled base-isolated buildings subjected to El Centro earthquake.

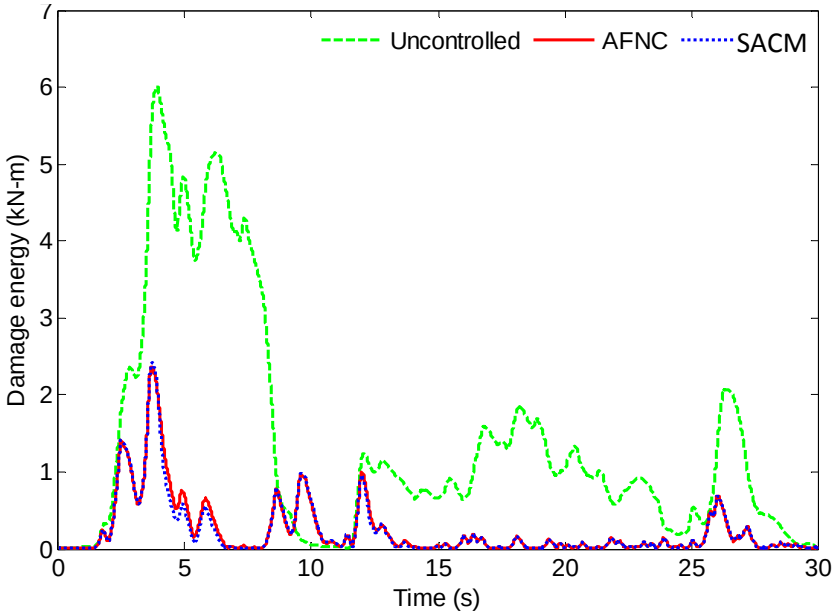

Figure 7.14: Time histories of damage energy for uncontrolled and controlled base-isolated buildings subjected to El Centro earthquake.

8. SEMI-ACTIVE ADAPTIVE CONTROL OF SEISMICALLY EXCITED 20-STORY NONLINEAR BUILDING

The effectiveness of using the SACM to improve the performance of a structure with linear behavior was studied in the previous sections. The SACM was compared to other control methods such as fuzzy control, clipped optimal control, passive control systems, Lyapunov controller etc. Using the SACM to control the structural performance was satisfactory. Particularly, the SACM was very successful in reducing the maximum acceleration. In this section, the structural response of a nonlinear building controlled with the SACM is studied and the performance of the SACM in controlling nonlinear systems is assessed.

8.1. Case Study

To study the performance of the adaptive controller, numerical simulation of a 20-story building with nonlinear behavior is performed and the responses of the controlled structure are evaluated. This building is a steel moment resisting frame (SMRF) designed as part of a SAC steel project for the Los Angeles area; it has been used as a benchmark control problem (Ohtori et al. 2004). Although this building is not actually constructed, it meets the requirements of the seismic code. The building is an office building designed for gravity, wind, and seismic loads. The North-South frame of the 20-story structure has five fully moment-resisting bays and its East-West frame has

six moment-resisting bays (Figure 8.1). It is 30.48 m by 36.54 m in plan, and 80.77 m in elevation (Ohtori et al. 2004). The seismic mass of the ground, first and 20^{th} level are 5.32×10^5 kg, 5.63×10^5 kg and 5.84×10^5 kg, respectively. The seismic mass of the second level to 19^{th} level is 5.52×10^5 kg. The first ten natural frequencies of the 20-story benchmark structure are 0.261, 0.753, 1.30, 1.83, 2.40, 2.44, 2.92, 3.01, 3.63, and 3.68 Hz. The nonlinear behavior of the structure is a result of structural members yielding. As shown in Figure 8.2, a bilinear hysteresis model is used to model the yielding and the formation of plastic hinges of structural members (Ohtori et al. 2004). It is assumed that the plastic hinges occur at moment resisting column-column and column-beam connections. The Newmark-β method is used to solve the nonlinear equations of motion. More details about this benchmark problem and the nonlinear model can be found in Ohtori et al. (2004).

It is assumed that two MR dampers are located on the first to seventeenth stories and one MR damper is located on each of the top three stories. The capacity of each MR damper is 1000 kN. The Bouc-Wen model is used to model the dynamic behavior of MR dampers (Yoshida and Dyke 2005).

To evaluate the proposed adaptive control strategy, the performance of the 20-story building is studied when the structure is subjected to the El Centro, the Hachinohe, the Northridge and the Kobe earthquakes with different PGA levels (0.5, 1 and 1.5 times the magnitude of the El Centro, Hachinohe; 0.5 and 1 times the magnitude of Northridge and Kobe). The absolute peak acceleration of the earthquakes records are 3.42, 2.25,

8.27 and 8.18 m/s^2, respectively. For the SACM, the value of σ, T and $\overline{T}$ are chosen to be 0, 10 $I_{20\times20}$ and 1 $I_{20\times20}$, respectively.

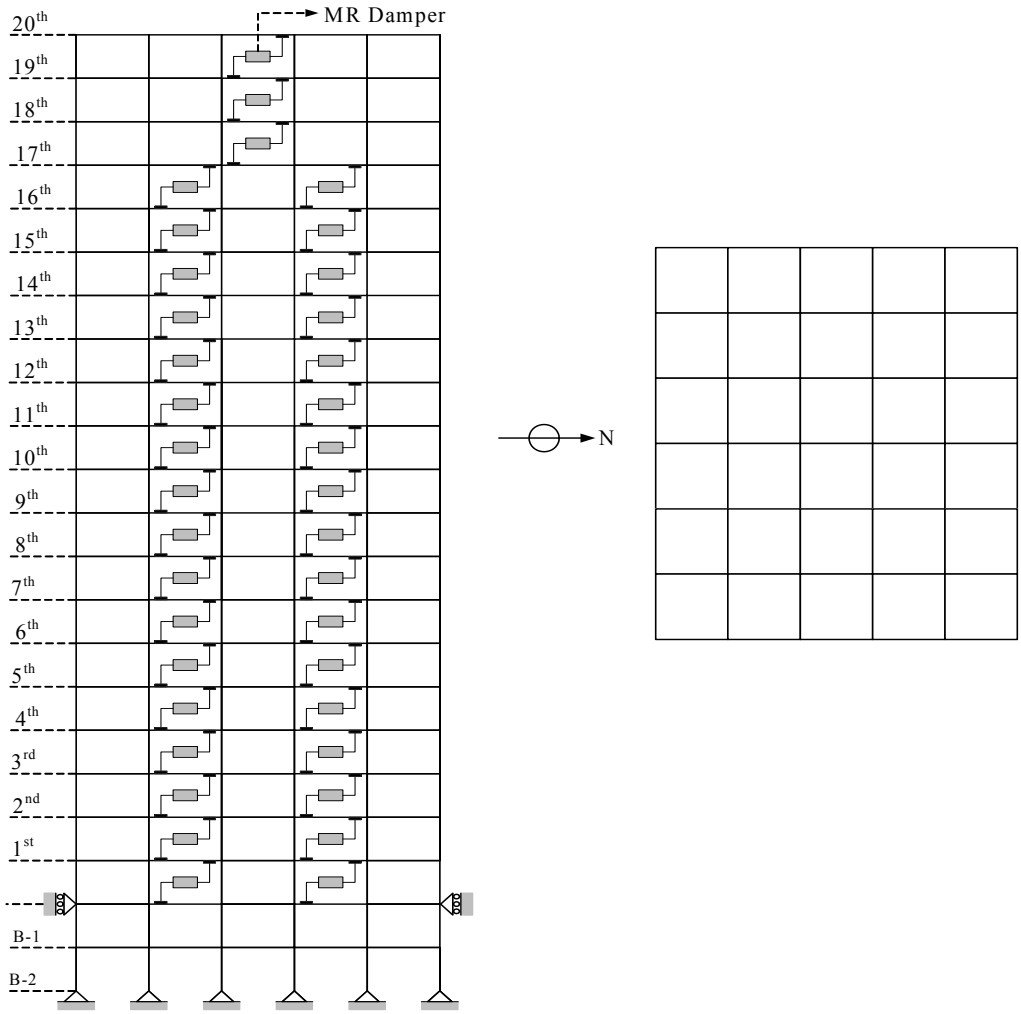

Figure 8.1: 20-story benchmark building N-S MRF.

The output of the plant is defined as the velocities of each story. As mentioned in Section 2.3, the order of control command, model output and plant output should be equal. There is at least one MR damper at each story, then the order of control command,

u_p, is 20 assuming that the MR dampers at one story generate equal forces. Therefore the order of plant output should be 20, but it is not logical to have one sensor at each story for tall buildings with many degrees of freedom. A Kalman estimator is designed to calculate the velocities of all stories if there are five sensors measuring velocities of the 5^{th}, 8^{th}, 12^{th}, 15^{th} and 20^{th} stories. The matrices Q and R are selected as 37 and $I_{20\times20}$ for Kalman estimator.

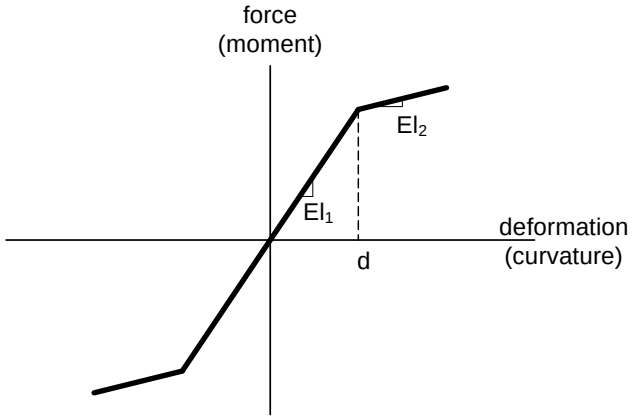

Figure 8.2: Bilinear hysteresis model for structural member bending.

8.2. Results and Discussions

Table 8.1 compares the maximum displacement, velocity, acceleration and interstory drift of the controlled structure with the response of the uncontrolled structure. It can be seen that the SACM significantly reduces the peak displacement and drift. In particular, the maximum floor displacements decrease by 71%, 73%, and 77% for El Centro with 0.5, 1 and 1.5 intensity. The results show that the SACM is also effective in decreasing the maximum acceleration. The maximum acceleration of the controlled structure is 54%, 55% and 30% less than the maximum acceleration of the uncontrolled

structure for El Centro with 0.5, 1 and 1.5 intensity. Table 8.1 shows that the maximum drift of the controlled structure is about 46%, 44% and 37% of the maximum drift of the uncontrolled structure while the maximum velocity of the controlled structure is 37%, 38% and 33% of the maximum velocity of the uncontrolled structure for El Centro with 0.5, 1 and 1.5 intensity, respectively. The results presented in Table 8.1 for other earthquakes also show that the SACM is very effective in reducing the structural response of the building.

The profiles of maximum story drift and acceleration are shown in Figures 8.3 to 8.6. It can be seen that the SACM decreases the maximum drift of each floor and it never increases the interstory drift comparing the performance of the uncontrolled structure. Also, these figures show that the maximum acceleration of the structure is significantly reduced when MR damper and the SACM are used to control the performance of the structure, although in some cases the maximum acceleration on a specific floor may increase. Figures 8.7 to 8.14 illustrate the time histories of the first floor and roof displacement, velocity and acceleration when the building subjected to different earthquakes. Due to the development of plastic connections, permanent drifts and displacements may occur when the structure is subjected to severe earthquakes.

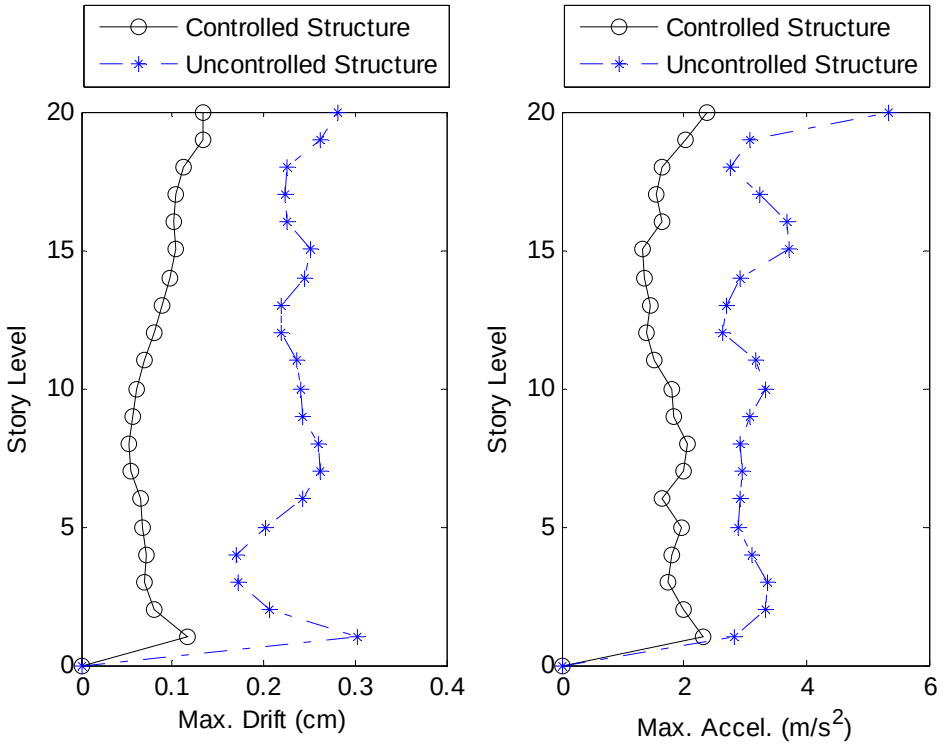

Figure 8.3: Maximum interstory drift and absolute acceleration for each floor of the structure subjected to El Centro earthquake (intensity =1).

As shown in Figures 8.11 and 8.13, the permanent displacement for the first floor is significantly reduced by using the SACM and MR dampers to control the structural behavior. It can be concluded that the SACM can improve the performance of the controlled structure significantly. Figure 8.15 illustrates the maximum force generated by the MR damper which was used to control the nonlinear building. It can be noted that larger forces are needed for the first eight stories while the force that is generated by the MR damper installed between the 16^{th} and 17^{th} floors is smallest when El Centro and Hachinohe are applied to the structure. As shown in Figure 8.15, larger forces are required to control the performance of the structure under the Northridge and the Kobe earthquakes which are more severe earthquakes.

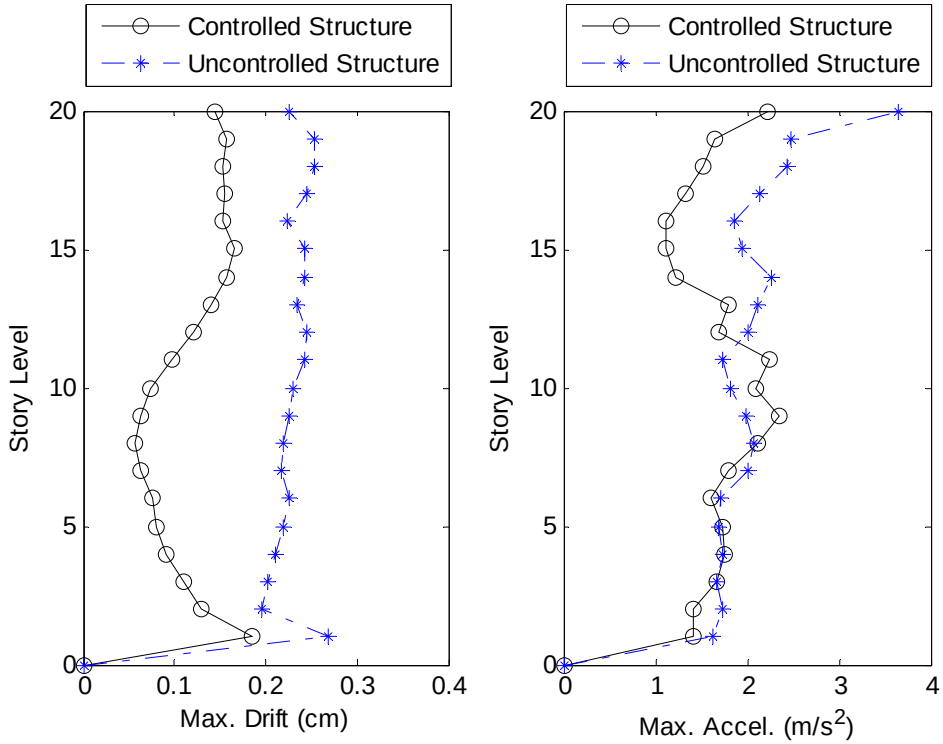

Figure 8.4: Maximum interstory drift and absolute acceleration for each floor of the structure subjected to Hichanohe earthquake (intensity =1).

To evaluate the SACM and compare its performance with that of other control methods, fourteen evaluation criteria defined in the benchmark control problem (Ohtori et al. 2004) are used. The summary of evaluation criteria for the nonlinear benchmark problem is presented in Figure 8.16. The evaluation criteria for the SACM and passive-on are calculated and presented in Tables 8.2 and 8.3, respectively. Table 8.4 summarizes the computed performance indices for the modified clipped optimal control (MCOC) adopted from Yoshida et al. (2004). Yoshida et al. assumed that four MR dampers were located on the first eight stories, three MR dampers were located on the next nine stories and two MR dampers were located on the top three stories. The total number of MR dampers used in the Yoshida et al. work was 65 while 37 MR dampers

are used in this study to control the performance of the 20-story building with the SACM and passive-on. Results presented in Tables 8.2 and 8.4 show that, although a lesser number of MR dampers is used in the structure controlled with the SACM, the SACM is more successful than the MCOC in reducing the structural response, especially the drift ratio. Although the structure controlled with passive-on has smaller maximum drift than the one controlled with the SACM, passive-on increases the acceleration of the structure 2~7 times.

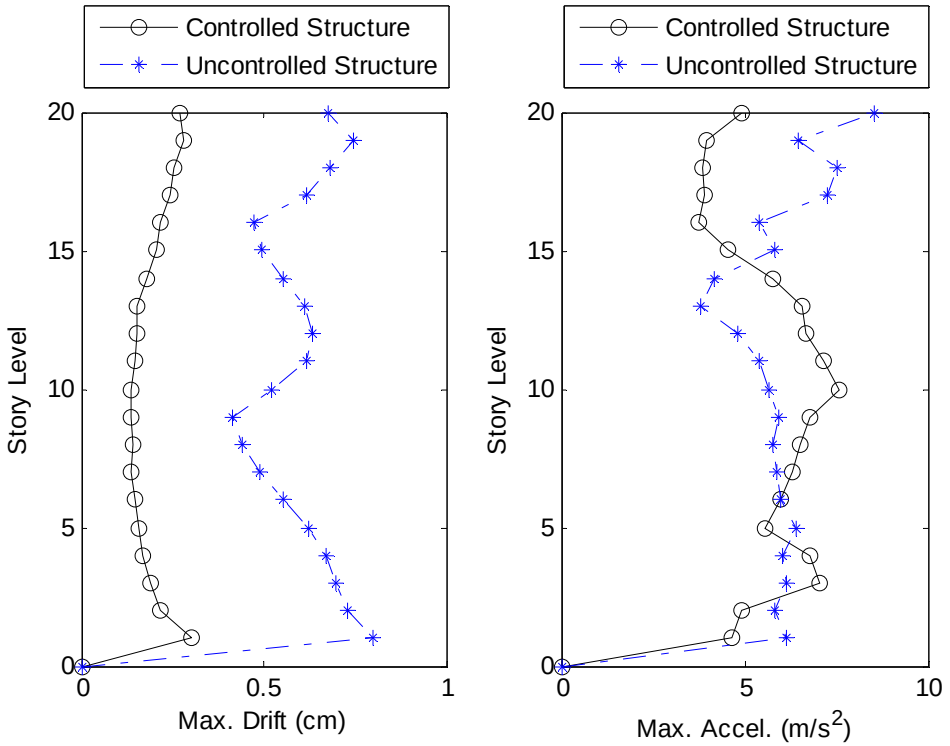

Figure 8.5: Maximum interstory drift and absolute acceleration for each floor of the structure subjected to Northridge earthquake (intensity =1).

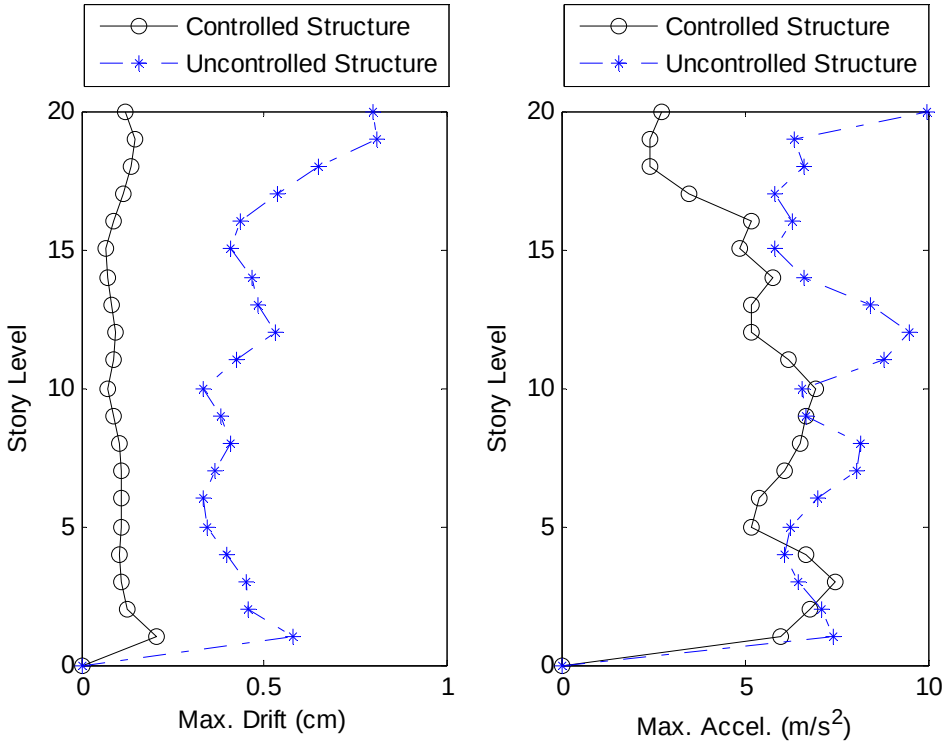

Figure 8.6: Maximum interstory drift and absolute acceleration for each floor of the structure subjected to Kobe earthquake (intensity =1).

The results show that the amount of energy dissipated through structural yielding is reduced more in the SACM than the MCOC and passive-on except for the structure under the 1.5-scaled El Centro where the MCOC is more successful. The SACM is capable of reducing the ductility ratio by 27% to 83% which shows that it is more effective than the MCOC. However, comparison of J_7 reveals that passive-on is somewhat more effective than the SACM in reducing the ductility.

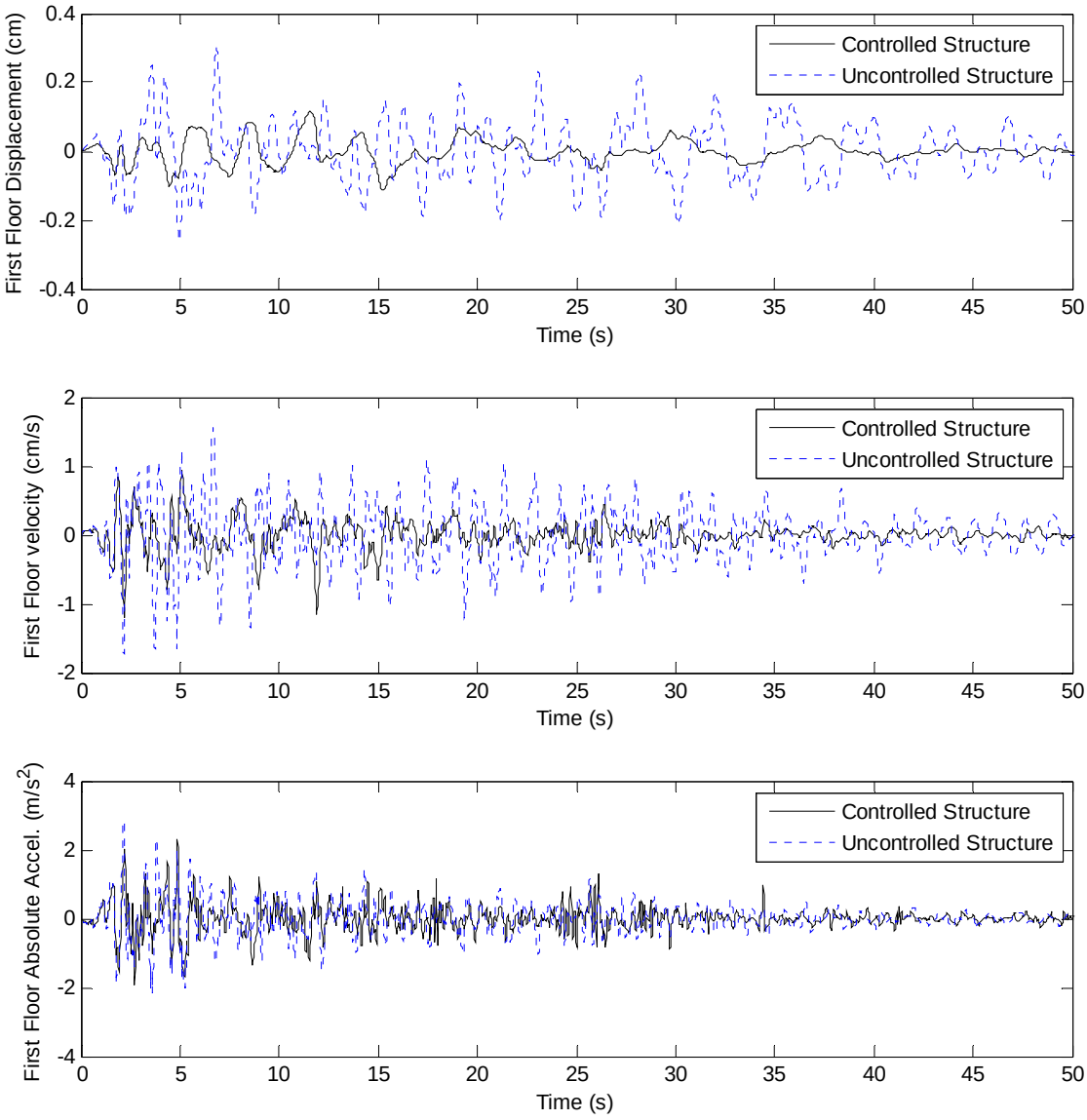

Figure 8.7: Time histories of first floor acceleration, velocity and displacement of uncontrolled and controlled structures subjected to El Centro earthquake (intensity =1).

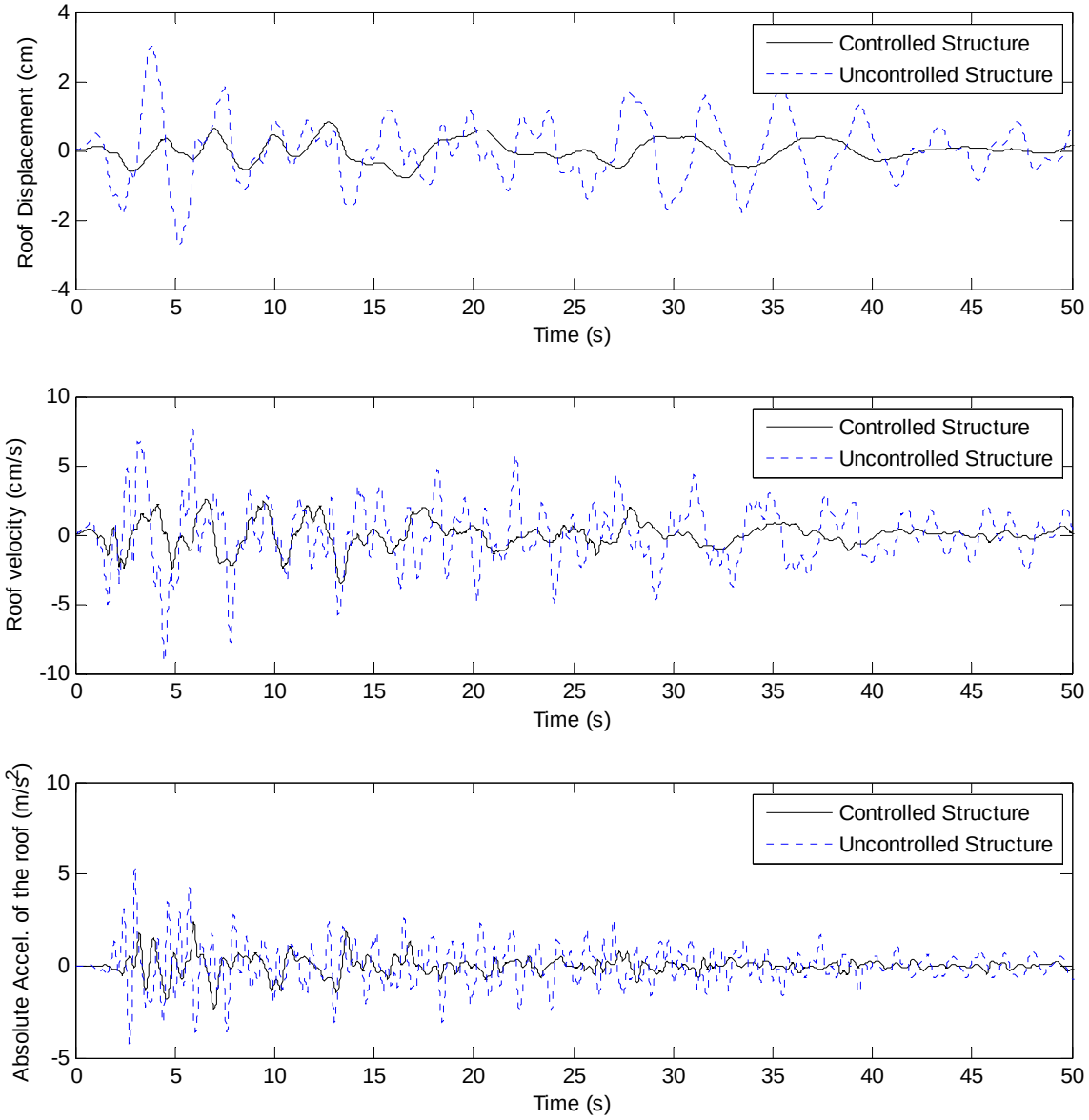

Figure 8.8: Time histories of top floor acceleration, velocity and displacement of uncontrolled and controlled structures subjected to El Centro earthquake (intensity =1).

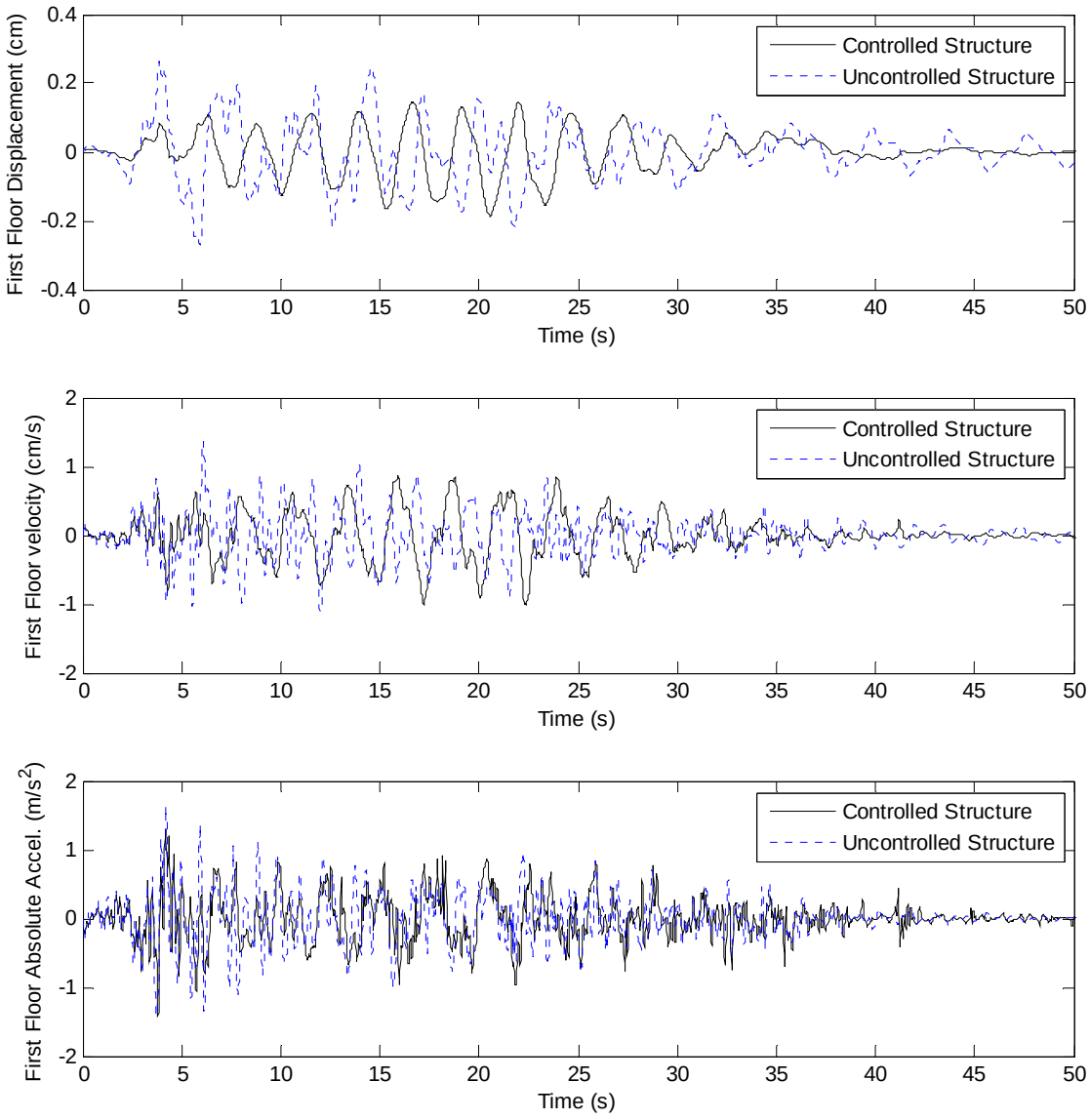

Figure 8.9: Time histories of first floor acceleration, velocity and displacement of uncontrolled and controlled structures subjected to Hichanohe earthquake (intensity =1).

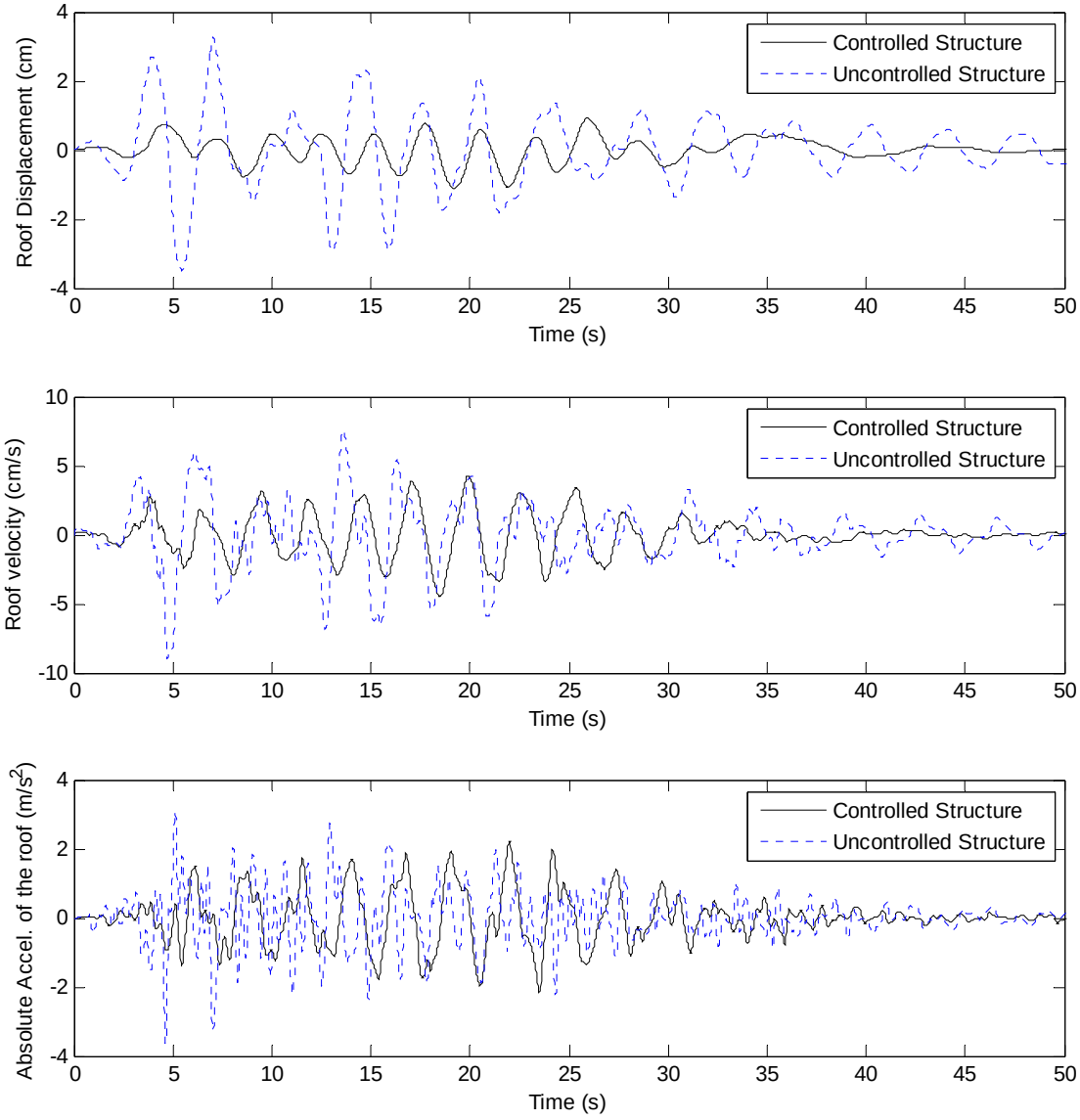

Figure 8.10: Time histories of top floor acceleration, velocity and displacement of uncontrolled and controlled structures subjected to Hichanohe earthquake (intensity =1).

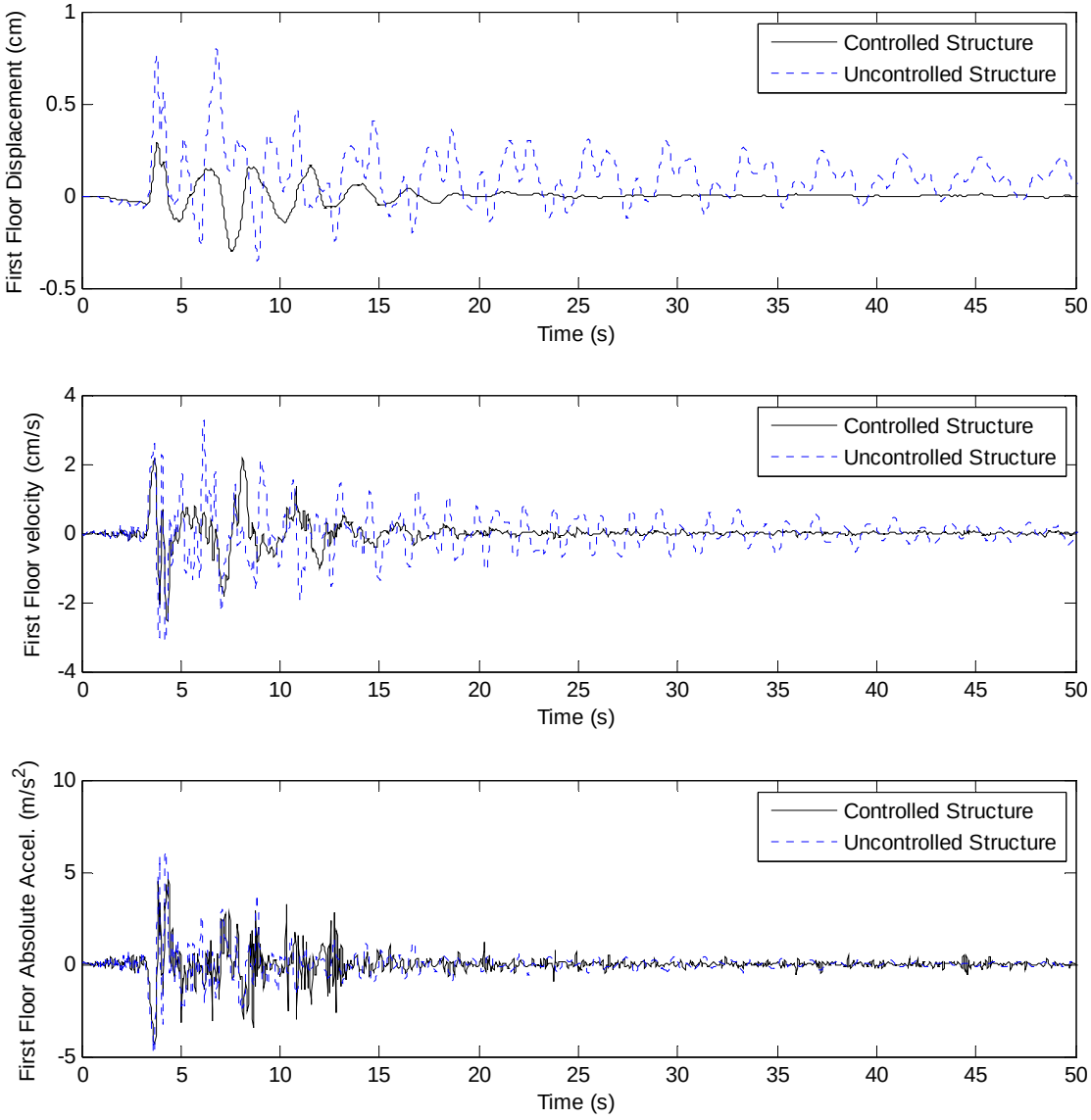

Figure 8.11: Time histories of first floor acceleration, velocity and displacement of uncontrolled and controlled structures subjected to Northridge earthquake (intensity =1).

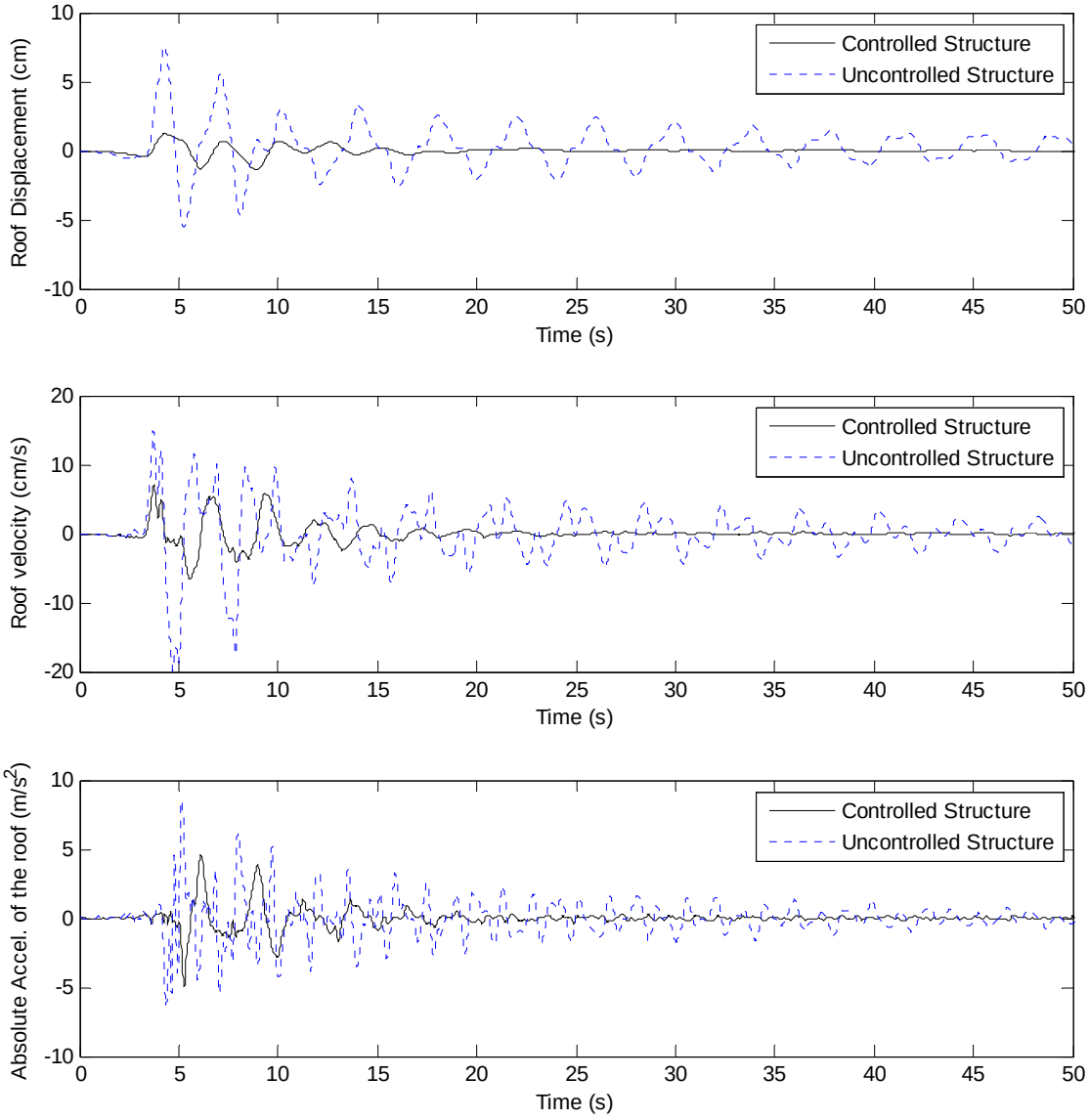

Figure 8.12: Time histories of top floor acceleration, velocity and displacement of uncontrolled and controlled structures subjected to Northridge earthquake (intensity =1).

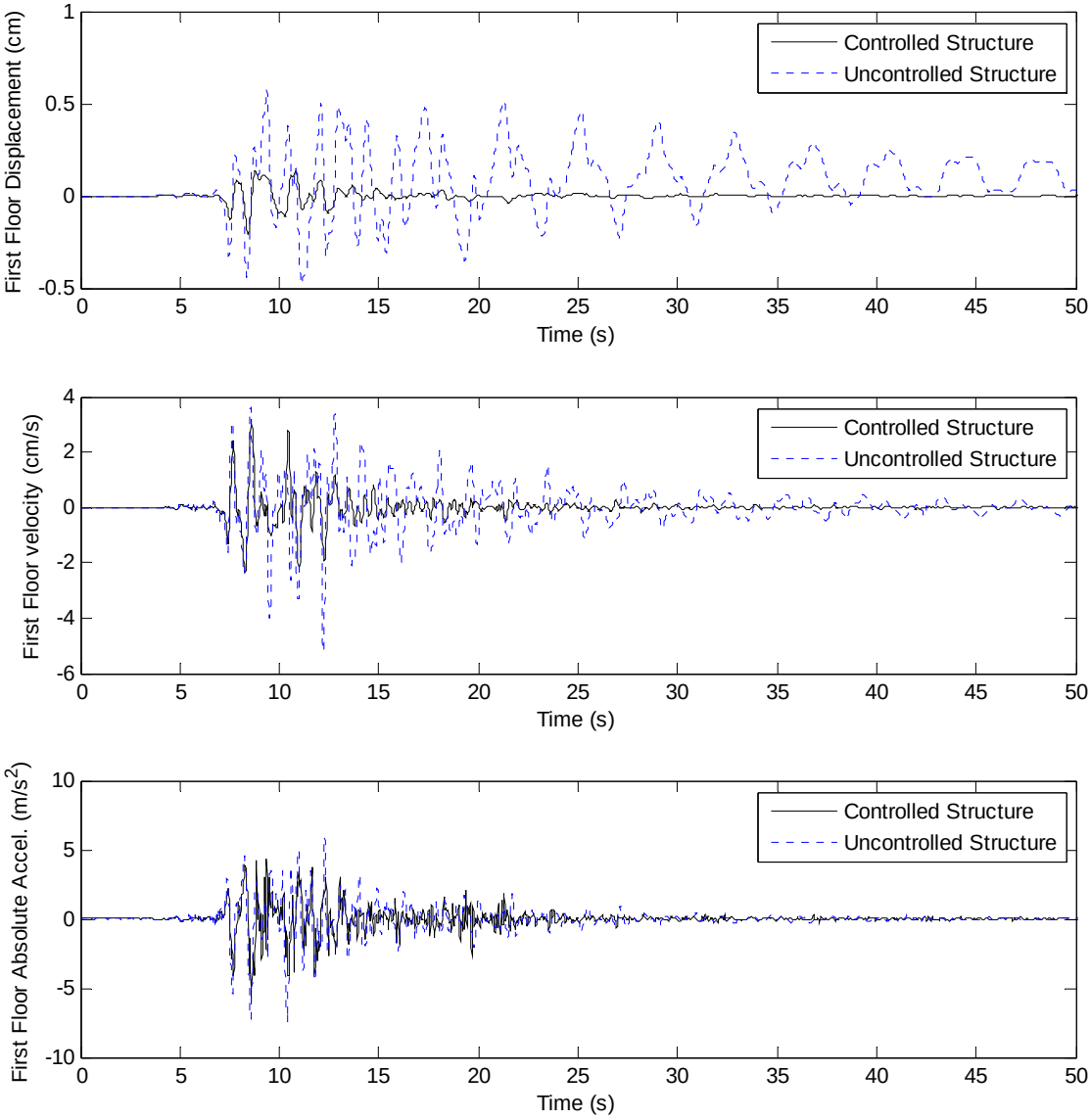

Figure 8.13: Time histories of first floor acceleration, velocity and displacement of uncontrolled and controlled structures subjected to Kobe earthquake (intensity =1).

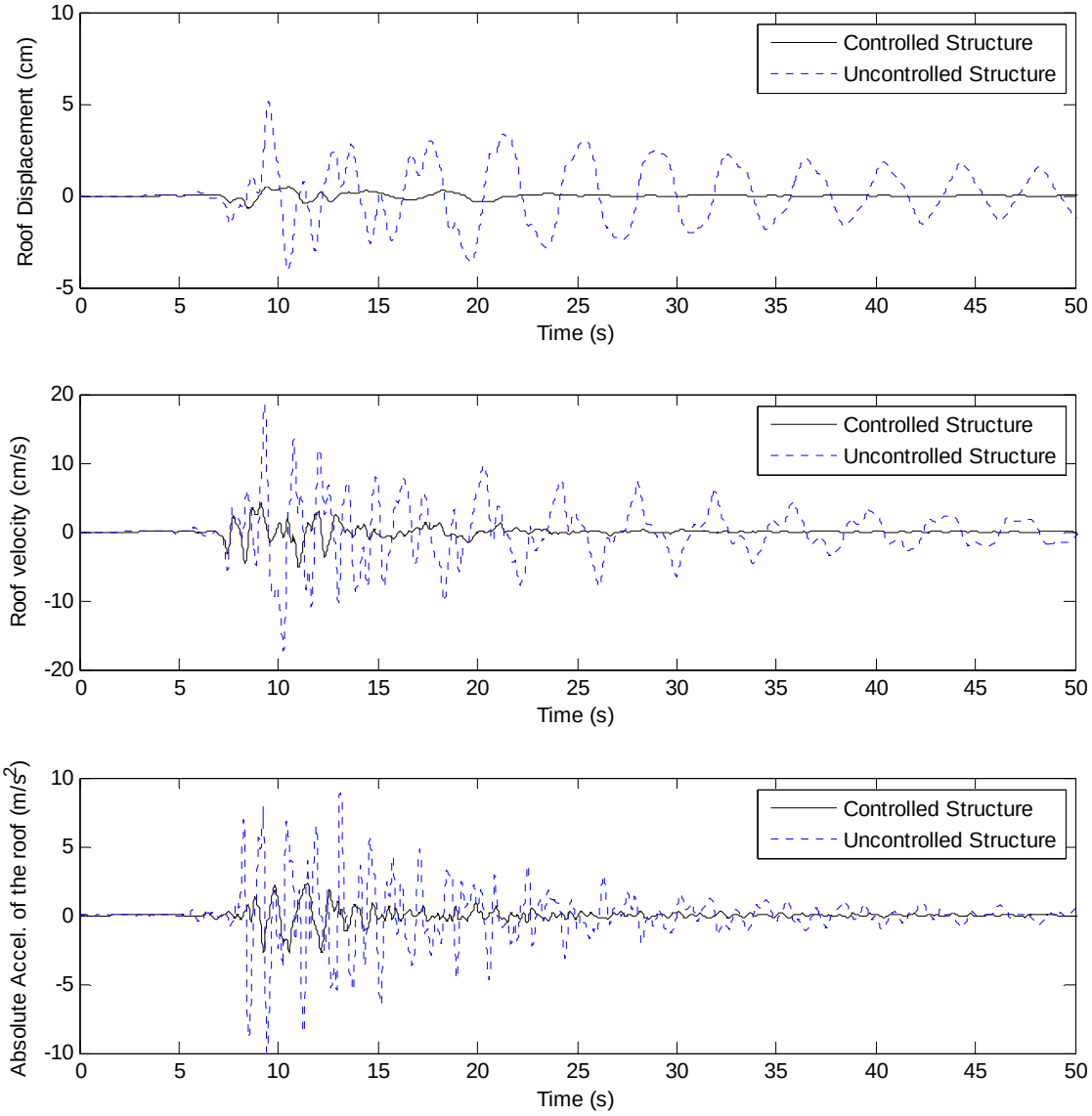

Figure 8.14: Time histories of top floor acceleration, velocity and displacement of uncontrolled and controlled structures subjected to Kobe earthquake (intensity =1).

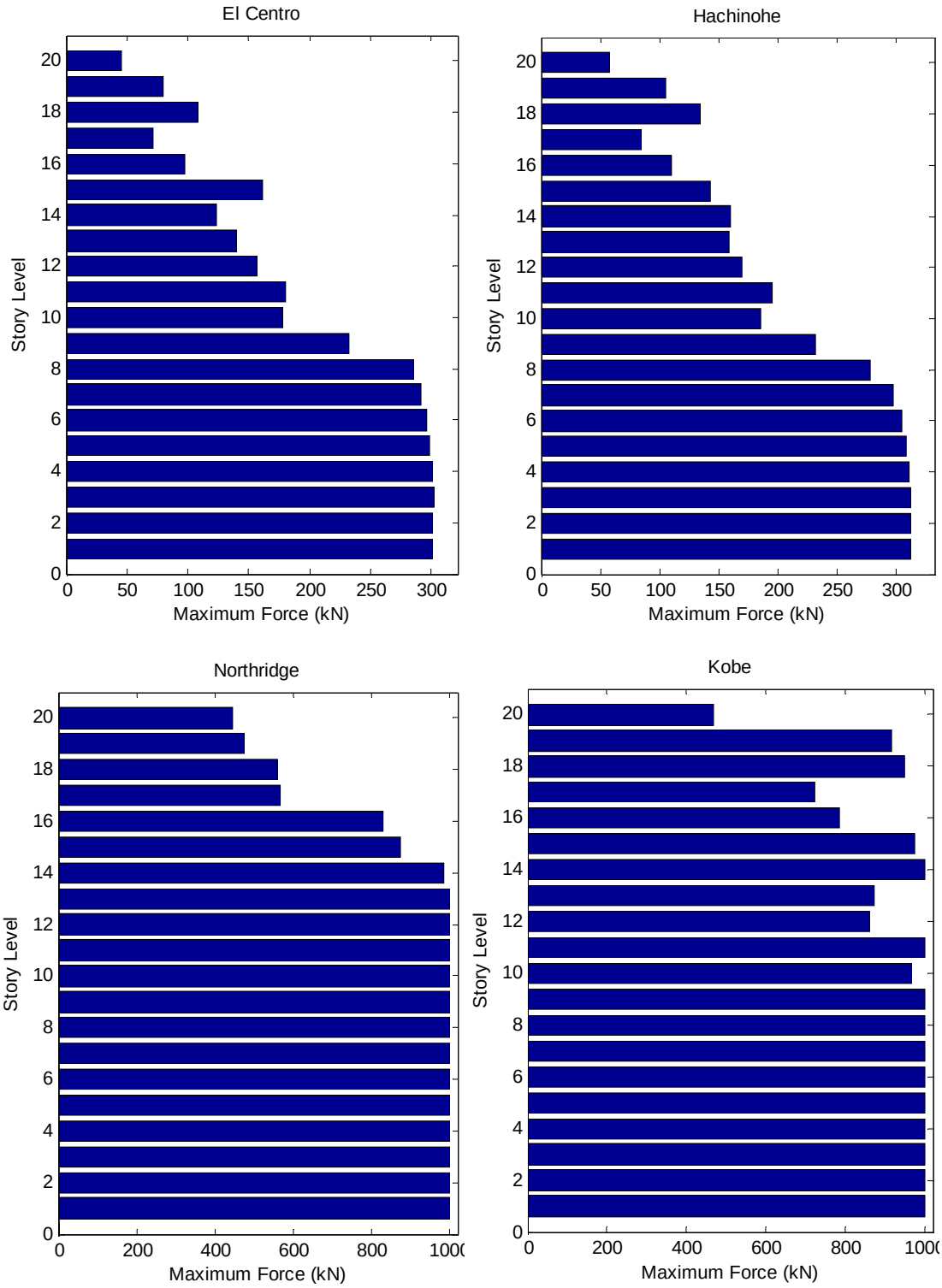

Figure 8.15: Maximum force generated by one MR Damper at each story (intensity =1) for different earthquake.

Interstory Drift Ratio $J_1 = \max\left\{\frac{\max\frac{\lvert d_i(t)\rvert}{h_i}}{\delta^{\max}}\right\}$	Level Acceleration $J_2 = \max\left\{\frac{\max\lvert \ddot{x}_{ai}(t)\rvert}{\ddot{x}_a^{\max}}\right\}$	Base Shear $J_3 = \max\left\{\frac{\max\lvert \sum m_i \ddot{x}_i(t)\rvert}{F_b^{\max}}\right\}$
Normed Interstory Drift Ratio $J_4 = \max\left\{\frac{\max\frac{\lVert d_i(t)\rVert}{h_i}}{\lVert \delta^{\max}\rVert}\right\}$	Normed Level Acceleration $J_5 = \max\left\{\frac{\max\lVert \ddot{x}_{ai}(t)\rVert}{\lVert \ddot{x}_a^{\max}\rVert}\right\}$	Normed Base Shear $J_6 = \max\left\{\frac{\lVert \sum m_i \ddot{x}_i(t)\rVert}{\lVert F_b^{\max}\rVert}\right\}$
Ductility $J_7 = \max\left\{\frac{\max\frac{\lvert \phi_i(t)\rvert}{\phi_{yi}}}{\phi^{\max}}\right\}$	Dissipated Energy $J_8 = \max\left\{\frac{\max\frac{\int dE_j}{F_{yj}\cdot\phi_{yi}}}{E^{\max}}\right\}$	Plastic Connections $J_9 = \max\left\{\frac{N_d^C}{N^d}\right\}$
Normed Ductility $J_{10} = \max\left\{\frac{\max\frac{\lVert \phi_i(t)\rVert}{\phi_{yi}}}{\lVert \phi^{\max}\rVert}\right\}$	Control Force $J_{11} = \max\left\{\frac{\max\lvert f_l(t)\rvert}{W}\right\}$	Control Device Stroke $J_{12} = \max\left\{\frac{\max\lvert y_i^a(t)\rvert}{x^{\max}}\right\}$
Control Power $J_{13} = \max\left\{\frac{\max\left[\sum \Phi_l(t)\right]}{\dot{x}^{\max}W}\right\}$	Normed Control Power $J_{14} = \max\left\{\frac{\sum\frac{1}{t_f}\int_0^{t_f}\Phi_l(t)}{\dot{x}^{\max}W}\right\}$	

Figure 8.16: Summary of evaluation criteria for the nonlinear benchmark problem (Ohtori et al. 2004).

Table 8.1: Maximum response of the controlled 20-story building.

		Controlled	Uncontrolled
El Centro intensity =0.5	max displ. (cm)	0.44157	1.5219
	max vel. (cm/s)	1.6992	4.5783
	max drift (cm)	0.069803	0.15087
	max acc. (m/s^2)	1.2073	2.6696
	max force kN	51.2952	
El Centro intensity =1	max displ. (cm)	0.81874	3.0439
	max vel. (cm/s)	3.524	9.1566
	max drift (cm)	0.1345	0.30174
	max acc. (m/s^2)	2.3664	5.3392
	max force kN	301.8697	
El Centro intensity =1.5	max displ. (cm)	1.0288	4.5352
	max vel. (cm/s)	4.3834	13.0069
	max drift (cm)	0.15721	0.42158
	max acc. (m/s^2)	5.4173	7.7856
	max force kN	994.806	
Hachinohe intensity =0.5	max displ. (cm)	0.59731	1.7397
	max vel. (cm/s)	2.3439	4.5122
	max drift (cm)	0.10152	0.13474
	max acc. (m/s^2)	1.2289	1.8291
	max force kN	48.8397	
Hachinohe intensity =1	max displ. (cm)	1.107	3.4795
	max vel. (cm/s)	4.5007	9.0244
	max drift (cm)	0.186	0.26948
	max acc. (m/s^2)	2.3465	3.6582
	max force kN	311.9414	
Hachinohe intensity =1.5	max displ. (cm)	1.4233	4.9178
	max vel. (cm/s)	5.9384	12.684
	max drift (cm)	0.21673	0.39353
	max acc. (m/s^2)	4.8011	4.7152
	max force kN	750.3641	
Northridge intensity =0.5	max displ. (cm)	0.84867	4.894
	max vel. (cm/s)	4.0279	16.6159
	max drift (cm)	0.18202	0.48627
	max acc. (m/s^2)	4.2137	6.0076
	max force kN	1000	
Northridge intensity =1	max displ. (cm)	1.3628	7.5036
	max vel. (cm/s)	7.4291	20.3901
	max drift (cm)	0.3019	0.80084
	max acc. (m/s^2)	7.5723	8.5107
	max force kN	1000	
Kobe intensity =0.5	max displ. (cm)	0.38378	3.1409
	max vel. (cm/s)	3.3781	13.1453
	max drift (cm)	0.12354	0.51703
	max acc. (m/s^2)	2.8478	7.4945
	max force kN	382.5348	
Kobe intensity =1	max displ. (cm)	0.70539	5.1734
	max vel. (cm/s)	6.0974	18.458
	max drift (cm)	0.20549	0.81154
	max acc. (m/s^2)	7.4894	9.9741
	max force kN	1000	

Table 8.2: Evaluation criteria for the structure controlled with SACM.

	Intensity	El Centro	Hachi	Northridge	Kobe	Max. Value
J_1	0.5	0.4974	0.6848	0.4063	0.2885	0.6848
	1	0.4792	0.6557	0.3783	0.1844	
	1.5	0.3729	0.5556			
J_2	0.5	0.4522	0.6719	0.7014	0.38	1.0182
	1	0.4432	0.6414	0.8897	0.7509	
	1.5	0.6958	1.0182			
J_3	0.5	0.428	0.7979	0.5643	0.3074	0.7979
	1	0.4448	0.7465	0.6697	0.6159	
	1.5	0.5349	0.7278			
J_4	0.5	0.2979	0.6623	0.2644	0.1915	0.6623
	1	0.2836	0.6153	0.0989	0.0415	
	1.5	0.23	0.4936			
J_5	0.5	0.3311	0.716	0.3446	0.296	0.716
	1	0.3058	0.6565	0.4268	0.4123	
	1.5	0.3078	0.5554			
J_6	0.5	0.3201	0.6076	0.2646	0.1626	0.6076
	1	0.2946	0.5826	0.3604	0.2741	
	1.5	0.2648	0.5084			
J_7	0.5	0.4275	0.7299	0.3344	0.1816	0.7299
	1	0.4135	0.6711	0.2807	0.1794	
	1.5	0.3016	0.4764			
J_8	0.5	-	-	2.01E-07	3.75E-06	5.06E-06
	1	-	-	8.8E-08	7.71E-07	
	1.5	5.06E-06	0.000000763			
J_9	0.5	-	-	0	0	0
	1	-	-	0	0	
	1.5	0	0			
J_{10}	0.5	0.4283	0.7997	0.2498	0.1952	0.7997
	1	0.3806	0.7367	0.0887	0.0433	
	1.5	0.2749	0.5932			
J_{11}	0.5	0.0009	0.0009	0.0184	0.007	0.0184
	1	0.0056	0.0057	0.0184	0.0184	
	1.5	0.0183	0.0138			
J_{12}	0.5	0.0459	0.0584	0.0372	0.0393	0.0584
	1	0.0442	0.0535	0.0402	0.0397	
	1.5	0.0347	0.0441			
J_{13}	0.5	0.0005	0.0007	0.0085	0.0037	0.0178
	1	0.0029	0.0035	0.0151	0.0178	
	1.5	0.0082	0.0084			
J_{14}	0.5	0	0	0	0	0.0002
	1	0.0001	0.0001	0.0002	0.0001	
	1.5	0.0001	0.0002			

Table 8.3: Evaluation criteria for the structure controlled with Passive-on.

	Intensity	El Centro	Hachi	Northridge	Kobe	Max. Value
J_1	0.5	0.45403	0.599633	0.246119	0.165611	0.599633
	1	0.291675	0.359135	0.26919	0.155374	
	1.5	0.285066	0.328686			
J_2	0.5	5.018644	7.220535	2.29239	1.876086	7.220535
	1	2.617318	3.662916	1.633237	1.405283	
	1.5	1.816152	3.009723			
J_3	0.5	1.013003	1.309018	0.459556	0.382767	1.309018
	1	0.631106	0.757154	0.635394	0.556436	
	1.5	0.578882	0.565312			
J_4	0.5	0.441866	0.57709	0.173229	0.110958	0.57709
	1	0.353438	0.35904	0.065105	0.03566	
	1.5	0.326092	0.32098			
J_5	0.5	18.02094	25.37194	8.68098	9.177282	25.37194
	1	8.990937	12.55535	6.836219	6.884289	
	1.5	6.135995	8.602495			
J_6	0.5	2.072777	2.244844	0.734777	0.953611	2.244844
	1	1.081219	1.140641	0.689236	0.781872	
	1.5	0.764556	0.80064			
J_7	0.5	0.386808	0.566806	0.218301	0.115013	0.566806
	1	0.32554	0.369639	0.245051	0.159865	
	1.5	0.285888	0.289319			
J_8	0.5	-	-	0.000315	0.000402	0.004496
	1	-	-	8.23E-05	2.12E-05	
	1.5	0.000242	0.004496			
J_9	0.5	-	-	0	0	0
	1	-	-	0	0	
	1.5	0	0			
J_{10}	0.5	0.660441	0.71776	0.175014	0.133938	0.71776
	1	0.558675	0.47168	0.072527	0.042684	
	1.5	0.454532	0.421204			
J_{11}	0.5	0.018406	0.018406	0.018406	0.018406	0.018406
	1	0.018406	0.018406	0.018406	0.018406	
	1.5	0.018406	0.018406			
J_{12}	0.5	0.041866	0.043998	0.022758	0.022577	0.043998
	1	0.031991	0.028923	0.037042	0.033748	
	1.5	0.030116	0.024534			
J_{13}	0.5	0.080993	0.091803	0.024221	0.030675	0.091803
	1	0.04584	0.047931	0.024054	0.026459	
	1.5	0.032572	0.034991			
J_{14}	0.5	0.033175	0.03539	0.009377	0.012065	0.03539
	1	0.017937	0.018043	0.008057	0.008792	
	1.5	0.011976	0.012558			

Table 8.4: Evaluation criteria for the structure controlled with Modified Clipped Optimal Control (MCOC) (Yoshida and Dyke 2005).

	Intensity	El Centro	Hachi	Northridge	Kobe	Max. Value
J_1	0.5	0.6957	0.7867	0.691	0.5495	0.906
	1	0.645	0.7707	0.906	0.5324	
	1.5	0.6007	0.818			
J_2	0.5	0.6149	0.8171	0.7167	0.6228	0.8195
	1	0.5568	0.7673	0.8195	0.741	
	1.5	0.6156	0.8175			
J_3	0.5	0.8145	1.0519	1.0019	0.766	1.0793
	1	0.8283	1.0507	1.0777	1.0793	
	1.5	0.9612	1.0623			
J_4	0.5	0.5568	0.7761	0.4557	0.3563	1.1881
	1	0.5261	0.7553	1.1881	0.1716	
	1.5	0.5206	0.7649			
J_5	0.5	0.5656	0.6647	0.4043	0.4237	0.6647
	1	0.4833	0.59	0.4909	0.548	
	1.5	0.462	0.5699			
J_6	0.5	0.6733	0.823	0.5091	0.4395	0.823
	1	0.6303	0.784	0.7429	0.6352	
	1.5	0.6179	0.7831			
J_7	0.5	0.6992	0.9569	0.6837	0.4292	0.9569
	1	0.7098	0.9367	0.9276	0.4985	
	1.5	0.6533	0.8999			
J_8	0.5	—	—	0.0351	0	0.2567
	1	—	—	0.2546	0.0719	
	1.5	0	0.2567			
J_9	0.5	—	—	0.2083	0	0.6979
	1	—	—	0.6979	0.5833	
	1.5	0	0.3256			
J_{10}	0.5	0.6136	0.7519	0.3858	0.3394	1.2044
	1	0.5875	0.7288	1.2044	0.207	
	1.5	0.5137	0.8343			
J_{11}	0.5	0.002092	0.002315	0.00647	0.007067	0.00943
	1	0.00382	0.004334	0.009429	0.009408	
	1.5	0.005435	0.006041			
J_{12}	0.5	0.07083	0.07562	0.07372	0.08558	0.09833
	1	0.07125	0.07395	0.09833	0.08767	
	1.5	0.07095	0.07793			
J_{13}	0.5	0.000009	0.000011	0.000009	0.000011	1.3E-05
	1	0.000009	0.000011	0.00001	0.000013	
	1.5	0.00001	0.000012			
J_{14}	0.5	0.000001	0.000001	0	0	1E-06
	1	0.000001	0.000001	0	0	
	1.5	0.000001	0.000001			

9. PROBABILISTIC INDIRECT ADAPTIVE CONTROL METHOD

Classical control methods may fail to improve the performance of the controlled structure in the presence of uncertainties, because these methods do not consider the model errors, measurement errors or other uncertainties in the control process. Recently, probabilistic control methods which consider some of the uncertainties have been developed and used to improve the performance of the structural systems. Monte Carlo simulation method (Stengel and Ray 1991; Marrison and Stengel 1995), first and second order reliability methods with a linear-quadratic-regulator (LQR) (Field et al. 1996; Spencer et al. 1994), and probability integrals to determine the optimal gain for an active mass driver (May and Beck 1998) are some of the probabilistic or stochastic robust control theories that have been used to control the behavior of the structure. Yuen (2002) introduced a probabilistic robust control approach in 2002. In this approach, engineering judgment or system identification can be utilized to obtain probabilistic descriptions of all possible structural models which are used in the selection of controllers to achieve optimum performance (Yuen 2002a).

Hwang et al. (2005) developed a probabilistic algorithm for active control of structures. In this method, the probability density function of structural energy is used. The control force is obtained by the probability that the structural energy exceeds a specified target critical energy, and the Lyapunov controller design method is used to determine the direction of the control forces (Min et al. 2003). This probabilistic active control method was both numerically and experimentally verified (Hwang et al. 2005).

In Scruggs et al. (2006), the uncertain ground motion is modeled as a stochastic process, and a probability-based active control method is used to control the performance of the structure with active base isolation systems. This method was applied to an eight-story base isolation benchmark model (Scruggs et al. 2006). The objective of this approach is to minimize the probability of failure which is defined as a maximum allowable response of the system such as drift or acceleration.

In the research done by Ni et al., (2004) stochastic optimal semi-active control based on statistical linearization and optimal linear control was developed and used to control the performance of tall building structures equipped with magneto-rheological tuned liquid column damper (MR-TLCD). The structure was assumed to be under random wind excitation and the proposed control approach did not depend on the external excitation. A semi-active control strategy which addressed structural modeling uncertainties was used to control the behavior of a structure with Magnetorheological (MR) dampers by Yuen et al. (2007) A robust reliability-based active linear control methodology and clipped-optimal control algorithm were used to calculate the forces generated by the MR dampers. Yuen et al. (2007) considered the uncertainties in the modeling of the structure and future unknown excitations in their analysis.

In this section, a probabilistic indirect adaptive control method (PIACM) is developed and its performance is compared with the performance of the SACM. As mentioned in Section 2, there are two types of adaptive control methods, direct and indirect adaptive approaches. An indirect method is an approach with two steps. The first step is system identification of the controlled system and the second step is the control

algorithm. For PIACM, a probabilistic system identification based on Bayesian theory is used for system identification and the LQG is selected as the control approach. The block diagram of PIACM is shown in Figure 9.1. A two degree of freedom system is used to compare the performance of the developed method with that of the SACM.

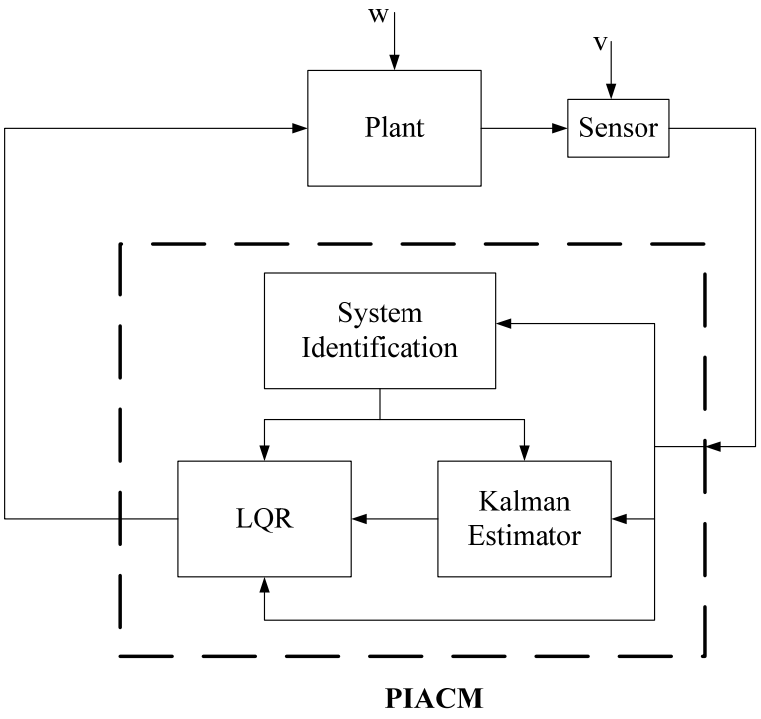

Figure 9.1: Block diagram of the developed probabilistic indirect adaptive control method (PIACM).

9.1. A Probabilistic System Identification Method Using Bayesian Theory

In this section, a Bayesian Structural model updating method adopted from Yuen et al. (2006) is used to update structural parameters of the controlled system. This method uses incomplete modal data, such as natural frequencies and mode shapes, to calculate the structural parameters of the controlled system (Yuen et al. 2006). It is

assumed that the dynamic behavior of the structure is characterized by the following equation,

$$M\,\ddot{x}(t) + C(\boldsymbol{\theta})\,\dot{x}(t) + K(\boldsymbol{\theta})\,x(t) = F(t)\,. \tag{9.1}$$

where M, $C(\boldsymbol{\theta})$ and $K(\boldsymbol{\theta})$ are the mass, damping and stiffness matrices of the structure. The vector $\boldsymbol{\theta}=[\theta_1,\theta_2,\ldots\theta_n]^T$ parameterizes the stiffness matrix,

$$K(\boldsymbol{\theta}) = K_0 + \sum_{j=1}^{n} \theta_j K_j\,, \tag{9.2}$$

where K_j is a substructure stiffness matrix which models the contribution of a portion of the structure to the overall stiffness matrix. It is assumed that $\boldsymbol{\phi} = [\phi_1, \phi_2, \ldots, \phi_m]$ and $\boldsymbol{\omega} = [\omega_1, \omega_2, \ldots, \omega_m]$ are m mode shapes and natural frequencies of the structure, with m less than or equal to the total number of degrees of freedom of the structure. The goal of this method is to calculate the most probable values for $\boldsymbol{\theta}$ which satisfy the equation of motion and measured modal characteristics of the structure. A statistical method based on Bayesian probabilistic framework is used to describe the uncertainties that arise from measurement noise, modeling error and none unique solution (Vanik 1997; Vanik et al. 2000). The probability density function (PDF) for the natural frequencies and mode shapes is

$$p(\boldsymbol{\omega}^2, \boldsymbol{\phi} | \boldsymbol{\theta}) = c_1\, exp\left[-\frac{1}{2} J_0(\boldsymbol{\omega}^2, \boldsymbol{\phi} | \boldsymbol{\theta}) \right], \tag{9.3}$$

where c_1 is a normalizing constant and

$$J_0(\boldsymbol{\omega}^2, \boldsymbol{\phi} | \boldsymbol{\theta}) = \begin{bmatrix} (K(\boldsymbol{\theta}) - \omega_1^2 M)\phi_1 \\ \vdots \\ (K(\boldsymbol{\theta}) - \omega_m^2 M)\phi_m \end{bmatrix}^T \Sigma_{eq}^{-1} \begin{bmatrix} (K(\boldsymbol{\theta}) - \omega_1^2 M)\phi_1 \\ \vdots \\ (K(\boldsymbol{\theta}) - \omega_m^2 M)\phi_m \end{bmatrix}. \quad (9.4)$$

A Gaussian PDF as a probability model for the eigenvalue equation errors is chosen for this prior PDF. The variable Σ_{eq}^{-1} is the prior covariance matrix which controls the size of equation errors. The uncertainty in the equation errors for each mode is assumed to be independent and identically distributed, therefore $\Sigma_{eq}^{-1} = \sigma_{eq}^2 I_{dm \times dm}$, where σ_{eq}^2 is the equation-error variance (Yuen 2002). Equation (9.5) shows the prior PDF for all the unknown parameters which are $\boldsymbol{\theta}$, $\boldsymbol{\omega}$, and $\boldsymbol{\phi}$,

$$p(\boldsymbol{\omega}^2, \boldsymbol{\phi}, \boldsymbol{\theta}) = p(\boldsymbol{\omega}^2, \boldsymbol{\phi} | \boldsymbol{\theta}) p(\boldsymbol{\theta}) . \quad (9.5)$$

The prior PDF $p(\boldsymbol{\omega}^2, \boldsymbol{\phi}, \boldsymbol{\theta}) = p(\boldsymbol{\omega}^2, \boldsymbol{\phi} | \boldsymbol{\theta}) p(\boldsymbol{\theta})$ can be taken as a Gaussian distribution with mean $\boldsymbol{\theta_0}$ and covariance matrix Σ_θ (Yuen et al. 2002). The measurement error ε is introduced to build the likelihood function,

$$\begin{bmatrix} \hat{\boldsymbol{\omega}}^2 \\ \hat{\boldsymbol{\Psi}} \end{bmatrix} = \begin{bmatrix} \boldsymbol{\omega}^2 \\ \Gamma \boldsymbol{\phi} \end{bmatrix} + \varepsilon . \quad (9.6)$$

A Gaussian probability with zero mean and covariance matrix Σ_ε is selected for ε. $\hat{\boldsymbol{\omega}}^2$ and $\hat{\boldsymbol{\Psi}}$ are the modal parameters estimated from dynamic test data. The posterior PDF for the unknown parameters based on Bayes' Theorem is,

$$p(\boldsymbol{\omega}^2, \boldsymbol{\phi}, \boldsymbol{\theta} | \hat{\boldsymbol{\omega}}^2, \hat{\boldsymbol{\Psi}}) = c_2 p(\hat{\boldsymbol{\omega}}^2, \hat{\boldsymbol{\Psi}} | \boldsymbol{\omega}^2, \boldsymbol{\phi}, \boldsymbol{\theta}) p(\boldsymbol{\omega}^2, \boldsymbol{\phi} | \boldsymbol{\theta}) p(\boldsymbol{\theta}) . \quad (9.7)$$

Equation (9.7) must be maximized to calculate the most probable values of the unknown parameters (Yuen et al. 2006). In other word, $J(\boldsymbol{\omega}^2, \boldsymbol{\phi}, \boldsymbol{\theta})$ should be minimized to find the most probable values if,

$$\begin{aligned} J(\boldsymbol{\omega}^2, \boldsymbol{\phi}, \boldsymbol{\theta}) &= -2\, p(\boldsymbol{\omega}^2, \boldsymbol{\phi}, \boldsymbol{\theta} \left| \hat{\boldsymbol{\omega}}^2, \hat{\boldsymbol{\Psi}} \right.) \\ &= c_3 + (\theta - \theta_0)^T \Sigma_\theta^{-1} (\theta - \theta_0) + \sigma_{eq}^{-2} \sum_{i=1}^{m} \left\| (K(\boldsymbol{\theta}) - \omega_i^2 M)\phi_i \right\| \cdot \\ &+ \begin{bmatrix} \hat{\boldsymbol{\omega}}^2 - \boldsymbol{\omega}^2 \\ \hat{\boldsymbol{\Psi}} - \Gamma\boldsymbol{\phi} \end{bmatrix}^T \Sigma_\varepsilon^{-1} \begin{bmatrix} \hat{\boldsymbol{\omega}}^2 - \boldsymbol{\omega}^2 \\ \hat{\boldsymbol{\Psi}} - \Gamma\boldsymbol{\phi} \end{bmatrix} \end{aligned} \tag{9.8}$$

Yuen et al. (2006) suggested to use an iterative linear optimization method to calculate the most probable value for **θ** (Yuen et al. 2006).

9.2. Results

The probabilistic indirect adaptive control method developed in the previous section is examined using a mathematical model of a 2 DOF shear structure. A typical model is depicted in Figure 9.2. It is assumed that an ideal active device with capacity of 5000 kN is located between the ground and the first story of the structure.

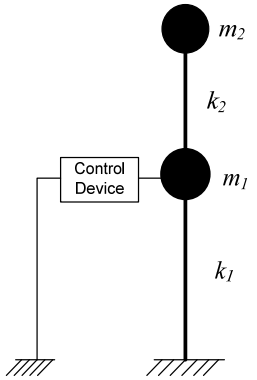

Figure 9.2: The model of 2 DOF Structure.

The substructure stiffness matrices are $K_1 = \begin{bmatrix} k_1 & 0 \\ 0 & 0 \end{bmatrix}$ and $K_2 = \begin{bmatrix} k_2 & -k_2 \\ -k_2 & k_2 \end{bmatrix}$.

Therefore, the stiffness matrix of the structure is equal to $K = \theta_1 K_1 + \theta_2 K_2$. Table 9.1 shows values of mass and stiffness of each story of the structure.

Table 9.1: Specification of the structure.

m_1	m_2	k_1	k_2
478 ton	478 ton	2.0298×10^8 N/m	1.1452×10^8 N/m

To calculate the most probable value of $\boldsymbol{\theta}$, the response of the structure subjected to the Kobe earthquake is measured for each time interval of 2 seconds. Then using the modal frequency domain decomposition method (Brincker et al. 2000; Brincker et al. 2001), the mode shapes and natural frequency of each time interval are calculated ($\hat{\boldsymbol{\omega}}^2$ and $\hat{\boldsymbol{\Psi}}$). Twenty five calculated mode shapes and natural frequencies are used to calculate the most probable value of $\boldsymbol{\theta}$ (Table 9.2). Also, it is assumed that 30% stiffness reduction occurred at each story. The above procedure is applied to the damaged case to calculate the most probable value of $\boldsymbol{\theta}$ for the damaged structure as is shown in Table 9.2.

Table 9.2: Most probable value of θ.

	θ_1	θ_2
Undamaged	1.0239	1.0197
Damaged	0.7236	0.7230

To study the effectiveness of PIACM, its performance is compared with the performance of the SACM. For the SACM, the value of σ, T and $\overline{T}$ are chosen to be 0.1, 100 and 100, respectively. For the PIACM, the weighting matrices for the LQG are chosen as,

$$Q = (0.5)\begin{bmatrix} K(\theta) & 0 \\ 0 & M \end{bmatrix} \tag{9.9}$$

$$R = 100 \tag{9.10}$$

$$Q_n = 1000 \tag{9.11}$$

$$R_n = 0.1\,. \tag{9.12}$$

The indirect adaptive control can deal with uncertainties caused by noisy measurement and model error. The Kalman estimator deals with the measurement noise and probabilistic system identification can compensate model error. Table 9.3 shows the performance of the developed PAICM and the SACM. The maximum acceleration and drift of the controlled structure under the Kobe earthquake are shown in Table 9.3. It is assumed that the velocity of the first story is measured by some sensors and a Gaussian noise is added to the output measurement to have noisy measurements.

Table 9.3: Maximum structural response of the 2-DOF structure controlled by SACM, PIACM and LQG.

		Max. Drift (cm)	**Max. Acceleration (m/s^2)**
Undamaged Case	Uncontrolled	8.37	20.5
	SACM	6.23	13.73
	PIACM	6.25	14.17
Damaged Case	Uncontrolled	14.57	25.28
	SACM	7.76	13.70
	PIACM	8.61	13.70

The results presented in Table 9.3 show that for the undamaged case, the SACM decreases the maximum drift to 74% of the uncontrolled maximum drift while the PIACM reduces the maximum drift to 75% of the uncontrolled maximum drift. The results show that the SACM is more effective than the PIACM in reducing the maximum

acceleration for undamaged case. By studying the performance of the SACM and the PIACM, it can be concluded that the SACM can deal with both presence of noise in measurement and any change in the characteristics of the structure. The maximum acceleration obtained by the SACM for undamaged and damaged cases are 13.73 m/s^2 and 13.7 m/s^2 which shows that stiffness reduction does not affect the performance of the SACM in reducing the maximum acceleration. The maximum drifts obtained by the SACM point to the same conclusion. Table 9.3 shows that the PIACM is also successful in reducing the maximum drift and acceleration in the presence of measurement noise or any change in the structural parameters.

The performance of the case study explained in Section 6 is controlled with the PIACM and results are presented in Table 9.4. The total stiffness matrix is calculated by

$$K = \theta_1 K_1 + \theta_2 K_2 + \cdots + \theta_6 K_6, \tag{9.13}$$

where

$$K_1 = 297\begin{bmatrix} 1 & 0 & 0 & 0 & 0 & 0 \\ 0 & 0 & 0 & 0 & 0 & 0 \\ 0 & 0 & 0 & 0 & 0 & 0 \\ 0 & 0 & 0 & 0 & 0 & 0 \\ 0 & 0 & 0 & 0 & 0 & 0 \\ 0 & 0 & 0 & 0 & 0 & 0 \end{bmatrix}, K_2 = 297\begin{bmatrix} 1 & -1 & 0 & 0 & 0 & 0 \\ -1 & 1 & 0 & 0 & 0 & 0 \\ 0 & 0 & 0 & 0 & 0 & 0 \\ 0 & 0 & 0 & 0 & 0 & 0 \\ 0 & 0 & 0 & 0 & 0 & 0 \\ 0 & 0 & 0 & 0 & 0 & 0 \end{bmatrix}. \tag{9.14}$$

$$K_3 = 297\begin{bmatrix} 0 & 0 & 0 & 0 & 0 & 0 \\ 0 & 1 & -1 & 0 & 0 & 0 \\ 0 & -1 & 1 & 0 & 0 & 0 \\ 0 & 0 & 0 & 0 & 0 & 0 \\ 0 & 0 & 0 & 0 & 0 & 0 \\ 0 & 0 & 0 & 0 & 0 & 0 \end{bmatrix}, \ldots, K_6 = 297\begin{bmatrix} 0 & 0 & 0 & 0 & 0 & 0 \\ 0 & 0 & 0 & 0 & 0 & 0 \\ 0 & 0 & 0 & 0 & 0 & 0 \\ 0 & 0 & 0 & 0 & 0 & 0 \\ 0 & 0 & 0 & 0 & 0 & 0 \\ 0 & 0 & 0 & 0 & 0 & 1 \end{bmatrix}$$

As presented in Table 9.4, the SACM and PIACM are both successful in decreasing the structural drift, but the SACM is more effective in reducing the maximum acceleration and displacement.

Table 9.4: Maximum structural response of the 6-story structure controlled by SACM and PIACM.

	Max. Displacement (cm)	**Max. Drift (cm)**	**Max Acc. (cm/s^2)**
Uncontrolled	1.32	0.3	148.16
PIACM	0.9	0.2	109.2
SACM	0.7	0.19	92.3

10. SUMMARY, CONCLUSIONS AND FUTURE WORK

10.1. Summary and Conclusion

In this dissertation, the SACM was modified to actively and semi-actively control the structural response of buildings subjected to earthquakes. The effectiveness of SACM to control the structural performance was investigated by several numerical examples. In Section 4, the SACM was used to control a three-story building from the SAC Phase II project. The goal was to use the SACM to mitigate the effect of damage in the structural response of the building and make the damaged structure behave like an undamaged structure. First, active devices that can produce any desired force were applied to control the behavior of the damaged structure and force it to behave like an undamaged one. The results show that using the adaptive control method and ideal active devices to control the structure is a powerful tool to achieve the desired performance, and the error between the response of the controlled damaged structure and the undamaged structure's response is negligible. Then MR dampers, one of the most promising semi-active devices for use in vibration control applications, were utilized to produce the required forces calculated from adaptive control to make the damaged structure behave similarly to the undamaged structure. The damaged structure can track the undamaged structure acceptably when it is controlled with MR dampers and its behavior is improved.

In Section 5, the SACM was used to optimize the structural response of an undamaged and a damaged structure using Magnetorheological (MR) dampers and

hydraulic actuators. For the SACM, the model, which is a system with a desired behavior, was defined in a way that the controlled system always had a better result than the uncontrolled system. The performance of the proposed control method is independent of the characteristics of the external loads, and it can be effective even in the presence of noise in output measurement or of any change in the characteristics of the controlled structure. The three-story building designed for the SAC Phase II project for the Los Angeles region was used to study the effectiveness of using the SACM to control the behavior of the structure subjected to the earthquake. Three suites of earthquake records with different probabilities of exceedence, developed for the SAC steel project, were applied to the three-story building to study the performance of the structure. The large-scale MR dampers and hydraulic actuators were used in the simulation as control devices. The results show that the performance of the structure is improved by using the SACM with MR dampers or hydraulic actuators for the undamaged case. The evaluation criteria for controlled damaged and undamaged structural responses in the presence of output-measurement noise show that the MR damper and the SACM have the potential for improving the seismic behavior of the civil structure. The response of the controlled structure subjected to different seismic loads shows that the SACM can enhance the performance of the controlled structure independently of the external excitations applied to the structure. The results show that the SACM can improve the performance of the structure in the presence of noise or damage. While instability can occur when hydraulic actuators are used, the MR damper never makes the structure unstable since it is a semi-active device and cannot inherently

insert energy into the structural systems. Therefore, the semi-active systems are significantly more robust and stable than active systems.

The SACM and a genetic-based fuzzy set were used to control the behavior of a structure equipped with MR dampers in Section 6. A numerical example was studied and the performance of the controllers developed by the SACM and fuzzy theory were compared with those of other semi-active control algorithms as well as passive operation of MR dampers. The results show that developed controllers can significantly decrease the peak displacement and drift of the structure while simultaneously reducing maximum absolute acceleration. Also, it is shown that the controllers proposed in this study can compensate for a change in the structural parameters due to possible damage in the structure and successfully perform under various excitation cases. It can be concluded that semi-active operation of MR dampers using proposed control strategies can effectively improve the response of the structure during a seismic event.

The goal of Section 7 was to investigate the effectiveness of two adaptive control strategies (the SACM and fuzzy logic control) that are employed to modulate the normal force of variable friction dampers installed in a base-isolated building. The adaptive controllers aim to simultaneously reduce the deformations of the isolation system and superstructure accelerations of the isolated building during various types of seismic excitations. The results from numerical simulations with several ground motions demonstrate that variable friction dampers that operated as semi-active devices by employing adaptive control strategies developed in this study, can effectively improve

the response of base-isolated buildings against both far-field and near-field ground motions.

In Section 8, the effectiveness of the SACM to control the performance of a nonlinear building equipped with MR dampers was investigated. The adaptive controller aims to simultaneously reduce drift and acceleration of the twenty-story building during seismic excitations. The results from numerical simulations demonstrate that MR dampers, operating as semi-active devices employing adaptive control strategy, can effectively improve the response of the structure against seismic excitations. By comparing the performance of the SACM with the MCOC and passive-on, it can be concluded that the SACM is more successful in improving the structural response of the twenty-story building with nonlinear behavior.

A probabilistic indirect adaptive control method (PIACM) is developed in Section 9. The PIACM combines a probabilistic system identification method based on Bayesian theory and the LQG. A numerical example was used to study the performance of the PIACM and compare its result with that of the SACM. The result showed that the PIACM was effective in reducing the structural response and could compensate the effects of measurement noise and any change in structural parameters. Also, it was concluded that the SACM performed effectively and was slightly better than the PIACM. In conclusion, both the SACM and the PIACM were successful in controlling the behavior of the structure under earthquake but the SACM was simpler than the PIACM, which shows that its implementation to control the structural response is more practical.

10.2. Future Work

The effectiveness of using the SACM to reduce the structural response of buildings under earthquakes was studied by analyzing several numerical examples in this dissertation. The performance of the SACM can be investigated experimentally and advantages and disadvantages of using it by comparing to other control methods can be studied through some experimental examples. A real-time hybrid simulation benchmark study with large-scale MR damper was recently developed by Phillips et al. (2010). The SACM can be used to control the newly developed benchmark structure and its performance can be compared with the performance of other control methods.

The parameters of the SACM, Y_{max}, σ, T and $\overline{T}$, were chosen by trial and error. It is possible to define a way that these parameters are chosen and changed automatically through the control process. Also, it is possible to use the SACM in Structural Health Monitoring. For example, by studying the control command of the SACM it can be determined if any change occurs in the structural characteristics of the structure.

The SACM can be utilized to control the performance of structures equipped with newly developed control devices other than the ones used in this dissertation and its effectiveness can be studied numerically and experimentally. Also, the SACM can be used to control the performance of civil engineering systems other than buildings, such as bridges. In this study, the SACM was used to improve the performance of the constructed buildings. It is suggested to consider the use of the SACM and control devices in the design process of buildings.

The effect of using the SACM with active or semi-active devices can be considered in the Life Cycle Cost Analysis (LCCA) of civil engineer systems. LCCA is one of the American Society of Civil Engineers (ASCE) policies and is recommended to be used in the design process to estimate the total cost of projects. It is worth assessing the effect of using the SACM and control devices on reducing the total cost of planning, design, construction, operation, maintenance and other reasonable anticipated costs of the life of the civil engineering project.

REFERENCES

Abe, M., Y. Fujino and S. Kimura (1998). "Active Tuned Liquid Damper (TLD) with Magnetic Fluid." *Proc., SPIE* 3329: 620-623.

Adeli, H. and A. Saleh (1999). *Control, Optimization, and Smart Structures: High-Performance Bridges and Buildings of the Future*, John Wiley & Sons, Inc, New York.

Ahlawat, A. S. and A. Ramaswamy (2001). "Multi-objective Optimal Structural Vibration Control Using Fuzzy Logic Control System." *ASCE Journal of Structural Engineering,* 127(11): 1330-1337.

Al-Dawod, M., B. Samali, K. Kwok and F. Naghdy (2004). "Fuzzy Controller for Seismically Excited Nonlinear Buildings." *Journal of Engineering Mechanics* 130(4): 407-415.

Barkana, I. (1987). "Parallel Feedforward and Simplified Adaptive Control." *International Journal of Adaptive Control and Signal Processing,* 1(2): 95-109.

Barkana, I. (2005a). "Gain Conditions and Convergence of Simple Adaptive Control." *International Journal of Adaptive Control and Signal Processing,* 19(1): 13-40.

Barkana, I. (2005b). "Classical and Simple Adaptive Control for Nonminimum Phase Autopilot Design." *Journal of Guidance, Control, and Dynamics,* 28(4): 631-638.

Barkana, I. (2008). "A Modified Invariance Principle and Gain Convergence in Adaptive Control." *Proc., IEEE 25th Convention of Electrical and Electronics Engineers*, Israel, 800-804.

Barkana, I., R. Fischl and P. Kalata (1991). "Direct Position Plus Velocity Feedback Control of Large Flexible Space Structures." *IEEE Transactions on Automatic Control,* 36(10): 1186-1188.

Barkana, I. and A. Guez (1990). "Simple Adaptive Control for a Class of Non-linear Systems with Application to Robotics." *International Journal of Control,* 52(1): 77-99.

Barkana, I. and H. Kaufman (1993). "Simple Adaptive Control of Large Flexible Space Structures." *IEEE Transactions on Aerospace and Electronic Systems,* 29(4): 1137-1149.

Barkana, I., M. C. M. Teixeira and L. HSU (2006). "Mitigation of Symmetry Condition in Positive Realness for Adaptive Control." *Automatica,* 42(9): 1611-1616.

Barroso, L. R., S. E. Breneman and H. A. Smith (2002). "Performance Evaluation of Controlled Steel Frames Under Multilevel Seismic Loads." *ASCE Journal of Structural Engineering,* 128(11): 1368 -1378.

Barroso, L. R., J. G. Chase and S. Hunt (2003). "Resettable Smart Dampers for Multi-level Seismic Hazard Mitigation of Steel Moment Frames." *Journal of Structural Control,* 10(1): 41-58.

Bitaraf, M. and L. R. Barroso (2009). "Structural Performance Improvement Using MR Dampers with Adaptive Control Method." *Proc., American Control Conference (ACC09)* St. Louis, Missouri, 598-603.

Bitaraf, M., L. R. Barroso and S. Hurlebaus (2010a). "Adaptive Control to Mitigate Damage Impact on Structural Response." *Journal of Intelligent Material Systems and Structures,* 21(6): 607-619.

Bitaraf, M., S. Hurlebaus and L. R. Barroso (2010b). "Active and Semi-Active Adaptive Control for Undamaged and Damaged Building Structures under Seismic Load." *Computer-Aided Civil and Infrastructure Engineering*: accepted.

Bitaraf, M., O. E. Ozbulut and S. Hurlebaus (2010c). "Adaptive Control of Base-Isolated Buildings Using Piezoelectric Friction Dampers against Near-Field Earthquake." *Proc., SPIE Smart Structures and Materials/Nondestructive Evaluation and Health Monitoring Conference*. San Diego, CA, 7643: 76432E-11

Bitaraf, M., O. E. Ozbulut, S. Hurlebaus and L. R. Barroso (2010d). "Application of Semi-active Control Strategies for Seismic Protection of Buildings with MR Dampers." *Engineering Structures,* 32(10): 3040-3047.

Brincker, R., L. Zhang and P. Andersen (2000). "Output Only Modal Analysis by Frequency Domain Decomposition." *Proc., 25th Int. Seminar on Modal Analysis (ISMA)*. Leuven, Belgium. 2: 717-723.

Brincker, R., L. Zhang and P. Andersen (2001). "Modal Identification of Output-only Systems Using Frequency Domain Decomposition." *Smart Materials and Structures,* 10(3): 441-445.

Brogan, W. L. (1991). *Modern Control Theory*, Prentice-Hall, Englewood Cliffs, NJ.

Casciati, F., G. Magonette and F. Marazzi (2006). *Technology of Semiactive Devices and Applications in Vibration Mitigation*, Wiley & Sons, Chichester.

Chang, C. C. and P. N. Roschke (1998). "Neural Network Modeling of a Magnetorheological Dampers." *Journal Inteligent Material Systems and Structures,* 9: 755-764.

Chase, J. G., K. J. Mulligan, A. Gue, T. Alnot, G. Rodgers, J. B. Mander, R. Elliott, B. Deam, L. Cleeve and D. Heaton (2006). "Re-shaping Hysteretic Behaviour Using Semi-active Resettable Device Dampers." Engineering Structures 28: 1418–1429.

Chen, C. (2007). *Development and Numerical Simulation of Hybrid Effective Force Testing Method*. Ph.D. Dissertation, Department of Civil and Enviromental Engineering, Lehigh University, Bethlehem, PA.

Chen, G. and C. Chen (2004). "Semiactive Control of the 20-Story Benchmark Building with Piezoelectric Friction Dampers." *Journal of Engineering Mechanics,* 130(4): 393-400.

Chen, Z. Q., X. Y. Wang, J. M. Ko, Y. Q. Ni, B. F. Spencer, G. Yang and J. H. Hu (2004). "MR Damping System for Mitigating Wind-Rain Induced Vibration on Dongting Lake Cable-Stayed Bridge" *Wind and Structures,* 7(5): 293-304.

Cheryy, S. and A. Filiatrault (1993). "Seismic Response Control of Buildings Using Friction Dampers." *Earthquake Spectra,* 9(3): 447-466.

Choi, K. M., S. W. Cho, H. J. Jung and I. W. Lees (2004). "Semi-active Fuzzy Control for Seismic Response Reduction Using Magnetorheological Dampers." *Earthquake Engineering and Structural Dynamics,* 33(6): 723-736.

Christenson, R., Y. Z. Lin, A. Emmons and B. Bass (2008). "Large-Scale Experimental Verification of Semiactive Control through Real-Time Hybrid Simulation." *ASCE Journal of Structural Engineering,* 134(4): 522-534.

Chung, L. L., R. C. Lin, T. T. Soong and A. M. Reinhorn (1989). "Experimental Study of Active Control for MDOF Seismic Structures." *Journal of Engineering Mechanics,* 115(8): 1609-1627.

Crassidis, J. L. and J. L. Junkins (2004). *Optimal Estimation of Dynamic Systems*, Chapman & Hall/CRC, New York.

Deb, K., A. Pratap, S. Agrawal and T. Meyarivan (2002). "A Fast Elitist Non-dominated Sorting Genetic Algorithm for Multi-objective Optimization: NSGA-II." *IEEE Trans Evolut Comput.,* 6(2): 182-97.

DeSilva, A. W. (1989). *Control Sensors and Actuators*, Prentice Hall, Englewood Cliffs, NJ.

Dosho, T. and H. Ohmori (1997). "New Design Method of Simple Adaptive Control for Systems with Arbitrary Relative Degree." *Proc., 36th IEEE Conference on Decision and Control*, Inst. of Electrical and Electronics Engineers, Piscataway, NJ, 2: 1914 - 1917.

Dyke, S. J. and B. F. Spencer (1996). "Seismic Response Control Using Multiple MR Dampers." *Proc., 2nd Int. Workshop on Struct. Control*, Hong Kong University of Science and Technology Research Center.

Dyke, S. J., B. F. Spencer, P. Quast and M. K. Sain (1995). "The Role of Control–structure Interaction in Protective System Design." *ASCE Journal of Eng. Mechanics,* 121: 322–38.

Dyke, S. J., B. F. Spencer, P. Quast, M. K. Sain, D. C. Kaspari and T. T. Soong (1996a). "Acceleration Feedback Control of MDOF Structures." *Journal of Engineering Mechanics,* 122(9): 907-918.

Dyke, S. J., B. F. Spencer, M. K. Sain and J. D. Carlson (1996b). "Modeling and Control of Magnetorheological Dampers for Seismic Response Reduction." *Smart Materials and Structures,* 5: 565-575.

Erkus, B., M. Abe and Y. Fujino (2002). "Investigation of Semi-active Control for Seismic Protection of Elevated Highway Bridges." *Engineering Structures,* 24: 281-293.

Faravelli, L. and T. Yao (1996). "Use of Adaptive Networks in Fuzzycontrol of Civil Engineering Structures." *J. Microcomput. Civ. Eng.,* 12: 67–76.

Feng, Q. and M. Shinozuka (1990). "Use of a Variable Damper for Hybrid Control of Bridge Response Under Earthquake." *U.S. Nat. Workshop on Struct. Control Res*. University of Southern California, Los Angeles: 107-112.

Field, R. V., P. G. Voulgaris and L. A. Bergman (1996). "Probabilistic Stability Robustness of Structural Systems." *Journal of Engineering Mechanics,* 122(10): 1012-1021.

Gardoni, P., A. D. Kiureghian and K. M. Mosalam (2002). "Probabilistic Capacity Models and Fragility Estimates for Reinforced Concrete Columns Based on Experimental Observations." *Journal of Engineering Mechanics,* 128(10): 1024 -1038

Gaul, L., S. Hurlebaus, J. Wirnitzer and H. Albrecht (2008). "Enhanced Damping of Lightweight Structures by Semi-active Joints." *Acta Mechanica,* 195: 249-261.

Gaul, L. and R. Nitsche (2001). "The Role of Friction in Mechanical Joints." *Applied Mechanics Reviews,* 54(2): 93-106.

Gilbert, E. G. (1963). "Controllability and Observability in Multivariable Control Systems." *Journal of the Society for Industrial and Applied Mathematics, Series A: Control* 2(1): 128-150.

Ha, Q. P., N. M. Kwok, M. T. Nguyen, J. Li and B. Samali (2008). "Mitigation of Seismic Responses on Building Structures Using MR Dampers with Lyapunov-Based Control." *Structural Control and Health Monitoring,* 15: 604-621.

He, W. L., A. K. Agrawal and J. N. Yang (2003). "Novel Semiactive Friction Controller for Linear Structures against Earthquakes." *Journal Structural of Engineering,* 129(7): 941-950.

Hirai, J., M. Naruse and H. Abiru (1996). "Structural Control with Variable Friction Damper for Seismic Response." *Proc., 11th World Conference on Earthquake Engineering,* Paper No. 1934, Amsterdam.

Hoang, N., Y. Fujino and P. Warnitchai (2008). "Optimal Tuned Mass Damper for Seismic Applications and Practical Design Formulas." *Engineering Structures,* 30: 707-715.

Housner, G. W., L. A. Bergman, T. K. Caughey, A. G. Chassiakos, R. O. Claus, S. F. Masri, R. E. Skelton, T. T. Soong, B. F. Spencer and J. T. P. Yao (1997). "Structural Control: Past, Present, and Future." *Journal of Engineering Mechanics,* 123(9): 897-971.

Huang, W., P. L. Gould, R. Martinez and G. S. Johnson (2004). "Non-linear Analysis of a Collapsed Reinforced Concrete Chimney." *Earthquake Engineering and Structural Dynamics,* 33(4): 485-498.

Huo, L., G. Song, H. Li and K. Grigoriadis (2008). "$H\infty$ Robust Control Design of Active Structural Vibration Suppression Using an Active Mass Damper." *Smart Materials and Structures,* 17(1): 1-10.

Hurlebaus, S. and L. Gaul (2006). "Smart Structure Dynamics." *Mechanical Systems and Signal Processing,* 20: 255-281.

Hwang, J. S., K. W. Min, S. H. Lee and H. Kim (2005). "Probabilistic Approach for Active Control of Structures: Experimental Verification." *Earthquake Engineering and Structural Dynamics,* 34(3): 207-225.

Inaudi, J. A. (1997). "Modulated Homogeneous Friction: A Semi-active Damping Strategy." *Earthquake Engineering and Structural Dynamics,* 26(3): 361-376.

Ishioka, T., M. Watakabe, S. Inai, T. Yamamoto and O. Chiba (2010). "Response Control Performance of Active Mass Damper Using Variable Gain Control System Applied to Super-High-Rise Building." *Proc., Fifth World Conference on Structural Control and Monitoring*, Tokyo, Japan, 5WCSCM-058.

Jansen, L. M. and S. J. Dyke (2000). "Semiactive Control Strategies for MR Dampers: Comparative Study." *ASCE Journal of Eng. Mechanics,* 126(8): 795-803.

Jiang, X. and H. Adeli (2008). "Dynamic Fuzzy Wavelet Neuroemulator for Non-linear Control of Irregular Building Structures." *International Journal for Numerical Methods in Engineering,* 74: 1045-1066.

Jinping, O. and L. Hui (2009). "Design Approaches for Active, Semi-Active and Passive Control Systems Based on Analysis of Characteristics of Active Control Force." *Earthquake Engineering and Engineering Vibration,* 8(4): 493-506.

Johnson, E. A., G. A. Baker, B. F. Spencer and Y. Fujino (2007). "Semiactive Damping of Stay Cables." *Journal of Engineering Mechanics,* 133(1): 1-11.

Johnson, E. A. and B. Erkus (2007). "Dissipativity and Performance Analysis of Smart Dampers via LMI Synthesis." *Structural Control and Health Monitoring*, 14(3): 471-496.

Johnson, E. A., J. Ramallo, B. F. Spencer and M. K. Sain (1998). "Intelligent Base Isolation Systems." *Proc,. 2nd World Conference on Structural Control*, Kyoto, Japan, 1, 367–376.

Jung, H. J., K. M. Choi, B. F. Spencer and I. W. Lee (2006). "Application of Some Semi-active Control Algorithms to a Smart Base-isolated Building Employing MR Dampers." *Structural Control and Health Monitoring,* 13(693-704).

Jung, H. J., B. F. Spencer, Y. Q. Ni and I. W. Lee (2004). "State of Art of Semiactive Control Systems Using MR Fluid Dampers in Civil Eng. Application." *Structural Engineering and Mechanics,* 17(3-4): 493-526.

Kamath, G. M. and N. Wereley (1997). "Nonlinear Viscoelastic-Plastic Mechanism-Based Model of an Electroheological Damper." *J. Guidance, Control Dynamics,* 20(6): 1125-1132.

Kannan, S. and H. M. Uras (1995). "Active Control of Building Seismic Response by Energy Dissipation." *Earthquake Engineering and Structural Dynamics,* 24(5): 747-759.

Kaufman, H., I. Barkana and K. Sobel (1994). *Direct Adaptive Control Algorithms, Theory and Applications*, Springer, New York.

Kerber, F., S. Hurlebaus, B. M. Beadle and U. Stöbener (2007). "Control Concepts for an Active Vibration Isolation System." *Mechanical Systems and Signal Processing,* 21: 3042–3059.

Kim, H. and H. Adeli (2005). "Hybrid Control of Smart Structures Using a Novel Wavelet-Based Algorithm." *Computer-Aided Civil and Infrastructure Engineering,* 20: 7-22.

Kim, Y., S. Hurlebaus and R. Langari (2010). "Model-Based Multi-input, Multi-output Supervisory Semi-active Nonlinear Fuzzy Controller." *Computer-Aided Civil and Infrastructure Engineering,* 25: 387–393.

Kim, Y., R. Langari and S. Hurlebaus (2008). "Semiactive Nonlinear Control of a Building with a Magnetorheological Damper System " *Mechanical Systems and Signal Processing,* 23(2): 300-315.

Kitano, H. (1994). "Neurogenetic Learning: An Integrated Method of Designing and Training Neural Networks Using Genetic Algorithms." *Physica D: Nonlinear Phenomena,* 75: 225-238.

Kozodoy, D. A. and P. D. Spanos (1995). "Robustly Stable Active Control." *Journal of Structural Control*, 2 (1): 65–77.

Lee, D. Y. and N. M. Wereley (2002). "Analysis of Electro- and Magneto-Rheological Flow Mode Dampers Using Herschel-Bulkley Model." *Proc., SPIE Smart Structure and Materials Conference*, Newport Beach, CA, 3989, 244.

Li, H., M. Liu, J. Li, X. Guan and J. Ou (2007). "Vibration Control of Stay Cables of the Shandong Binzhou Yellow River Highway Bridge Using Magnetorheological Fluid Dampers." *Journal of Bridge Engineering,* 12(4): 401-409.

Loh, C.-H., P.-Y. Lin and N.-H. Chung (1999). "Experimental Verification of Building Control Using Active Bracing System." *Earthquake Engineering and Structural Dynamics,* 28(10): 1099-1119.

Lu, L. Y. and G. L. Lin (2009). "A Theoretical Study on Piezoelectric Smart Isolation System for Seismic Protection of Equipment in Near-Fault Areas." *Journal of Intelligent Material and Systems Structures,* 20: 217-232.

Marrison, C. I. and R. F. Stengel (1995). "Stochastic Robustness Synthesis Applied to a Benchmark Problem." *International Journal of Robust Nonlinear Control,* 5(1): 13-31.

May, B. S. and J. L. Beck (1998). "Probabilistic Control for the Active Mass Driver Benchmark Structural Model." *Earthquake Engineering and Structural Dynamics,* 27(11): 1331-1346.

McCormick, J., R. DesRoches, et al. (2006). "Seismic Vibration Control Using Superelastic Shape Memory Alloys." *Journal of Engineering Materials and Technology,* 128(3): 294-301.

McClamroch, N. H. and H. P. Gavin (1995). "Closed Loop Structural Control Using Electrorheological Dampers." *Proc., Am. Control Conf.* , American Automatic Control Council, Washington, DC., 6: 4173 - 4177.

Min, K. W., J. S. Hwang, S. H. Lee and L. Chung (2003). "Probabilistic Approach for Active Control Based on Structural Energy." *Earthquake Engineering and Structural Dynamics,* 32(15): 2301-2318.

Morita, K., T. Fujita, S. Ise, K. Kawaguchi, T. Kamada and H. Fujitani (2001). "Development and Application of Induced Strain Actuators for Building Structures." *Proc., of SPIE,* 4330, 426.

Morse, W. and K. Ossman (1990). "Model Following Reconfigurable Flight Control System for the AFTI/F-16." *Journal of Guidance, Control, and Dynamics,* 13(6): 969-976.

Nagarajaiah, S., Y. Q. Mao and S. Saharabudhe (2006a). "Nonlinear, Seismic Response Spectra of Smart Sliding Isolated Structures with Independently Variable MR Dampers and Variable Stiffness SAIVS System." *Structural Engineering and Mechanics,* 24(3): 375-393.

Nagarajaiah, S. and S. Sahasrabudhe (2006b). "Seismic Response Control of Smart Sliding Isolated Buildings Using Variable Stiffness Systems: An Experimental and Numerical Study." *Earthquake Engineering and Structural Dynamics,* 35(2): 177-197.

Narasimhan, S. and S. Nagarajaiah (2006). "Smart Base Isolated Buildings with Variable Friction Systems: H-Infinity Controller and SAIVF Device." *Earthquake Engineering and Structural Dynamics,* 35(8): 921-942.

Ng, C. L. and Y. L. Xu (2007). "Semi-Active Control of a Building Complex with Variable Friction Dampers." *Engineering Structures,* 29: 1209-1225.

Ni, Y. Q., Z. G. Ying, J. Y. Wang, J. M. Ko and B. F. Spencer (2004). "Stochastic Optimal Control of Wind-Excited Tall Buildings Using Semi-Active MR-Tlcds." *Probabilistic Engineering Mechanics,* 19(3): 269-277.

Nishitani , A. and Y. Inoue (2001). "Overview of the Application of Active/semiactive Control to Building Structures in Japan." *Earthquake Engineering and Structural Dynamics,* 30(11): 1565-1574.

Ohtori, Y., R. E. Christenson, B. F. Spencer, Jr. and S. J. Dyke (2004). "Benchmark Control Problems for Seismically Excited Nonlinear Buildings." *ASCE Journal of Eng. Mechanics,* 130(4): 366-387.

Ozbulut, O. E., M. Bitaraf and S. Hurlebaus (2010). "Adaptive Control of Base-isolated Structures against Near-Field Earthquakes Using Variable Friction Dampers." *Structural Design of Tall and Special Buildings*: under review.

Padgett, J. E. and R. DesRoches (2008). "Seismic Performance of a Passive Control Technology for Bridges Using Shape Memory Alloys." *Proc., The 18th Analysis and Computation Specialty Conference (A&C)*, Vancouver, BC, Canada, 315:1-11.

Phillips, B. M., Z. Jiang, J. M. Ricles, S. J. Dyke, Y. Chae, B. F. Spencer, R. E. Christenson and A. Agrawal (2010). "Real-Time Hybrid Simulation Benchmark Study with a Large-Scale MR Damper." *Proc., Fifth World Conference on Structural Control and Monitoring*. Tokyo, Japan: 5WCSCM-092.

Quast, P., B. F. Spencer, M. K. Sain and S. J. Dyke (1995). "Microcomputer Implementation of Digital Control Strategies for Structural Response Reduction." *Microcomp. in Civ. Engrg.: Spec. Issue on New Dir. in Compo Aided Struct. Sys. Anal. Des. and Optimization,* 10: 1325.

Reinhorn, A. M., T. T. Soong, R. C. Lin, Y. P. Wang, Y. Fukao, H. Abe and M. Nakai (1989). "1:4 Scale Model Studies of Active Tendon. Systems and Active Mass Dampers for Aseismic Protection." National Center for Earthquake Engineering Research, Technical report, *Report No. NCEER-89-0026,* Buffalo, NY.

Sahasrabudhe, S. and S. Nagarajaiah (2005a). "Experimental Study of Sliding Isolated Buildings with MR Dampers." *Journal of Structural Engineering,* 131(7): 1025-1034.

Sahasrabudhe, S. and S. Nagarajaiah (2005b). "Experimental Study of Sliding Base-Isolated Buildings with Magnetorheological Dampers in Near-Fault Earthquakes." *ASCE Journal of Structural Engineering* 131(7): 1025-1034.

Sakamoto, M., T. Kobori, T. Yamada and M. Takahashi (1994). "Practical Applications of Active and Hybrid Response Control Systems and Their Verifications by Earthquake and Strong Wind Observations." *Proc., 1st World Conf. on Struct. Control*, Los Angeles, CA, WP90:99.

Sanchez, E., T. Shibata and L. A. Zadeh (1997). *Genetic Algorithms and Fuzzy Logic Systems: Soft Computing Perspectives,* World Scientific Publishing, River Edge, NJ.

Sasajima, K., A. Kubo, T. Yasuda, N. Yamaura and T. Tsukitani (2010). "Effectiveness of Compensation Algorithm for Active Mass Damper." *Proc., Fifth World Conference on Structural Control and Monitoring*. Tokyo, Japan: 5WCSCM-051.

Scruggs, J. T., A. A. Taflanidis and J. L. Beck (2006). "Reliability-Based Control Optimization for Active Base Isolation Systems." *Structural Control and Health Monitoring,* 13(2-3): 705-723.

Shibata, H., D. Li, T. Fujinaka and G. Maruoka (1996). "Discrete-time Algorithm for Generalized Simplified Adaptive Control and Its Application to DC Motor Control." *IEEE International Symposium on Industrial Electronics,* 1: 248-253.

Shook, D. A., P. N. Roschke and O. E. Ozbulut (2008). "Superelastic Semi-active Damping of a Base-isolated Structure." *Structural Control and Health Monitoring,* 15: 746-768.

Sivaselvan, M. V., A. M. Reinhorn, X. Shao and S. Weinreber (2008). "Dynamic Force Control with Hydraulic Actuators Using Added Compliance and Displacement Compensation." *Earthquake Engineering and Structural Dynamics,* 37: 1785-1800.

Skogestad, S. and I. Postlethwaite (2005). *Multivariable Feedback Control, Analysis and Design*, John Wiley & Sons Ltd, New York.

Sobel, K., H. Kaufman and L. Mabius (1982). "Implicit Adaptive Control for a Class of MIMO Systems." *IEEE Transactions on Aerospace and Electronic Systems,* 18(5): 576-590.

Somerville, P. (1997). "Develop Suites of Time Histories.", SAC Joint Venture Steel Project Phase II Report, Woodward-Clyde Federal Services, Pasadena, CA.

Spencer, B. F., R. E. Christenson and S. J. Dyke (1999). "Next Generation Benchmark Control Problems for Seismically Excited Buildings." *Proc., 2nd World Conf. on Structural Control*, Kyoto, Japan, Wiley, New York, 2: 1135–1360.

Spencer, B. F., S. J. Dyke and H. S. Deoskar (1998). "Benchmark Problems in Structural Control: Part I - Active Mass Driver System." *Earthquake Engineering and Structural Dynamics,* 27(11): 1127-1139.

Spencer, B. F., S. J. Dyke, M. K. Sain and J. D. Carlson (1997). "Phenomenological Model of a Magnetorheological Damper." *ASCE Journal of Eng. Mechanics,* 123(3): 230-238.

Spencer, B. F., D. C. Kaspari and M. K. Sain (1994). "Reliability-Based Optimal Structural Control." *Proc., American Control Conference,* Baltimore, MD, 1062-1066.

Spencer, B. F. and S. Nagarajaiah (2003). "State of the Art of Structural Control." *Journal of Structural Engineering,* 129(7): 845-856.

Stanway, R., J. L. Sproston and N. G. Stevens (1987). "Non-linear Modelling of an Electro-Rheological Vibration Damper." *Journal of Electrostatics,* 20(2): 167-184.

Stengel, R. F. and L. R. Ray (1991). "Stochastic Robustness of Linear Time-Invariant Control Systems." *IEEE Transactions on Automatic Control,* 36(1): 82-87.

Subramaniam, R. S., A. M. Reinhorn, M. A. Riley and S. Nagarajaiah (1996). "Hybrid Control of Structures Using Fuzzy Logic." *Microcomputers in Civil Engineering,* 11: 1-17.

Suhardjo, J., B. F. Spencer and A. Kareem (1992). "Frequency Domain Optimal Control of Wind Excited Buildings." *Journal of Engineering Mechanics,* 118(12): 2463-2481.

Symans, M. D. and S. W. Kelly (1999). "Fuzzy Logic Control of Bridge Structures Using Intelligent Semi-active Seismic Isolation Systems." *Earthquake Engineering and Structural Dynamics,* 28: 37-60.

Tsang, H. H., R. K. L. Su and A. M. Chandler (2006). "Simplified Inverse Dynamics Models for MR Fluid Dampers." *Engineering Structures,* 28: 327-341.

Tse, T. and C. C. Chang (2004). "Shear-Mode Rotary Magnetorheological Damper for Small-Scale Structural Control Experiments." *ASCE Journal of Structural Engineering,* 130(6): 904-911

Vanik, M. W. (1997). *A Bayesian Probabilistic Approach to Structural Health Monitoring*. Ph.D. Dissertation, Civil Eng. Dept., California Institute of Technology. Pasadena.

Vanik, M. W., J. L. Beck and S. K. Au (2000). "Bayesian Probabilistic Approach to Structural Health Monitoring." *Journal of Engineering Mechanics,* 126(7): 738-745.

Wang, D. H. and W. H. Liao (2005). "Modeling and Control of Magnetorheological Fluid Dampers Using Neural Networks." *Smart Materials and Structures,* 14: 111-126.

Warnitchai, P., Y. Fujino, B. M. Pacheco and R. Agret (1993). "An Experimental Study on Active Tendon Control of Cable-stayed Bridges." *Earthquake Engineering & Structural Dynamics,* 22(2): 93-111.

Wen, J. and M. Balas (1989). "Finite-Dimensional Direct Adaptive Control for Discrete-Time Infinite-Dimensional Hilbert Space." *Journal of Mathematical Analysis and Applications,* 143: 1-26.

Whiteley, D., T. Starkweather and C. Bogart (1990). "Genetic Algorithms and Neural Networks: Optimizing Connections and Connectivity." *Parallel Computing,* 14: 347-361.

Wilde, K., P. Gardoni and Y. Fujino (2000). "Base Isolation System with Shape Memory Alloy Device for Elevated Highway Bridges." *Engineering Structures*, 22: 222-229.

Wilde, K., P. Omenzetter and Y. Fujino (2001). "Suppression of Bridge Flutter by Active Deck-Flaps Control System." *Journal of Engineering Mechanics,* 127(1): 80-89.

Williams, S. R. (2004). *Fault Tolerant Design for Smart Damping Systems*. M.Sc. Thesis, Department of Civil Engineering. Washington University, St. Louis

Xu, Y. L. and B. Chen (2008). "Integrated Vibration Control and Health Monitoring of Building Structures Using Semi-Active Friction Dampers: Part I-Methodology." *Engineering Structures,* 30: 1789-1801.

Yang, G., B. F. Spencer, J. D. Carlson and M. K. Sain (2002). "Large-Scale MR Fluid Dampers: Modeling and Dynamic Performance Considerations." *Engineering Structures,* 24: 309-323.

Yasser, M., J. Phuah, J. Lu and T. Yahagi (2003). "A Method of Simple Adaptive Control for MIMO Nonlinear Continuous-time Systems Using Multifraction Neural Network." *Proc. IEEE/ASME International Conference on Advanced Intelligent Mechatronics*, Port Island, Kobe, Japan, 23-28

Yasser, M., A. Trisanto, A. Haggag, T. Yahagi, H. Sekiya and J. Lu (2007). "Simple Adaptive Control for SISO Nonlinear Systems Using Multiple Neural Networks." *Proc., SICE, 2007 Annual Conference*, Japan, 1287-1292.

Yi, F., S. Dyke, J. Caicedo and J. D. Carlson (2001). "Experimental Verification of Multi Input Seismic Control Strategies for Smart Dampers." *Journal of Engineering Mechanics,* 127(11): 1152-1164.

Yoshida, K., S. Yoshida and Y. Takeda (1999). "Semi-Active Control of Base Isolation Using Feedforward Information of Disturbance." *Proc., 2nd World Conf. on Structural Control*, Kyoto, Japan, 377–386.

Yoshida, O. and S. J. Dyke (2005). "Response Control in Full Scale Irregular Buildings Using MR Dampers." *ASCE Journal of Structural Engineering,* 131(5): 734-742.

Yoshida, O. and S. J. Dyke (2004). "Seismic Control of a Nonlinear Benchmark Building Using Smart Dampers." *Journal of Engineering Mech*anics, 130(4): 386-392.

Yuen, K., J. L. Beck and L. S. Katafygiotis (2002). "Probabilistic Approach for Modal Identification Using Non-stationary Noisy Response Measurements Only." *Earthquake Engineering and Structural Dynamics,* 31(4): 1007-1023.

Yuen, K., J. L. Beck and L. S. Katafygiotis (2006). "Efficient Model Updating and Health Monitoring Methodology Using Incomplete Modal Data without Mode Matching." *Structural Control and Health Monitoring,* 13(1): 91-107.

Yuen, K. V. (2002). *Model Selection, Identification and Robust Control for Dynamic Systems*, Ph.D. Dissertation, Civil Eng. Dept., California Institute of Technology. Pasadena.

Yuen, K. V., Y. Yuanfeng Shi, J. L. Beck and H. F. Lam (2007). "Structural Protection Using MR Dampers with Clipped Robust Reliability-Based Control." *Structural and Multidisciplinary Optimization,* 34(5): 431-443.

Zbikowski, R. and K. J. Hunt (1996). *Neural Adaptive Control Technology*. World Scientific Series in Robotics and Intelligent Systems, Singapore.

Zhang, S. and F. Luo (2009). "An Improved Simple Adaptive Control Applied to Power System Stabilizer." *IEEE Transactions on Power Electronics,* 24(2): 369-375.

Zhou, L., C. C. Chang and L. X. Wang (2003). "Adaptive Fuzzy Control for Nonlinear Building-magnetorheological Damper System." *Journal of Structural Engineering,* 129(7): 905-913.

Zhu, G., M. Rotea and R. E. Skelton (1997). "A Convergent Algorithm for the Output Covariance Constraint Control Problem." *SIAM J. Control and Optimization,* 35(1): 341-361.

VITA

Name: Maryam Bitaraf

Email Address: mbitaraf@tamu.edu; mrybitaraf@yahoo.com

Education: B.Sc., Civil Engineering, University of Tehran, 2003
M.Sc., Civil Engineering, University of Tehran, 2006
Ph.D., Civil Engineering, Texas A&M University, 2011

Research interests:
Structural Control
Structural Health Monitoring
Smart Structures
Numerical Methods